UNIVERSITY OF OKLAHOMA

GRADUATE COLLEGE

IMPACT OF SOIL PH ON THE LEACHING RATE OF DISPOSED LI-ION BATTERIES

A THESIS

SUBMITTED TO THE GRADUATE FACULTY

in partial fulfillment of the requirements for the

Degree of

MASTER OF SCIENCE IN ENVIRONMENTAL ENGINEERING

By

MICHAEL THOMAS SULLIVAN, JR.
Norman, Oklahoma
2021

IMPACT OF SOIL PH ON THE LEACHING RATE OF DISPOSED LI-ION BATTERIES

A THESIS APPROVED FOR THE

SCHOOL OF CIVIL ENGINEERING AND ENVIRONMENTAL SCIENCE

BY THE COMMITTEE CONSISTING OF

Dr. Keith Strevett

Dr. Mark Nanny

Dr. Tohren Kibbey

© Copyright by MICHAEL THOMAS SULLIVAN, JR. 2021

All Rights Reserved

Acknowledgements

I would like to thank my committee members, Dr. Tohren Kibbey and Dr. Mark Nanny, for their support and expertise to guide this thesis in the proper direction. I would like to thank Dr. Keith Strevett, for not only being my advisor through this project, but also being a mentor and great friend.

Table of Contents

List of Tables

List of Figures

Abstract

Lithium-ion batteries (LIB) are becoming the front-runner for rechargeable battery usage yet are rarely disposed of properly. Analysis of varying landfills and electronic waste recycling centers throughout the world show high levels of metal contamination in the nearby soil and water system, contaminating the environment and impacting the health of the surrounding communities. Depending on soil characteristics, the solubility of metals changes by either integrating into the soil or leaching into the water runoff. Though research has been performed with other battery types and electronic waste regarding the severity of the metal contamination over time, no published studies related to LIB were found. This study focused on evaluating the effect soil and water pH has on the leaching of LIB metals and the comparison to the MINEQL+ model of the systems. Dismantled LIB pieces were added to the two types of soil and water sample groups, which were amended to a pH of approximately 4.5 and 9.5, for one to twenty-four weeks. The soil and water samples analyzed by X-ray Fluorescence (XRF) for copper, manganese, nickel, cobalt, and aluminum. Cobalt was below the detection limit in both soil and water groups. The results from the soil samples show the basic soil having a significantly higher adsorption rate over the acidic soil for copper, nickel, and manganese ($p < 0.05$). There was no significant difference in aluminum adsorption between the soil groups. The MINEQL+ model utilized the two-layer adsorption model to qualitatively match the experimental results, with estimating through iteration the equilibrium constants for the metals in the soil. The results from the water samples show the acidic water having a significantly higher leaching rate over the basic water for copper, nickel, and manganese ($p < 0.05$). The leaching rate of aluminum was significantly higher in the basic water over the acidic water ($p < 0.05$). The MINEQL+ model utilized solubility parameters to qualitatively match the experimental results and determine the dominant metal species for ecological health risk. This study highlights the severity of LIB metal contamination into the environment based on soil and water pH. The results of this study aim to encourage the monitoring of soil and water pH surrounding

landfills and recycling centers as implementation steps to prevent further contamination of the surrounding environment by LIB.

Key Words: Lithium-ion battery, Soil pH, Heavy metal contamination, Adsorption Rate, Leaching Rate

Chapter I: Project Introduction

1.1 Introduction

Lithium-ion batteries (LIB) are becoming the front-runner for rechargeable battery usage and storage in household electronics, electric vehicles, and have been introduced as community power reserve stations. When comparing presently available batteries types (i.e., alkaline, lead-acid, nickel-metal hydride), LIB are consistently lighter weight, have no memory effects (lower life cycle), have a higher specific energy (run time), and have higher specific power (power output) (Zubi et al., 2018). These characteristics allow LIB to perform in a diverse set of applications, as previously mentioned.

As with every consumable product, there are ideal disposal procedures to limit the pollution into the environment; LIB are no different. LIB are often improperly discarded into the waste management system (landfills) rather than being recycled (Jacoby, 2019). Batteries disposed of in landfills leach their heavy metals during the degradation process into the soil and water systems nearby, polluting the environment. Even though recycling prevents reusable waste from entering landfills, the recycling centers create heavy metal contamination in the surrounding areas from the recycling process of batteries and other electronic waste. Heavy metal contamination from landfills and recycling centers into drinking water and agriculture can accumulate in the body, causing future health problems (Leyssens et al., 2017). There is a lack of knowledge on the effects soil characteristics have on LIB heavy metal leaching. Such characteristics include pH, cation exchange capacity, original metal content, redox conditions, and organic matter content. This research will examine the effects soil pH has on the LIB heavy metal leaching rate.

1.2 Research Question

The first research question in this study was: what effect does soil and water pH have on the adsorption and leaching of LIB metals such that soil and water contamination becomes a considerable risk?

The second research question in this study was: how does MINEQL+ modeling of the adsorption and leaching of LIB metals into soil and water compare to the experimental results?

1.3 Hypotheses

The first hypothesis for this study states that the integration and adsorption of LIB metals (manganese, cobalt, nickel, aluminum, and copper) into pH amended soil over a 24 week time period will be more significant in basic soil than acidic soil. Specifically, the copper and nickel will have the highest adsorption rates onto the soil compared to the other metals, notably at the basic pH range based on their affinity towards adsorption.

The second hypothesis for this study states that the dissolution of LIB metals into pH amended water over a 24 week time period will be more significant in acidic water than basic water. Specifically, cobalt and copper will have a higher leaching rate in the acidic water compared to the other metals based on solubility and the formation kinetics of metal compounds.

1.4 Objectives

The objective is to evaluate the effects soil and water pH has on the adsorption and leaching rate of LIB metals by creating homogenous soil samples for reproducibility, simulating the damaged LIB in landfills and recycling centers, and simulating the environment in which the LIB are located. With this, a 24 week timeline on the rate at which the LIB metals adsorb onto the soil

and leach into the water will be established and compared to MINEQL+ computer modeling of the systems.

Chapter II: Literature Review

2.1 Li-ion Battery Technology

The basic components of LIB are the same as other battery types: there is an anode, cathode, electrolyte solution, and a separator. The LIB anode is most commonly graphite with a copper current collector. The cathode is constructed of varying metals to promote a desired performance and uses an aluminum current collector. The most common cathodes in use are lithium cobalt oxide ($LiCoO_2$), lithium manganese oxide ($LiMn_2O_4$), and lithium nickel manganese cobalt oxide ($LiNi_xMn_yCo_zO_2$, $0 < x, y, z < 1$) (Zubi et al., 2018). The different cathodes are used depending on the output requirements, a high specific energy or high specific power or a combination of the two. The cathode is made up of sheets of the metal oxides where the lithium ions compose a layer in between the sheets. The electrolyte is can be a solution of lithium hexafluorophosphate, $LiPF_6$, in an organic solvent such as dimethyl carbonate; though a polymer gel made of polyvinylidene fluoride is becoming more common (M. Li et al., 2013). The separator only allows the lithium ions to transfer, preventing the anode and cathode from coming in contact. For LIB discharge, the lithium ions flow from the anode through the electrolyte to the cathode, releasing electricity to power the devices. When recharging the battery, the ions flow back to the anode to the original status until it is used again. This process is shown in Figure 2.1.

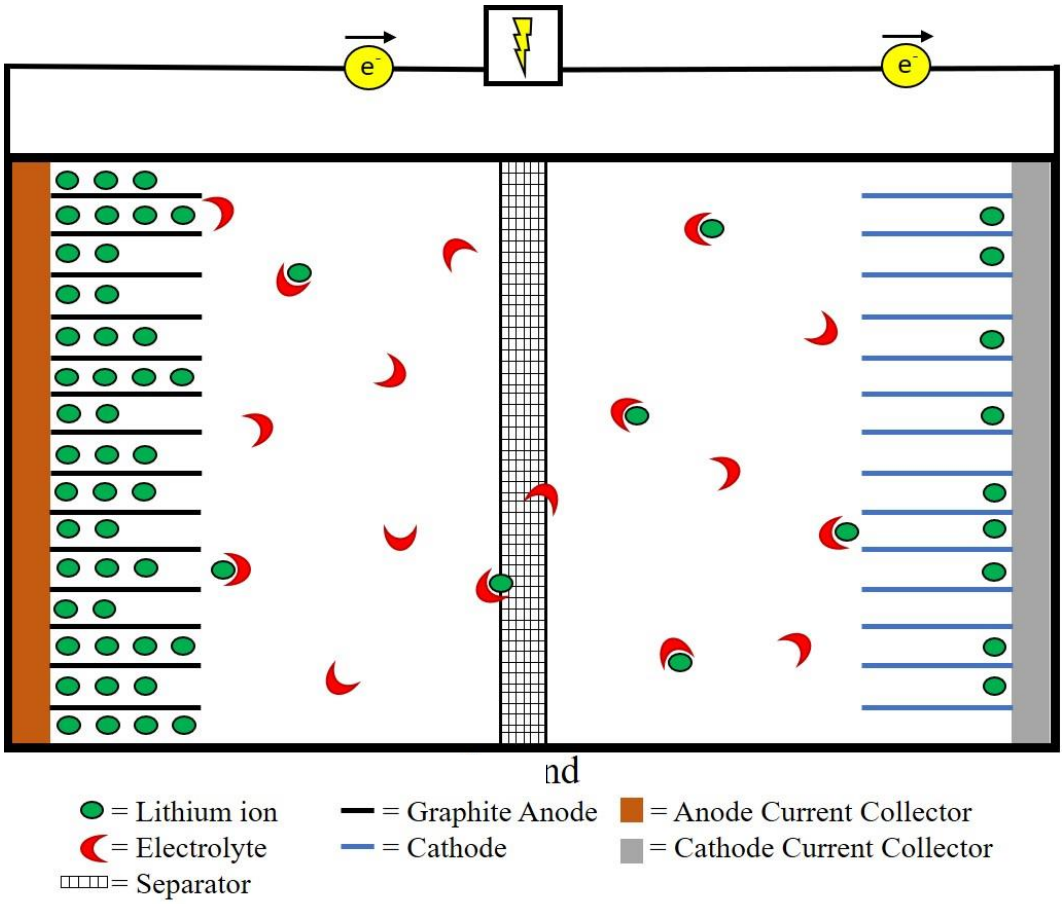

Figure 2.1: *Diagram of a lithium-ion battery cell.*

Lithium-ion technology has paved the way for reliable, high voltage and power output, lower storage weight, and high cycle life batteries (Zubi et al., 2018). $LiNi_xMn_yCo_zO_2$ (NMC) is becoming the front-runner for LIB because it possesses the benefits of nickel, manganese and cobalt. There are multiple combinations of these NMC batteries to better suit the designed task, such as a higher power output for power tools (higher Mn and Co content) or higher run time for energy cells (higher Ni content) (*BU-205: Types of Lithium-ion*, 2019).

2.2 Li-ion Battery Disposal

As with all other types of batteries, NMC LIB degrade with time due to side reactions between the internal metals. The nickel cycles between $Ni^{2+/3+}$ and $Ni^{3+/4+}$ oxidation states throughout the charging and discharging process. When the Ni^{2+} is present, it is capable of diffusing into the lithium layer where reactions with the nickel on the cathode sheet create highly reactive Ni^{4+}. This oxidation state of nickel can react with electrolytes, thickening the cathode-electrolyte interfaces, which reduces the number of available lithium ions, decreasing the battery's performance and longevity (T. Li et al., 2019). At higher voltages, the Ni^{4+} can produce CO_2 which increases electrode interfacial resistances for the lithium ion to insert onto and desert from the cathode, resulting in performance reduction. When the cathode is in a highly delithiated state (i.e., when there is little lithium inserted on the cathode), an electron from O^{2-} can transfer to Co^{4+}, reducing it to Co^{3+}. This releases O_2 into the battery cells that cause capacity and voltage fading and degrade the battery to the point of thermal runaway (Sharifi-asl et al., 2019). LIB do have a longer life than other common batteries but do not have a long life compared to the product in which they are used.

The average mobile phone LIB has a lifespan of just over two years, which is less than the mobile phone itself (Gu et al., 2017). When the LIB are replaced in any electronic device, like electronic waste (e-waste), they are either discarded into the trash can for the municipal waste system to pick up and dump into the landfill or they are properly recycled. Unfortunately, less than five percent of LIB are recycled throughout the world (Jacoby, 2019). That results in hundreds of thousands of metric tons of LIB disposed into landfills rather than being recycled. There are several reasons why the recycling rate is so low. First, there is little public information or advertisement regarding where and how to recycle LIB. Second, technology for LIB recycling

is very fluid, changing and updating every few years. Finally, there are contradictory identifications between governmental authorities relating to whether LIB are considered safe to discard into the waste system or are hazardous waste and must be recycled properly (Timpane, 2018). Regardless of where the LIB are discarded, there is contamination of the surrounding area, whether it be the landfill or the recycling center.

2.3 Environmental Effects

Soil has a vast array of characteristics based on location, fauna, temperature, organic matter content, cation exchange capacity (CEC), water content, and many others. The United States Department of Agriculture (USDA) has created a taxonomic system of twelve different groups, with a multitude of subgroups for each one. These groups differ based on the composition of the layers, or horizons, of the soil and the characteristics listed above (Fischer, 1999). Due to the complexity of these soil groups and to limit the scope of research, this study will focus on the pH of soil. The pH of soil around the world ranges from around a pH of one to over a pH of ten, with 30-40% of arable land on earth is acidic soil (Matsumoto, 2000). Depending on the soil pH, adsorption of metals changes. In basic soil conditions (pH>7), metal ions adsorb strongly to soil particle surfaces, thus not leaching into rain runoff or water systems and less available for plant uptake. In acidic soil conditions (pH<7), there is less affinity for the metal ions to adsorb to the soil particles, causing them to leach into the water and be more available for plant uptake. An example of this is aluminum and manganese present in pH<5 soil can reach toxic concentrations for plant uptake and human consumption (McCauley et al., 2017).

Adsorption for heavy metals have been studied with various soil parameters to determine the affinity metals have for the soil over the dissolved state in water. Nickel, copper, and zinc

adsorption edges based on soil pH show that the metals increase adsorption onto soil as the pH increases (Mamindy-Pajany et al., 2014). This reveals that the availability of the toxic metals for plant uptake or water transport diminishes in basic soil. Alloway (2019) affirms this statement with manganese and cobalt concentrations in sandy loam soil over a pH of 4.5 to 7.5. The manganese soil solution concentration sharply declined from 227 mM at pH 4.5 to 3.1 mM at pH 5.6 then to 0.34 mM at pH 7.5. Cobalt decreases from 0.13 mM to 0.03 mM over a similar pH increase. As pH increases from acidic conditions, metals generally decrease in availability and key nutrients become more available to plants (Jones & Olson-Rutz, 2020).

Although individually tested metals are shown to have their own adsorption edges, there is competition between metals to adsorb onto soil based on the metal's affinity toward the soil particles. This may cause one metal species to be more mobile in the soil and be more readily taken up by plants or transported via water runoff to contaminate other sites. Mamindy-Pajany et al. (2014) shows that in the presence of the other metals, nickel, copper, and zinc have a lower percent adsorbed onto the soil compared to the individual metal's percent adsorption. An exception to this is at higher pH soil and zinc adsorption, which after pH 6, the percent adsorbed is at approximately 100% for both individual zinc and the metal mixture. This analysis along with McCauley et al. (2017) and Sharma et al. (2018) can use effective nuclear charge, Z_{eff}, as a prediction for the adsorption of metals onto soil. As Z_{eff} increases, the high charge to size ratio allows stronger attraction and thus stronger binding to occur to the soil particles. A lower adsorption of the metal allows it to be available for agriculture uptake or transported via water systems to other areas. Regardless of the soil characteristics, heavy metals in LIB will leach into the soil and water systems, potentially reaching concentration levels that are considered dangerous to human health when ingested for a long period of time.

Since the creation of landfills, leachate contamination into the surrounding soil, surface water, and groundwater has been a concern (Perry & Dorian, 1987). Since the mid-20th Century though, regulations in the U.S. and other more developed countries have been put in place to curb the leachate from seeping out of official landfills. These regulations set by the United States Environmental Protection Agency (EPA) include installing a layer of impervious clay, geomembranes, and other impervious barriers into the future landfill site as well as leachate collection and treatment procedures at the source to prevent contamination (Agency, 1987). However, the EPA recognizes that these barriers can fail due to degradation over time or multiple errors in the installation process, causing leachate to escape into the surrounding environment sans treatment.

Common listed failures of these barriers include defective or low quality material; root penetration; cracking due to shrinking, swelling, and settlement; and degradation of the material (Agency, 1987; Council, 2007). The EPA requires multiple barriers stacked together to minimize the failure risk of the individual barriers. Nonetheless, the agency concludes, "based on what is known about the pressures placed on liners over time, is that any liner will begin to leak eventually" (Agency, 1982). The majority of the leachate produced in landfills occurs during its active life, when it is still being filled with waste, and directly after it is closed and capped with barriers to prevent water penetration. This leachate is monitored and treated to prevent contamination into the soil and water systems, however, elevated concentrations of hazardous metals due to the increase of electronic waste can cause issues in the treatment process, disallowing full removal of the metals before discharging the water into the environment (Jang & Townsend, 2003).

Electronic waste in landfills leach heavy metals into the nearby water systems. The leachate that contains these contaminants comes from rainwater permeating the soil to solubilize the heavy

metals in waste as well as surface runoff of exposed waste. The pH of landfill leachate varies depending on the phase of biological stabilization, with literature showing a pH range of 3.5 to 8.5 (Perry & Dorian, 1987). New landfills undergo an acid formulation phase, more currently called anaerobic acid phase, which is the fermentation and hydrolysis of waste into volatile organic fatty acids. This phase decreases the pH of the landfill and increases the heavy metal solubility in the leachate. Examples from Perry & Dorian (1987) is manganese; the concentration of Mn is 0.6 mg/L in every phase except for the acid formulation phase. During this phase, the concentration ranges from 0.6 to 41 mg/L; a drastic increase in Mn that is then integrated into the nearby water systems.

Although recycling is the ideal method of disposing LIB, recycling centers contribute to heavy metal contamination as well. Electronic waste recycling centers distribute heavy metals via flue gas into the air and via ash into the soil and water. (Leyssens et al., 2017). The air, soil, and water spread the heavy metals into the environment, polluting the water systems and agriculture for food. Lead-acid battery recycling centers and general electronic waste recycling centers around the world have been studied for their contamination impact on the nearby communities (Fujimori et al., 2016; Afolayan, 2018; J. Li et al., 2011).

One area that has been studied is the town of Guiyu, China, one of the larger electronic and battery recycling centers in China (J. Li et al., 2011). This town is in a rice growing region with a population of 150,000 and received approximately 15,000 metric tons of waste every day at the time of the study. The air, water, and soil were contaminated with heavy metals, which presents risks to human and environmental health. J. Li et al., (2011) examined soil and water around both current and abandoned recycling sites, then compared the results to previous measurements. The authors determined that many areas had one or more heavy metals well above China's

Environmental Quality Standards for Soils Grades I through III guide value. Grade I is the upper limit of the soil background level; this grade is used to screen potential drinking water and animal rangeland sites. Grade II is the maximum value of contamination for the purpose of agriculture. Grade III is land that should be rehabilitated due to the high concentrations of heavy metal contamination (J. Li et al., 2011). One example is the copper measurements, the Grade I and III levels are 90 and 300 mg/kg, respectively. Out of the nine soil samples collected, seven were higher than Grade I, with one sample at 12,700 mg/kg. These high levels of heavy metals in the soil will be transferred and accumulated into the agriculture on which humans depend.

A second location that has been studied is Olodo, Nigeria, which has a battery waste dumpsite with agriculture in the surrounding area. Afolayan (2018) analyzed the lead, cadmium, and iron concentrations in topsoil, surface water, and maize plants located near this dumpsite. The National Environmental Standards and Regulations Enforcement Agency (NESREA) for Nigeria has set limits for soil and water to be considered safe. For soil, the limits for lead and cadmium are 164 and 50 mg/kg, respectively, with no limit for iron. At all locations, sampled, the lead concentrations were at least 20 times the limit and the cadmium concentrations were at least 3.28 times the limit. In addition to the soil analysis, the stream running near the dumpsite was analyzed, 188 m upstream and 140 m downstream from the dumpsite. Unsurprisingly, the downstream water had lead, cadmium, and iron concentrations much higher than the upstream location, with maximum downstream measurements of 2.15 mg/L, 0.17 mg/L, and 12.90 mg/L, respectively, and upstream measurements of 0.55 mg/L for iron while lead and cadmium were below detectable limits. The NESREA water concentration limits of lead, cadmium, and iron are 0.050 mg/L, 0.01 mg/L, and 1.0 mg/L, respectively. These elevated concentrations cause aquatic pollution that will harm the ecosystem for miles downstream. When the maize was analyzed, all sections of the plant

(leaf, grain, stem, and root) averaged approximately 40.95±1.98 mg/L of lead and 2.84±0.19 mg/L of cadmium, with control maize having negligible concentrations. Iron is essential for photosynthesis, thus iron levels in the maize are not shown to be affected. These studies show that heavy metals leach into the environment regardless of location, however, there is a lack of research on the significance of soil characteristics effect on this contamination.

2.4 Human Health Effects

Heavy metals are generally linked to pollution and their negative environmental effects, yet some are required as micronutrients for healthy plant, animal, and microorganism life. Zinc, iron, copper, chromium, manganese, and cobalt are used in metabolic functions (Muhammad et al., 2020). However, when the heavy metal concentrations in soil and water become higher than the permissible limits established by the World Health Organization (WHO) and other governmental health institutions, they can have detrimental health effects to humans and animals (Brewer, 2010; Casalegno et al., 2015; Klotz et al., 2017; Kumar & Trivedi, 2016; Leyssens et al., 2017; Rivera-Mancía et al., 2011; Sidoryk-Wegrzynowicz, 2014; Yeganeh et al., 2013). The health effects can be provoked by acute (short term) or chronic (long term) exposure to elevated levels of the heavy metals. Chronic toxicity is the focus of the LIB metals due to their lower concentrations in the environment from battery waste, where bioaccumulation occurs slowly over time through the ingestion of contaminated food and water. The pollution of these heavy metals into the surrounding area has long lasting effects on the environment and those that live or work nearby. As previously said, the area around studied landfills and electronic waste recycling centers are shown to be contaminated with heavy metals to the point that the soil and water are considered unfit for human use due to the dangerous health effects caused by the ingestion and absorption of

these metals. To reiterate, the predominant metals in LIB are lithium, aluminum, and copper; with cobalt, manganese, and nickel present depending on the composition of the LIB.

Lithium is a common treatment for Bipolar disorder by increasing serotonin while hindering dopamine and norepinephrine release. As a neurological therapy drug, a long-term use of lithium can cause disorders such as seizures, altered mental status, and Parkinson's-like symptoms. In addition to this, lithium increases the possibility of hypothyroidism six-fold by disrupting the conversion and responsiveness to thyroid hormones (Mehus & Leroy, 2018). Although there is possible chronic toxicity of lithium, it has been shown that there is not a higher bioaccumulation of lithium when consuming water with an elevated concentration of the metal (Aral & Vecchio-Sadus, 2008).

Copper, the anode current collector, is useful in the functions of making red blood cells and the maintenance of nerve cells and the immune system but can cause negative health effects when built up in the body over time. The oxidation state of copper that is most prominent in causing health effects is copper (II). Inorganic copper (i.e., copper not bound to proteins in food) is the form of copper that has the toxic characteristics. Because organic copper is bound to proteins in food, it is easily digested in the liver and removed from the body. Inorganic copper is generally found in water systems due to copper pipes or contaminated water systems, thus it is readily available to transfer to the blood stream (Brewer, 2010). Excess copper in the body contributes to mitochondrial damage because of the generation of reactive oxygen species (ROS). These species damage DNA, proteins, and lipids, resulting in damaged cells that cannot fully function. Copper toxicity has been linked to liver diseases and neurodegenerative diseases such as Alzheimer's disease. To put values on copper toxicity, the amount of copper that increases Alzheimer's-like

diseases in rabbit models is 0.12 parts per million (ppm) in their drinking water (Sparks & Schreurs, 2003). This shows that very little copper is needed to potentially cause harm in humans.

Aluminum, the cathode current collector, is a natural component of food and water, and plays an essential role in medicine and some cosmetics. Exposure to aluminum from these sources is far below the tolerable weekly intake of 1 mg aluminum/kg body weight, set by the European Food Safety Authority (Klotz et al., 2017). Nonetheless, aluminum, like copper, causes negative health effects on the nervous system and brain when over exposed for an extended amount of time. A buildup of aluminum over time can lead to neurological degradation, resembling Alzheimer's disease and Amyotrophic Lateral Sclerosis (ALS). The excess aluminum damages the blood-brain barrier, increasing the permeability of the membrane and allowing aluminum and other contaminants to enter the brain and cause damage (Shaw & Tomljenovic, 2013). Excess aluminum increases lipid accumulation inside cells because it enhances lipogenesis (creation of lipids) and reduces β-oxidation (destruction of lipids) (Mailloux et al., 2011). The increase of lipids in cells may lead to cell dysfunction or cell death, causing further problems in the body.

Manganese is one of the possible metals to make up the cathode. It is an essential metal for the central nervous system by assisting in antioxidant defenses, ammonia detoxification, as well as other necessary mechanisms in the body. However, overexposure to manganese, regardless of oxidation state, can be catastrophic to these mechanisms (Williams et al., 2012). Manganese accumulation in the brain, called manganism, leads to psychiatric and motor function impairments, similar to Parkinson's disease (Guilarte, 2010). Manganese also is a source for hepatic encephalopathy, the decline in brain function because of liver disease. A healthy liver readily removes toxins from the body, with liver disease, however, the toxins are not adequately removed.

The lack of manganese removal from the liver allows the metal to accumulate in the brain, causing brain function impairments (Rivera-Mancía et al., 2011).

Cobalt is one of the possible metals to make up the cathode. It plays a necessary role in only one known biological function, the role of vitamin B_{12}, also called cyanocobalamin. Exposure to any other cobalt compound is considered toxic to the body. Cobalt accumulation can cause cardiovascular, neurological, and endocrine complications. The cobalt (II) ion (Co^{2+}) is the primary state for toxicity in the body because it is generally unbound ions circulating rather than protein-bound cobalt. The ions interact with cellular receptors, ion channels, and biomolecules, generating ROS and causing lipid peroxidation, interruption of thyroid iodine uptake, and mitochondrial disfunction (Leyssens et al., 2017). The results of these disruptions in the body by cobalt include hypothyroidism, cardiomyopathy, and hearing and visual impairment.

Nickel is one of the possible metals to make up the cathode. Nickel is the least understood metal with regards to its function in the body, with many theories based on where it is found in high concentrations. Nickel is present in DNA and RNA probably as a stabilizer for nucleic acids. It is also shown to aid in the absorption of iron and may activate enzymes that breakdown or utilize glucose (Kumar & Trivedi, 2016). Besides the skin nickel allergy that many people have, there are long term exposure effects in the body. Soluble nickel (II) compounds (i.e., nickel chloride or nickel nitrate) are more toxic than their more insoluble counterparts (i.e., nickel sulfide or nickel oxide). This can be explained by the easier uptake of soluble components in the body and the insoluble components pass through without interaction. The absorption of soluble nickel through drinking water leads to a higher nickel concentration in the liver, causing lipid peroxidation, glutathione peroxidase activity, and other destructive processes. Another location in the body that

nickel negatively affects is the seminal vesicle, causing a decrease in size and activity, leading to lower testosterone production (Casalegno et al., 2015).

With the dramatic rise in LIB in the past decade and future prediction in use, concerns over recycling and waste disposal will become even more prevalent and important to environmental and human health (Jacoby, 2019). Heavy metals from lead acid, cadmium, and alkaline batteries have been shown to leach into the soil and water systems in landfills and recycling centers, so it is reasonable to assume that LIB do the same, although little research has been published to confirm this. This study plans to fill that lack of published research by comparing the adsorbing rate into soil and the leaching rate into water of LIB metals based on the media's pH.

Chapter III: Experimental Setup and Methods

3.1 Introduction

X-Ray Fluorescence Spectroscopy (XRF) technology is over a century old, by Charles G. Barkla and Henry G. J. Moseley, where they discovered X-ray radiation from samples change based on the atomic number of the element (Shackley, 2018). However, it was not until the mid- to late- 20th Century that XRF technology expanded exponentially into the field and laboratory use that is seen today. The use for XRF instruments ranges from environmental assessments of contaminated sites, metal recycling plants, mining, industrial, and military use (Coronel et al., 2014; Crook et al., 2006; Kilbride et al., 2006; Reddivari, 2016; Rouillon & Taylor, 2016; Schneider et al., 2016; Shackley, 2018). Present XRF technology uses high-energy photons from the X-ray tube to excite electrons in the samples, which causes the fluorescence of secondary X-rays back to the spectrometer housed in the instrument. Each individual element, regardless of chemical bonds, emits its own specific secondary X-rays to distinguish it from other elements and based on the intensity of the spectrum peaks, the concentration in the sample can be found (Davis et al., 2011). Unlike other elemental analytical technology and procedures, including traditional XRF analysis, the field portable XRF instrument used in this study does not require destructive sample preparation, for analytical methods such as inductively coupled plasma mass spectrometry and atomic absorption (Davis et al., 2011; Mao et al., 2017; Uddin et al., 2016; Udristioiu et al., 2014). This non-destructive analysis of samples allows for quick and easy analysis with little to no sample preparation required and for samples to be saved for future analysis by other instruments if desired (Shackley, 2018).

3.1.1 XRF Technology for Soil Analysis

Field portable XRF instruments are most practical being used in remote locations because of the size and low weight of the instrument and ease of use. The XRF is widely used for the detection of trace metals in soils both in the field and in the laboratory, however, results in the field are generally reported as lower than results acquired in the laboratory. Moisture content in the soil greater than 20% causes X-ray scattering, which diminishes the detection capabilities of the XRF (Bastos et al., 2012; Crook et al., 2006; Sahraoui & Hachicha, 2016; Schneider et al., 2016). Particle size of the soil and organic content both contribute to inaccuracies and increase the limit of detection for multiple elements (Crook et al., 2006; Kilbride et al., 2006; J. Lin, 2009). With these contributing factors for poor XRF results, XRF use in the field is best for initial examinations, with laboratory analysis reserved for generating accurate results. Drying, removing organic matter, and passing the soil through at least a 250 μm or #60 sieve fraction will deliver the most accurate XRF data (J. Lin, 2009; Sikora, 2018). This study used these methods for metal concentration analysis in the LIB soil samples.

3.1.2 XRF Technology for Water Analysis

XRF analysis of liquids, especially water, can be difficult due to the X-ray scattering that the liquid creates. This scattering prevents the fluoresced X-rays from the sample from sufficiently reaching the detector on the XRF for measurements (Crook et al., 2006; IAEA, 1997; Pearson et al., 2017). There are multiple avenues to bypass this hurdle, mainly by precipitation of the metals. Methods include making metal hydroxides by raising the pH, using chelating agents to bind to the dissolved metals, and adding sodium sulfide to make metal sulfides that are insoluble at higher pH, or simply drying the solution entirely to pellet the metals from the water (Abe et al., 2006;

Gordeeva et al., 2003; IAEA, 1997; Peng et al., 2012; Rodrigues dos Santos et al., 2017). The precipitates formed by these methods can then be collected on a membrane filter to be accurately analyzed with the XRF instrument.

This study employed the use of ammonium pyrrolidine dithiocarbamate (APDC) as the chelating agent to metal ions. APDC has been used for decades to concentrate trace metals for analysis by XRF because APDC metal complexes are sparingly soluble in water (Gordeeva et al., 2003; IAEA, 1997; Kanchi et al., 2014; Orescanin et al., 2006; Pradzynski et al., 1976). Orescanin et al. (2006) determined that the optimal recovery of metals occurs with sufficient APDC and the water at pH 8. This study expands on these recommendations to analyze the metal concentration in the LIB water samples.

3.1.3 MINEQL+ Modeling

MINEQL+ is a powerful chemical equilibrium modeling system that incorporates user chemical inputs with its thermodynamic database to simulate experiments and predict chemical reactions in a system (Software, 2015). This program has been used to model and predict heavy metal solubility, adsorption, and precipitation in soil and aqueous environments. The models are often combined with physical experiments to compare the results between one another, which helps verify the physical results and show insight into the thermodynamic properties of the experiment (Al-Hamdan & Reddy, 2008; Magdaleno et al., 2014; Rodgher et al., 2012; Tolonen et al., 2016). There are multiple adsorption models to best fit the type of system that is being modelled. This study utilized the triple-layer adsorption model, which allows for adsorption onto the strong inner-layer surface as well as weaker outer-layer complexation, which includes at least one water molecule between the surface and the adsorbing metal ion. The equilibrium constants

for this model are modified, referred to intrinsic constants, $LogK^{int}$, due to ion concentration products for the bulk solution can vary with pH and solute concentration (Deverel & Fujii, 2012; Schecher & McAvoy, 2015). This study utilized this adsorption model to adjust the metals' $LogK^{int}$ values so that the MINEQL+ models align with the soil experimental results and compare these values with previous literature.

3.2 Methods for Soil Analysis

3.2.1 Soil Collection and pH Adjustment

Northeast of Cheney Reservoir in Reno County, Kansas is the Cheney Wildlife Area, which contains pristine soil, meaning soil that has not been converted to agriculture or urban use. Eleven kilograms of soil was collected with a stainless-steel shovel, from a 20 cm by 36 cm by 12 cm deep section, four centimeters below the surface. The soil was immediately stored in an airtight plastic container for further processing. A soil test was performed to determine the composition of the soil. Larger soil clods were broken apart my hand, sifted with a 0.375" to remove large stones and vegetation, then ground with a mortar and pestle. A U.S. Number 8 sieve was used to sift the soil once more to remove the remaining smaller pebbles and roots and then thoroughly mixed to make a homogenate soil bank to have near identical soil samples for each pH group. The organic matter (OM) and organic carbon (OC) were determined by the Loss-On-Ignition (LOI) method similar to Nelson & Sommers, 1996. Briefly, approximately 25 grams of soil was dried completely then ignited in a muffle furnace at 385℃ for 18 hours. Once cooled, the final mass was recorded, with the difference between the initial and final masses equaling the OM, reported as % wt. loss. The OC is calculated as 58% of the OM (Nelson & Sommers, 1996).

The initial pH and moisture content of the soil were determined based on the methods used by (Carter, 1993). With the initial pH, approximate amounts of sulfuric acid and calcium hydroxide were calculated based on five kilograms of soil for each pH group. Elemental sulfur or sulfuric acid and calcium hydroxide are commonly used to alter the soil pH for certain agriculture uses (*Acidifying the Soil*, 2012; Crozier & Hardy, 2018). To five kilograms of soil to be made for the acidic group, 650 mL of 5.1 M sulfuric acid and 100 mL of UltraPure water was added incrementally while stirring the soil, reaching a final pH of 4.43. To the other five kilograms of soil to be made for the basic group, 26.2 grams of calcium hydroxide and 600 mL of UltraPure water was added incrementally while stirring the soil, reaching a final pH of 9.50. The two soil groups were stored in their respective airtight plastic containers and UltraPure water added to the basic soil group to match the moisture content of the acidic soil after the addition of the sulfuric acid, for a final moisture content of 17.5% for both groups.

3.2.2 Dismantling Li-ion Batteries

Samsung 25R Li-ion NMC batteries were purchased for this experiment because of the nickel manganese cobalt oxide cathode. The LIB were fully discharged over three days by connecting them to a Sylvania 7506LL vehicle taillight bulb and a voltmeter confirmed zero volts. This lowered the risk of electric shock and thermal runaway. The LIB were cut with a Dremel tool into 0.5-1.0 cm cylinders, discarding the end pieces into a hazardous waste container. Each LIB piece was weighed prior to placing into the soil sample tube.

3.2.3 Soil Sample Timeline

The sample timeline included nine time points: 1, 2, 4, 6, 8, 12, 16, 20, and 24 weeks in which the LIB was embedded into the soil. There were three separate samples for each soil pH group at each time point, with soil reserved for a control group of samples for analysis. For both soil groups, twenty-five grams of the corresponding soil and one piece of LIB were added to Falcon 50 mL conical tubes. The tubes were placed onto a tissue culture rotator to spin at ten revolutions per minute to facilitate the adsorption of the LIB into the whole soil sample.

3.2.4 Laboratory Sample Analysis

The soil sample analysis preparation for the analysis by XRF closely followed the preparation procedure set up by McCumber & Strevett, 2017. When the time period for the sample ended the LIB was discarded into a hazardous waste container and the soil was air dried at 20 ℃ for two days. The dried soil was ground with a mortar and pestle, then passed through a #60 sieve and thoroughly mixed. The mortar and pestle were cleaned with KimWipes and the sieve was cleaned with coarse and soft brushes after every sample to minimize contamination between soil samples. The XRF sample cups were 32 mm in diameter and covered with 0.2 Mil (5 μm) thick polypropylene X-ray film. Enough soil was packed into circular XRF sample cups to cover the entire surface of the film. Glass wool was added to fill the remaining space in the sample cup so that the soil stayed pressed against the film. The sample cup was inserted into a test stand that secured the XRF with the X-ray tube window pointing down at the sample to allow a stable analysis. The XRF analyzed the soil sample with a runtime of 180 seconds. The range was set to mg/kg. The sample was analyzed two more times with a 60 degree rotation between scans. The remaining unused soil was kept in the Falcon conical tubes in case of further analysis is warranted.

Statistical analyses were performed on the datasets using Microsoft Excel. The Shapiro-Wilk test was used to determine the normality of the dataset, where a p-value greater than 0.05 passes the normality test and the data is normally distributed. A Student's t-Test at 95% confidence level ($p < 0.05$) was performed between the acidic and basic samples of the same time period to determine if there is a significant difference between the two groups.

3.3 Methods for Water Analysis

3.3.1 Water Sample Preparation and Timeline

The pH of both water sample groups was amended to match the pH of the soil sample groups. For the acidic water samples, three liters of UltraPure water were prepared with an addition of 0.25 M sulfuric acid to achieve a pH of 4.53. For the basic water samples, three liters of UltraPure water were prepared with an addition of calcium hydroxide to achieve a pH of 9.37. The LIB were dismantled and weighed in the same process as the soil samples. The sample timeline included nine time points: 1, 2, 4, 6, 8, 12, 16, 20, and 24 weeks in which the LIB was placed in the water. For both pH groups, 40 mL of water was added to Falcon 50 mL conical tubes then the LIB piece placed inside. The samples sat in darkness for the specified length of time until analysis.

3.3.2 Laboratory Sample Analysis

The water sample preparation for the analysis by XRF similarly followed the preparation procedures by Orescanin et al. (2006) with modification. The sample tubes were centrifuged at 2,000 rpm for ten minutes, after which the supernatant was transferred to a new Falcon conical tube to leave behind the LIB and particulates from the water. The centrifugation and supernatant

transfer were repeated once for the removal of any remaining particulates. Every sample's pH was adjusted to pH 8 with either 0.025 M H_2SO_4 or 0.1 M NaOH. Five milliliters of 2.5% (w/v) APDC was added to each tube and shaken for 30 minutes. After shaking, the samples were passed through a 47 mm, 0.45 μm Osmonics Inc. MicronSep mixed cellulose ester filter under vacuum. The filter paper was air dried prior to analysis. The filter paper was placed into a test stand and the XRF was locked in a stationary vertical position as described above. The XRF analysis time was set to 180 seconds and the range was set to ppm. The filter paper was analyzed two more times with a 60 degree rotation between scans. Linear calibration of each metal was performed to determine a relationship between the XRF ppm results of the filter paper and the actual concentration in the 40 mL sample. A solution of certified calibration standard solution containing 50 mg/L each of aluminum, cobalt, copper, manganese, and nickel was used in volumes of 5 mL, 10 mL, 20 mL, and 40 mL. Each volume was diluted to 40 mL and followed the same procedure as the samples. The slope of this linear relationship was used to correct the sample XRF ppm results to actual concentration of each LIB metal. Statistical analyses were performed on the datasets using Microsoft Excel. The Shapiro-Wilk test was used to determine the normality of the dataset, where a p-value greater than 0.05 passes the normality test and the data is normally distributed. A Student's t-Test at 95% confidence level ($p < 0.05$) was performed between the acidic and basic samples of the same time period to determine if there is a significant difference between the two groups.

3.4 Methods for MINEQL+ Modeling

3.4.1 Soil Modeling

MINEQL+ Version 5.00.0 was used to model the heavy metal adsorption onto the soil between pH 4.0 and 10.0 for the LIB metals: copper, aluminum, nickel, manganese, and cobalt. This study closely followed the "Two-Layer Adsorption" procedure in the MINEQL+ Manual, with slight modification (Schecher & McAvoy, 2015). Based on the findings by *Petrology of Banzet Lithologies*, 1989, the minerals chosen to represent the sand, silt, and clay include quartz, K-feldspar, and kaolinite, respectively. With the results of the soil composition from Chapter 3.2.1 and previous literature, a weighted average for the surface site density (0.0779 mmol/g), specific surface area (4.11 m^2/g), surface site concentration (0.0779 mM), solids concentration (1 g/L), and the initial surface complexation constants ($LogK^1$=4.36, $LogK^2$=-7.94) (Beckingham et al., 2016; Fan et al., 2019; Reich et al., 2010; Richter, 2015; Stillings & Susan, 1995; Tang et al., 2015). Previous literature carries a range of surface complexation constants for the three chosen minerals, thus, iterations of slight changes to the initial values were performed to match the experimental soil results. Equations 3.1 and 3.2 were used for the general reactions required in this model, with S as the mineral's surface, and M^{2+} as the adsorbing metal (Olin & Lehikoinen, 1997; Schecher & McAvoy, 2015; Walker et al., 1988).

$$SOH + M^{2+} \rightarrow SOHM^{2+} \qquad \text{LogK}^1 \qquad \textbf{Eq. 3.1}$$

$$SOM^{+} \rightarrow SO^{-} + M^{2+} \qquad \text{LogK}^2 \qquad \textbf{Eq. 3.2}$$

Into MINEQL+, the LIB metals were individually selected from the list of components and the Two-Layer Model with strong binding sites was chosen under the *Surface Opts*. Listed in

Table 3.1, two new aqueous species were inserted into the *Aqueous Species* Tableau with their respective LogK and stoichiometric coefficients. The total concentration of each component was added to the tableau, with the LIB metals at 0.001 M. Within the *RunTime Manager*, the Ionic Strength Correction was fixed at 0.01 M, based on the soil ionic strength determined by previous literature, and the solids concentration and specific surface area of the soil were entered into the *Adsorption Model* group (Foxboro, 1999; Survey, 2003).

Table 3.1: *Aqueous Species with the respective LogK and stoichiometric coefficients inserted into MINEQL+.*

Species	H_2O	H^+	Coul.	M^{2+}	$S_{(s)}OH$	Log K
SOHM	0	0	1	1	1	4.36
SOHM-1	0	0	-1	-1	1	-7.94

The model utilized the titration calculation using pH as the fixed ion choice, starting at pH 4, ending at pH 10, with 20 points. A pC – pH adsorption diagram was developed for each metal with the total metal adsorbed over the pH range. The results were compared to the soil experimental results, then adjusted the LogK values for SOHM and SOHM-1 species until the model and experimental results matched.

3.4.2 Water Modeling

MINEQL+ Version 5.00.0 was used to model the heavy metal solubility in water between pH 4.0 and 10.0 for the LIB metals: copper, aluminum, nickel, manganese and cobalt. The procedure for this model closely follows the "Calculating the Solubility of Pb and Cu" procedure in the MINEQL+ Manual (Schecher & McAvoy, 2015). The nickel, manganese, and cobalt metal

ions with a 0 M starting concentration and fixing the metal oxide in the Solids Mover, while copper and aluminum metal ions were set to 1 M starting concentration because these metals are in the base metal state. Ca^{2+} and SO_4^{2-} were included with a 10^{-3} M starting concentration to consider the calcium hydroxide and sulfuric acid used to amend the pH. The ionic strength correction entered was 10^{-3} M and utilized the titration calculation using pH as the fixed ion choice, starting at pH 4, ending at pH 10, with 20 points. A pC – pH diagram was developed for each metal with its dominant species and respective concentrations over the pH range. These results were compared to the water experimental results of this study.

Chapter IV: Results

4.1 Soil Analysis Results

The soil composition was determined to be 30.4% clay, 63.2% silt, and 6.4% sand, classified as silty clay loam by the *Soil Conservation Service State Soil Geographic Database.* The initial soil pH was 8.38 with a moisture content of 12.8%, to which the calcium hydroxide, sulfuric acid, and UltraPure water were added to the respective soil group to achieve an acidic soil pH of 4.43, a basic soil pH of 9.5 and a moisture content of 17.5%. The determination of OM and OC from the LOI method resulted in an OM of 6.14% and OC of 3.56%.

Out of the five LIB metals of interest, copper, manganese, nickel, and aluminum were measured above the detectable limit in both soil pH types along the 24 week timeline, with cobalt below the for the XRF for all samples. To confirm that cobalt was below the detection limit in the soil samples and not an instrument defect, LIB powder was analyzed with the XRF, detecting cobalt, with the results in Table A.1. In the control soils, copper and nickel levels were below the detection limit while manganese and aluminum were measured. To best represent the magnitude of LIB metal adsorbing onto the soil, the XRF results were normalized to the control base values by subtracting out the control base value from the sample results, with the control base values shown in Table A.2. Figures 4.1 through 4.4 show the normalized concentration for copper, manganese, nickel, and aluminum, respectively. The vertical axis, ΔC, is the concentration in soil corrected from the control. The line of best fit (solid line) is derived from the first order reaction rate equation, Equation 4.1, where C is the concentration of the metal, k is the rate constant, t is time, and C^* is the adsorption capacity. The reaction rate constant for both pH groups was 0.217, which was used in calculating the adsorption capacity of each metal. A 95% confidence level for the adsorption capacity was calculated via linear regression. The values for k, adsorption capacity,

and 95% confidence level for each sample group were determined, listed in Table 4.1. Non-normalized results are presented in the appendix, figures A.1 through A.4.

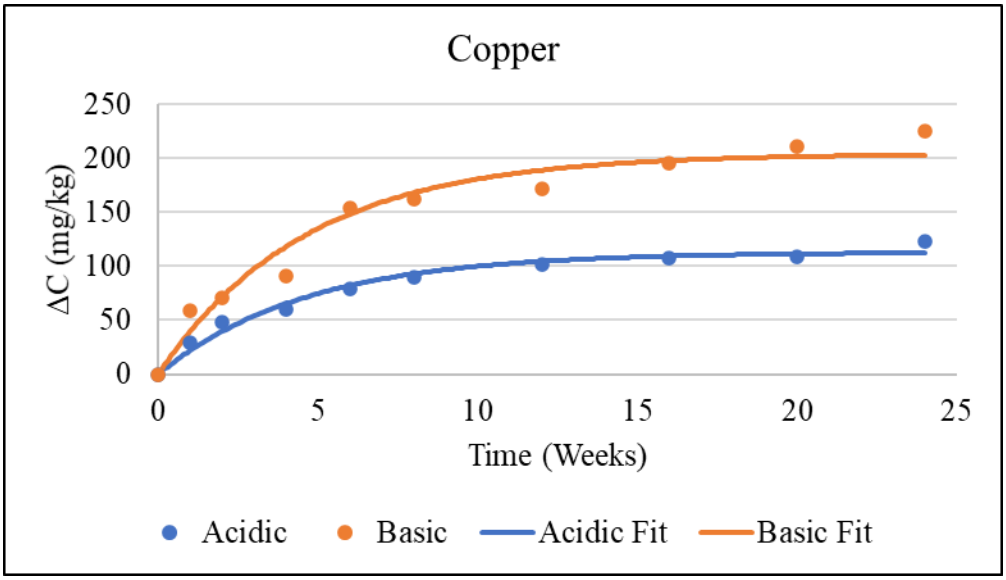

Figure 4.1: *Comparison of copper concentration in soil normalized to controls.*

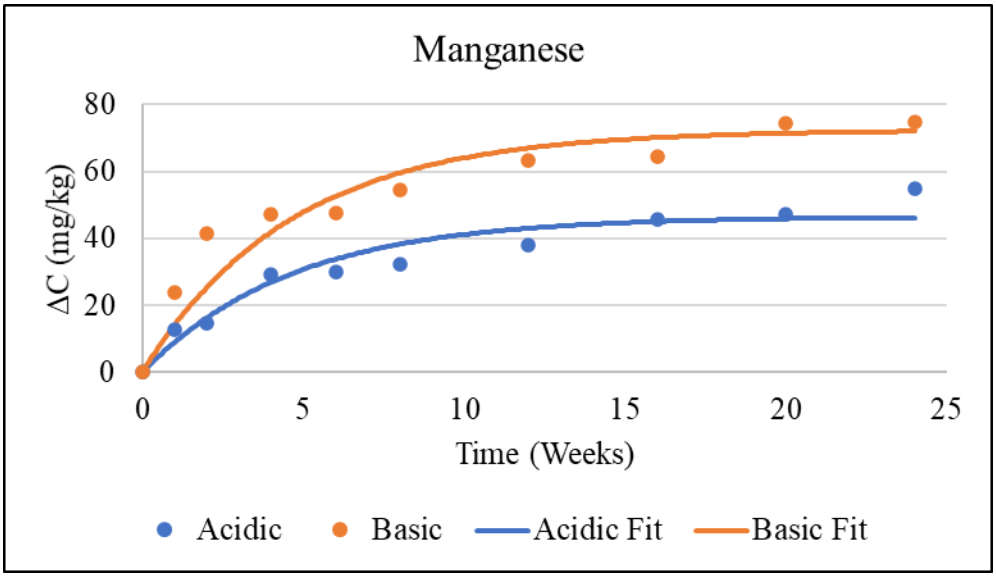

Figure 4.2: *Comparison of manganese concentration in soil normalized to controls.*

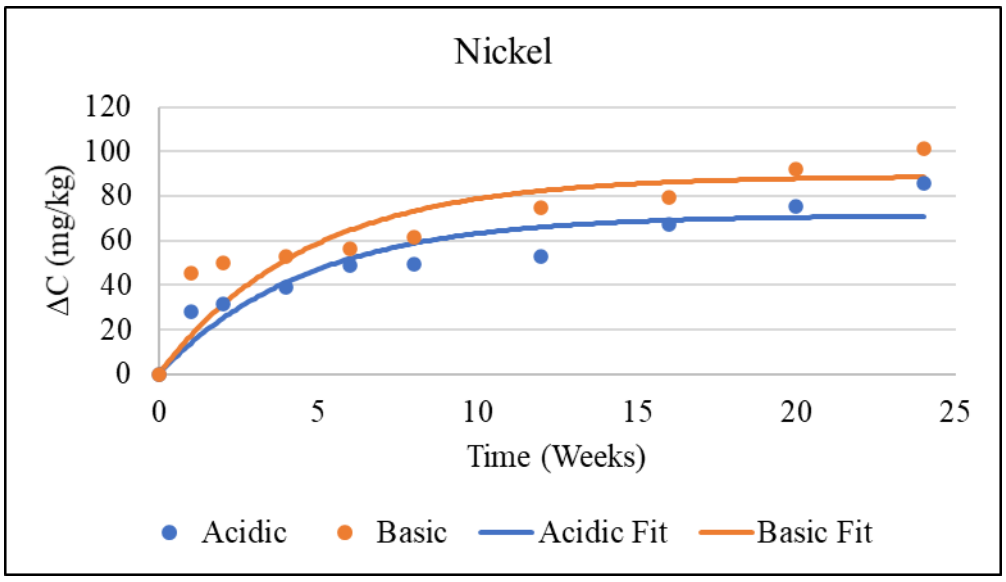

Figure 4.3: *Comparison of nickel concentration in soil normalized to controls.*

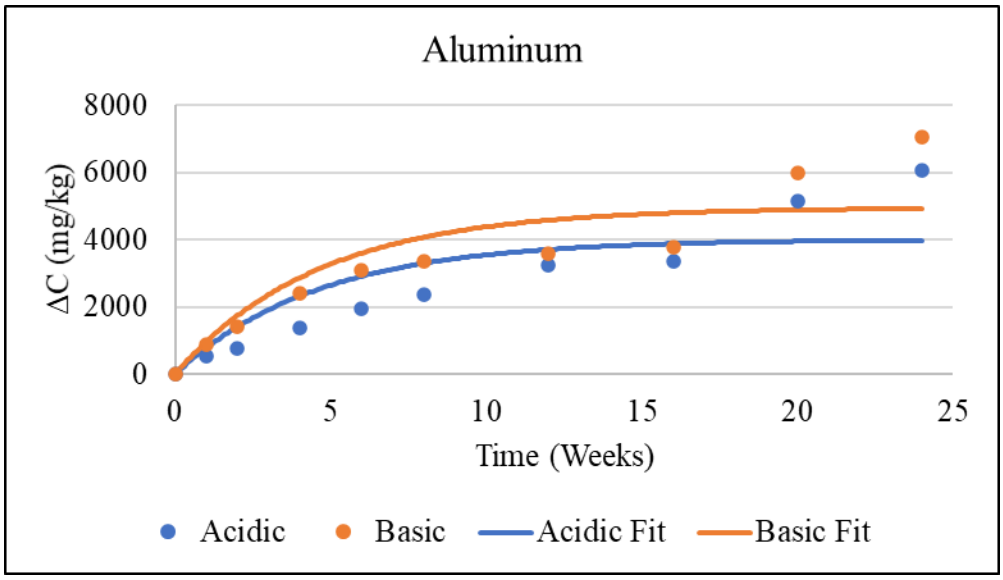

Figure 4.4: *Comparison of aluminum concentration in soil normalized to controls.*

$$C = C^* \cdot (1 - e^{-kt}) \qquad \textbf{Eq. 4.1}$$

Table 4.1: *First-order rate constant, k, and adsorption capacity, C^*, of LIB metals into acidic and basic soil.*

Rate Constant (k), Adsorption Capacity (C^*), and 95% Confidence Level (C.L)				
	Copper	**Nickel**	**Manganese**	**Aluminum**
k	0.217	0.217	0.217	0.217
Acidic C^* (mg/kg)	112.73	71.29	46.51	4,001.31
Basic C^* (mg/kg)	204.01	88.91	72.39	4,944.96
Acidic C^* C.L.	6.64	9.42	4.48	964.12
Basic C^* C.L.	14.77	13.51	7.00	973.34

The Shapiro-Wilk Test for normality results for copper, nickel, manganese, and aluminum in acidic soil and basic soil are in Tables 4.2 and 4.3, respectively. A sample p-value greater than 0.05 retains the null hypothesis that the sample group is normally distributed. A sample p-value less than 0.05 rejects the null hypothesis that the sample group is normally distributed.

Table 4.2: *Shapiro-Wilk Test for each metal in acidic soil over 24 weeks, $p > 0.05$ for all sample groups*

Acidic Soil Shapiro-Wilk Test, p-values				
Week	**Copper**	**Nickel**	**Manganese**	**Aluminum**
1	0.290	0.078	0.973	0.975
2	0.416	0.703	0.239	0.999
4	0.987	0.155	0.559	0.065
6	0.287	0.205	0.980	0.590
8	0.074	0.053	0.976	0.892
12	0.277	0.534	0.837	0.306
16	0.085	0.484	0.493	0.825
20	0.383	0.919	0.843	0.369
24	0.082	0.368	0.605	0.100

Table 4.3: *Shapiro-Wilk Test for each metal in basic soil over 24 weeks, $p > 0.05$ for all sample groups.*

Basic Soil Shapiro-Wilk Test, p-values				
Week	**Copper**	**Nickel**	**Manganese**	**Aluminum**
1	0.189	0.884	0.167	0.237
2	0.416	0.803	0.428	0.495
4	0.546	0.587	0.734	0.162
6	0.757	0.656	0.342	0.343
8	0.463	0.912	0.146	0.179
12	0.850	0.037	0.777	0.793
16	0.296	0.123	0.314	0.329
20	0.418	0.173	0.492	0.479
24	0.341	0.113	0.706	0.325

A Student's t-Test was performed for the LIB metals in each time period between the acidic and basic soil groups. A p-value less than 0.05 rejects the null hypothesis of no difference, confirming a significant difference between the metal concentrations in the two soil groups at the respective time period. A p-value greater than 0.05 cannot reject the null hypothesis, confirming no significant difference between the metal concentrations in the two soil groups at the respective time period. Table 4.4 is the result of the Student's t-Test for the soil groups, where aluminum at all time periods and nickel at the six week time period have a p-value greater than 0.05.

Table 4.4: *Student's t-Test for each metal between acidic and basic soil groups, bolded p-value is a rejection of the null hypothesis.*

Student's t-Test, p < 0.05				
Week	**Copper**	**Nickel**	**Manganese**	**Aluminum**
1	<0.0001	<0.0001	0.013	**0.527**
2	<0.0001	<0.0001	0.003	**0.285**
4	<0.0001	0.001	0.0001	**0.074**
6	<0.0001	**0.054**	0.007	**0.254**
8	<0.0001	0.0003	0.0003	**0.178**
12	<0.0001	<0.0001	0.0002	**0.817**
16	<0.0001	<0.0001	0.009	**0.854**
20	<0.0001	0.001	0.002	**0.935**
24	<0.0001	<0.0001	0.014	**0.964**

The comparison between acidic and basic soil groups for each time period with the respective standard deviations are in Figures 4.5 through 4.8. The p-value refers to the Student's t-Test for significant differences between the acidic and basic soils.

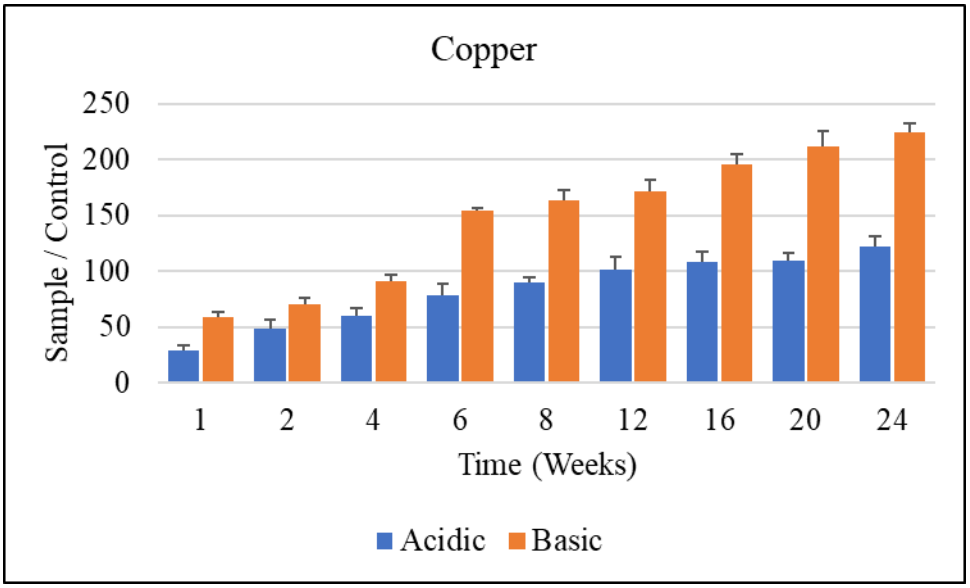

Figure 4.5: *Copper concentration comparison between acidic and basic soil, including standard deviation and Student's t-Test outliers.*

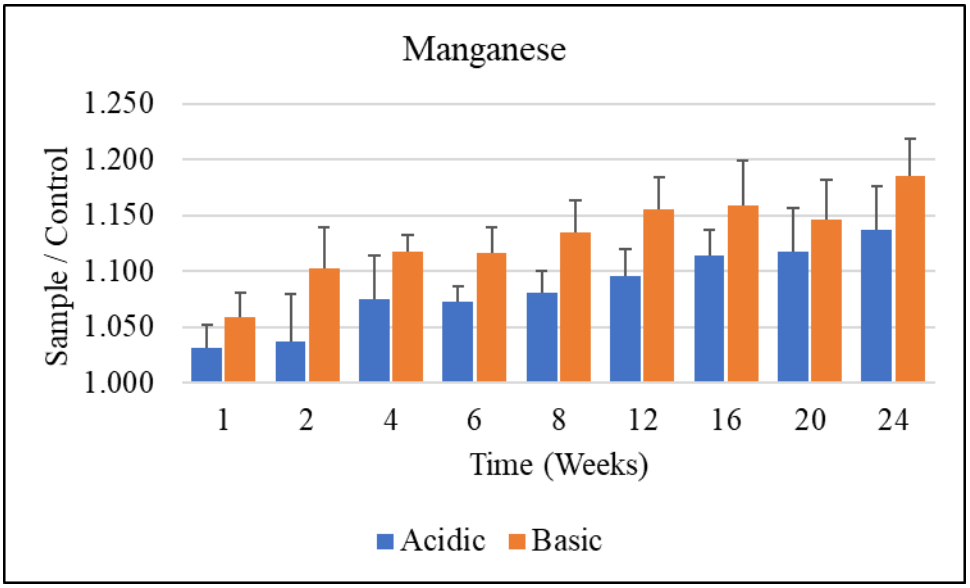

Figure 4.6: *Manganese concentration comparison between acidic and basic soil, including standard deviation and Student's t-Test outliers.*

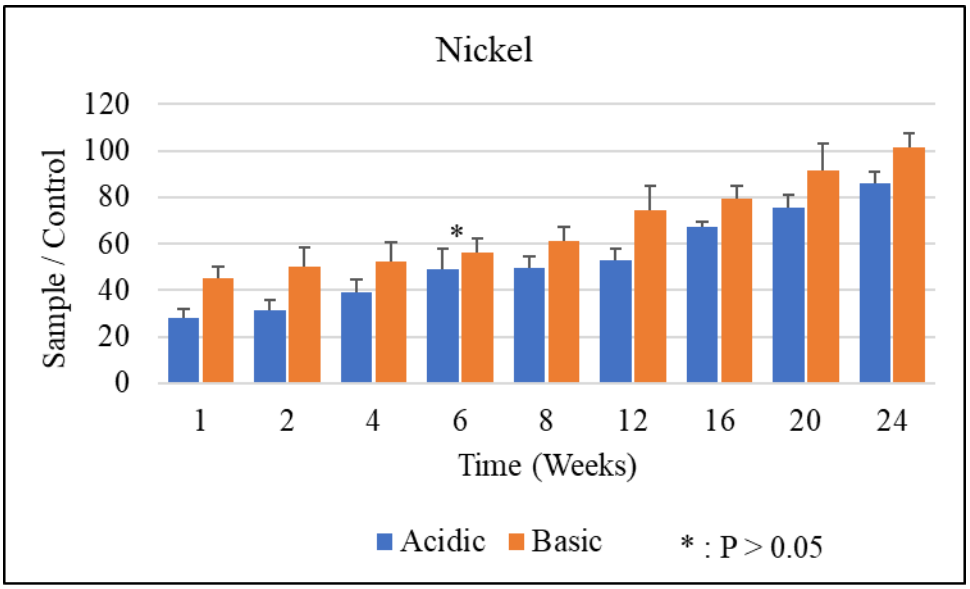

Figure 4.7: *Nickel concentration comparison between acidic and basic soil, including standard deviation and Student's t-Test outliers.*

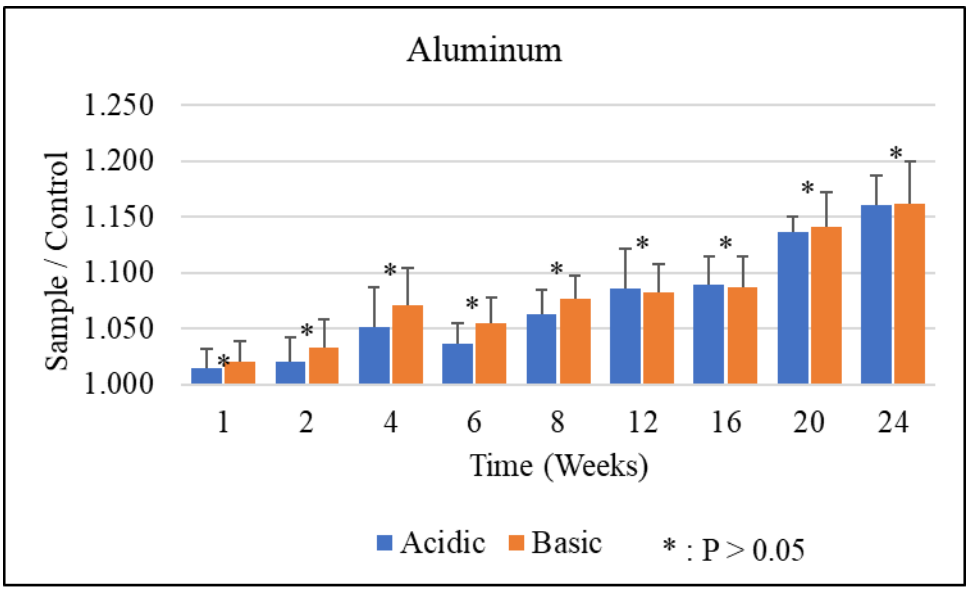

Figure 4.8: *Aluminum concentration comparison between acidic and basic soil, including standard deviation and Student's t-Test outliers.*

4.2 Water Analysis Results

Out of the five LIB metals of interest, copper, manganese, nickel, and aluminum were measured above the detectable limit in both water pH groups along the 24 week timeline, with cobalt below the detection limit for the XRF for all samples. To confirm that cobalt was below the detection limit in the water samples and not an instrument defect, LIB powder was analyzed with the XRF, detecting cobalt, with the results in Table A.1. A linear relationship was created from the certified standards to correct the XRF results to actual concentrations, shown in Figure A.5 and Table A.3. To best represent the magnitude of LIB metal leaching into the water, the XRF results were normalized to the control base values by subtracting out the control base value from the sample results, with the control base values shown in Table A.4. Figures 4.9 through 4.12 show the normalized concentration for copper, manganese, nickel, and aluminum, respectively. The line of best fit (solid line) is derived from the logistic growth rate equation, Equation 4.2,

where C is the concentration of the metal, k is the rate constant, t is time, b is the midway point, and S is the solubility limit. A 95% confidence level for the solubility limit was calculated via linear regression. The values for k, solubility limit, midway point, and 95% confidence level for each sample group were determined, listed in Table 4.5 Non-normalized results are presented in the appendix, figures A.6 through A.9. The pH of the acidic group increased from the starting pH of 4.53 to approximately a pH of 6 for the time points 20 and 24 weeks. The pH of the basic group was consistent throughout the entire sample group.

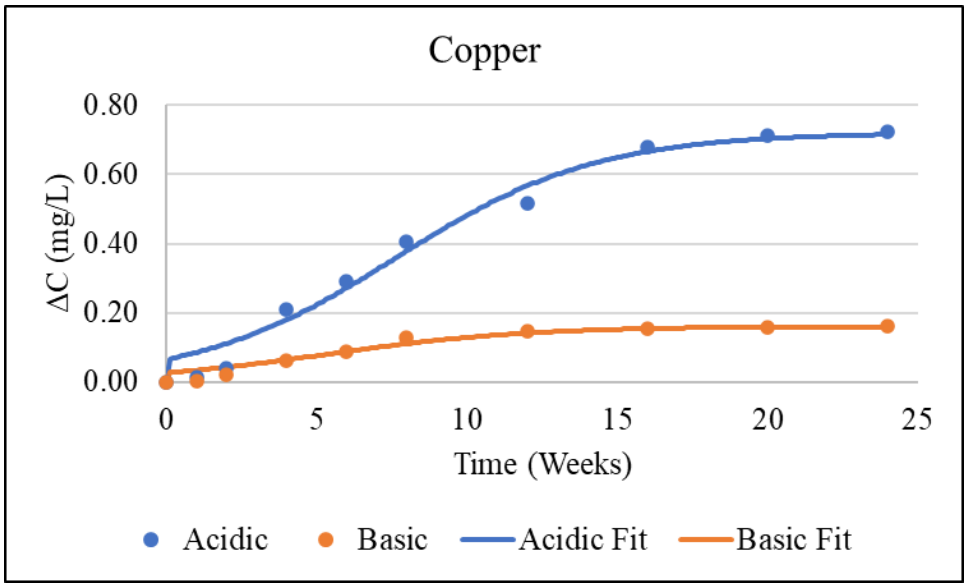

Figure 4.9: *Comparison of copper concentration in water normalized to controls.*

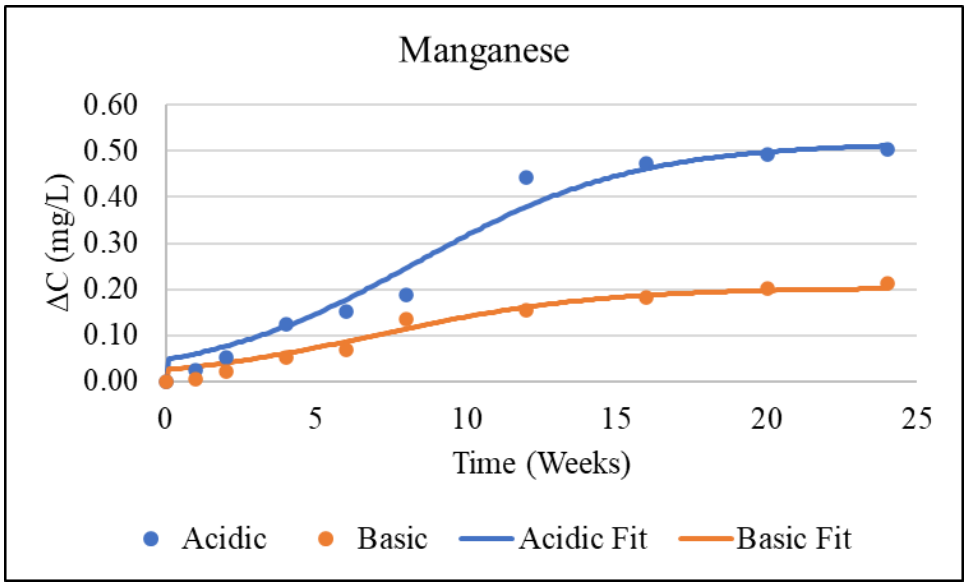

Figure 4.10: *Comparison of manganese concentration in water normalized to controls.*

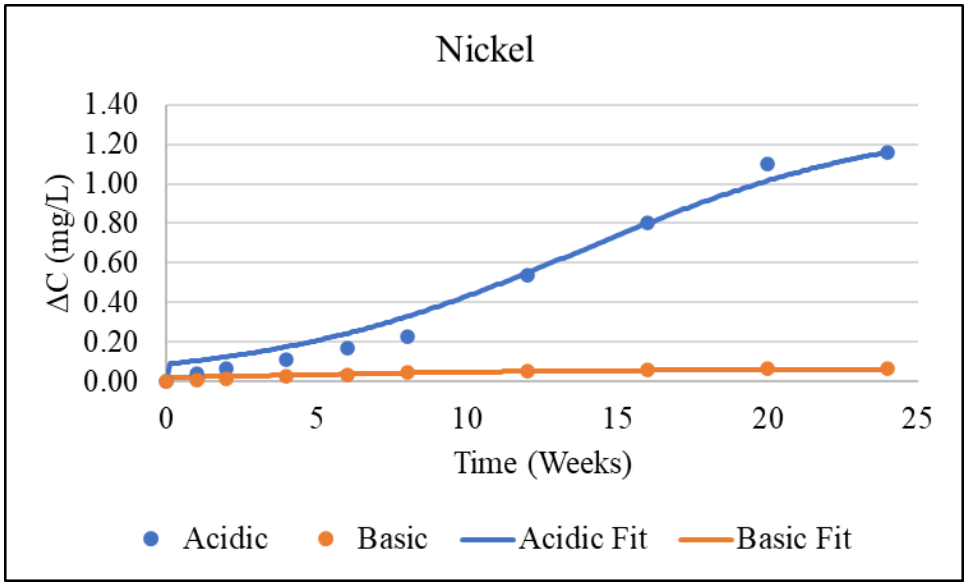

Figure 4.11: *Comparison of nickel concentration in water normalized to controls.*

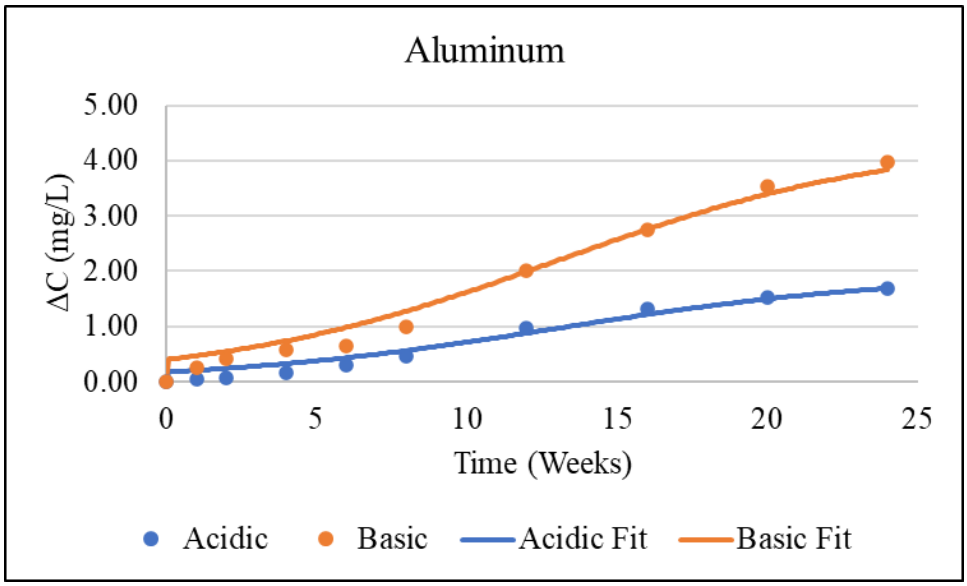

Figure 4.12: *Comparison of aluminum concentration in water normalized to controls.*

$$C = \frac{S}{1+be^{-kt}} \qquad \textbf{Eq. 4.2}$$

Table 4.5: *Logistic growth rate constant, k, and solubility limit, S, and midway point, b, of LIB metals into acidic and basic water.*

Rate Constant (k), Solubility Limit (S) and Midway Point (b)

	Copper	Nickel	Manganese	Aluminum
k	0.236	0.236	0.236	0.236
Acidic S (mg/L)	0.802	1.127	0.557	1.596
Acidic b (Weeks)	10	14	10	10
Acidic C.L.	0.050	0.107	0.042	0.192
Basic S (mg/L)	0.173	0.058	0.216	3.604
Basic b (Weeks)	5	2	7	10
Basic C.L.	0.015	0.009	0.018	0.314

The Shapiro-Wilk Test for normality results for copper, nickel, manganese, and aluminum in acidic water and basic water are in Tables 4.5 and 4.6, respectively. The only sample group that rejects the null hypothesis is copper at 12 weeks in the acidic water.

Table 4.6: *Shapiro-Wilk Test for each metal in acidic water over 24 weeks, bolded value is a rejection of the null hypothesis.*

Acidic Soil Shapiro Wilk Test, p > 0.05				
Week	**Copper**	**Nickel**	**Manganese**	**Aluminum**
1	0.642	0.771	0.179	0.079
2	0.785	0.086	0.439	0.567
4	0.541	0.861	0.457	0.552
6	0.229	0.669	0.090	0.216
8	0.485	0.327	0.952	0.155
12	**0.042**	0.734	0.171	0.162
16	0.114	0.489	0.169	0.563
20	0.457	0.699	0.484	0.456
24	0.088	0.567	0.589	0.731

Table 4.7: *Shapiro-Wilk Test for each metal in basic water over 24 weeks, p > 0.05 for all sample groups.*

Basic Soil Shapiro Wilk Test, p > 0.05				
Week	**Copper**	**Nickel**	**Manganese**	**Aluminum**
1	0.254	0.560	0.221	0.272
2	0.182	0.175	0.215	0.242
4	0.200	0.499	0.289	0.227
6	0.586	0.218	0.657	0.199
8	0.418	0.503	0.211	0.291
12	0.442	0.109	0.344	0.534
16	0.901	0.845	0.466	0.378
20	0.148	0.293	0.740	0.329
24	0.189	0.199	0.411	0.052

A Student's t-Test was performed for the LIB metals in each time period between the acidic and basic water groups. Table 4.7 is the result of the Student's t-Test for the water pH groups, with no group's p-value greater than 0.05.

Table 4.8: *Student's t-Test for each metal between acidic and basic water groups.*

Student's t-Test, $p < 0.05$				
Week	**Copper**	**Nickel**	**Manganese**	**Aluminum**
1	<0.0001	<0.0001	<0.0001	<0.0001
2	<0.0001	<0.0001	<0.0001	<0.0001
4	<0.0001	<0.0001	<0.0001	<0.0001
6	<0.0001	<0.0001	<0.0001	<0.0001
8	<0.0001	<0.0001	<0.0001	<0.0001
12	<0.0001	<0.0001	<0.0001	<0.0001
16	<0.0001	<0.0001	<0.0001	<0.0001
20	<0.0001	<0.0001	<0.0001	<0.0001
24	<0.0001	<0.0001	<0.0001	<0.0001

The comparison between acidic and basic water groups for each time period with the respective standard deviations are in Figures 4.13, 4.14, 4.15, and 4.16. The p-value refers to the Student's t-Test for significant differences between the acidic and basic soils.

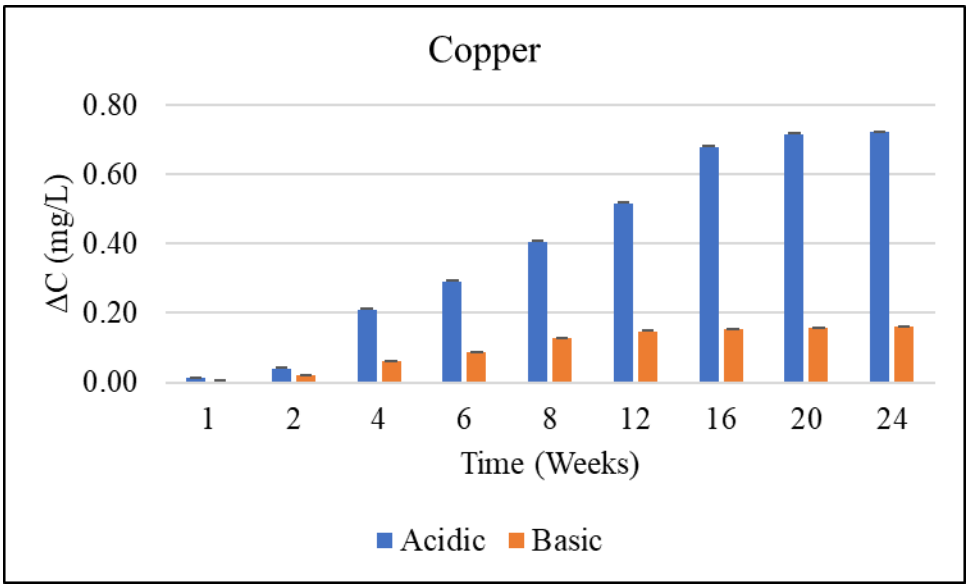

Figure 4.13: *Copper concentration comparison between acidic and basic water, normalized to the control, including standard deviation and Student's t-Test.*

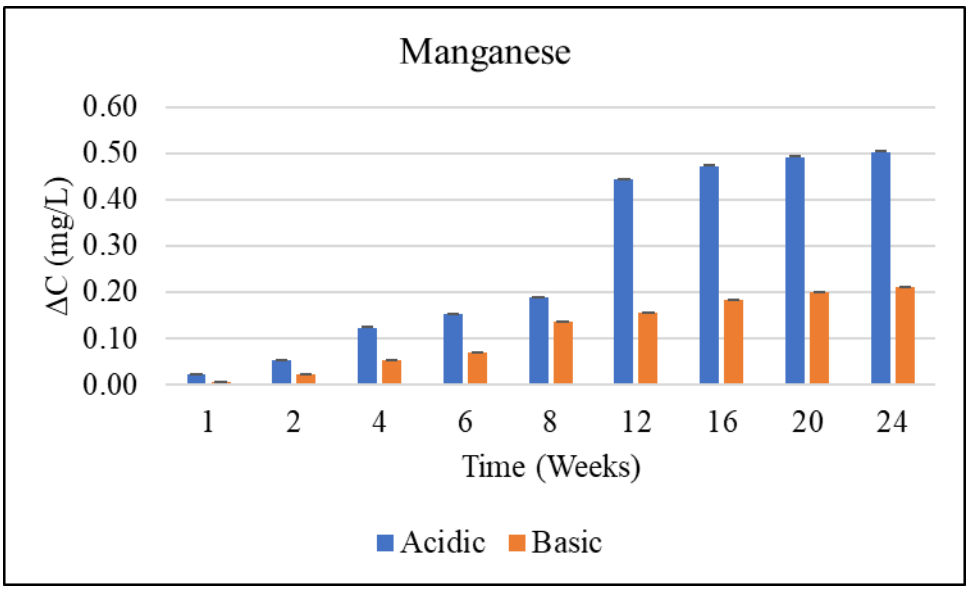

Figure 4.14: *Manganese concentration comparison between acidic and basic water, normalized to the control, including standard deviation and Student's t-Test.*

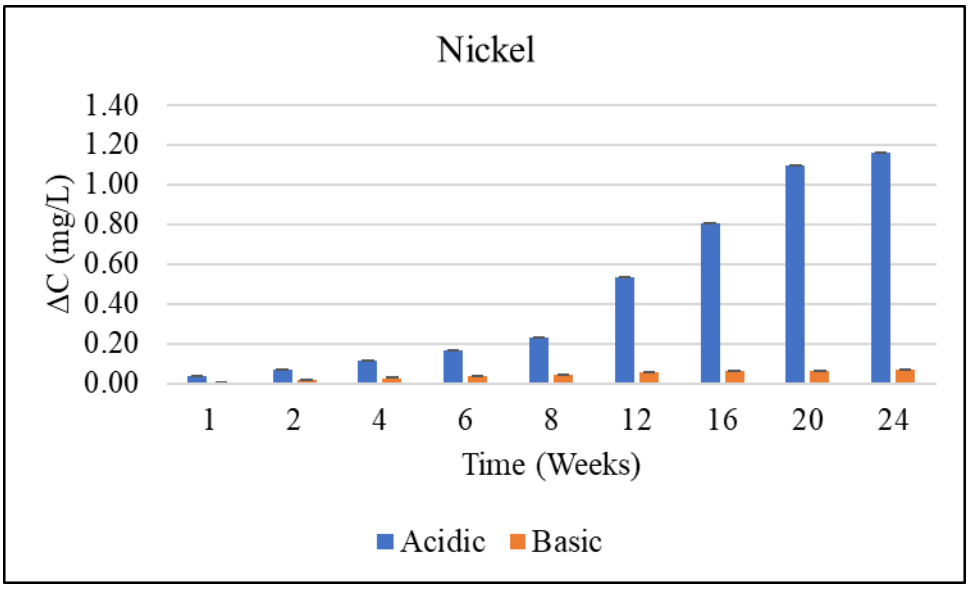

Figure 4.15: *Nickel concentration comparison between acidic and basic water, normalized to the control, including standard deviation and Student's t-Test.*

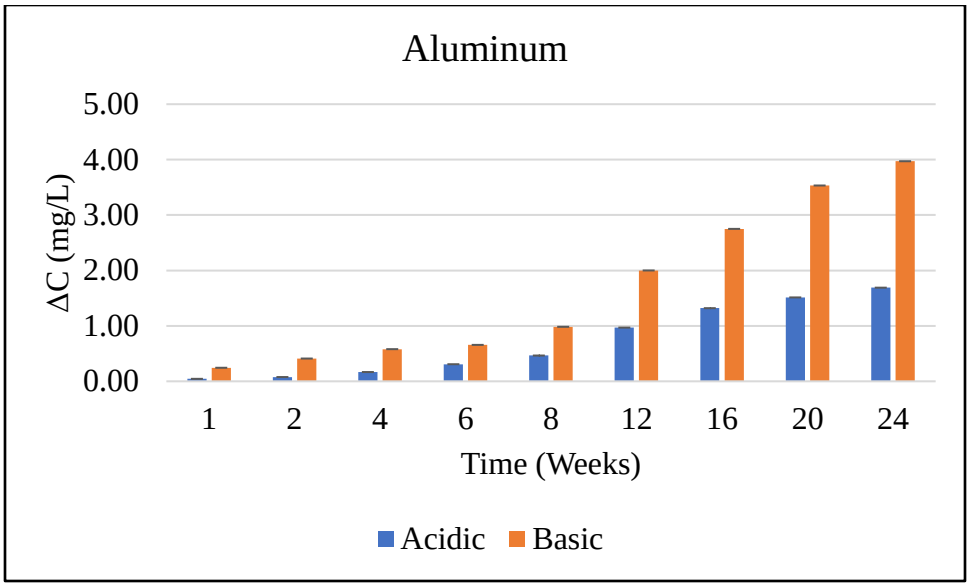

Figure 4.16: *Aluminum concentration comparison between acidic and basic water, normalized to the control, including standard deviation and Student's t-Test.*

4.3 MINEQL+ Modeling Results

4.3.1 Soil Modeling

MINEQL+ enabled the modeling of the adsorption of each LIB metal between pH 4 and pH 10. The LogK values for SOHM and SOHM-1, were determined to be 1 and -8.2, respectively, which were the best fit the experimental soil results. The pC – pH adsorption diagram for the total adsorption of each metal is provided in Figure 4.11. The pC – pH adsorption diagrams for each metal with their major dissolved species are Figures A.10 through A.14 in the Appendix.

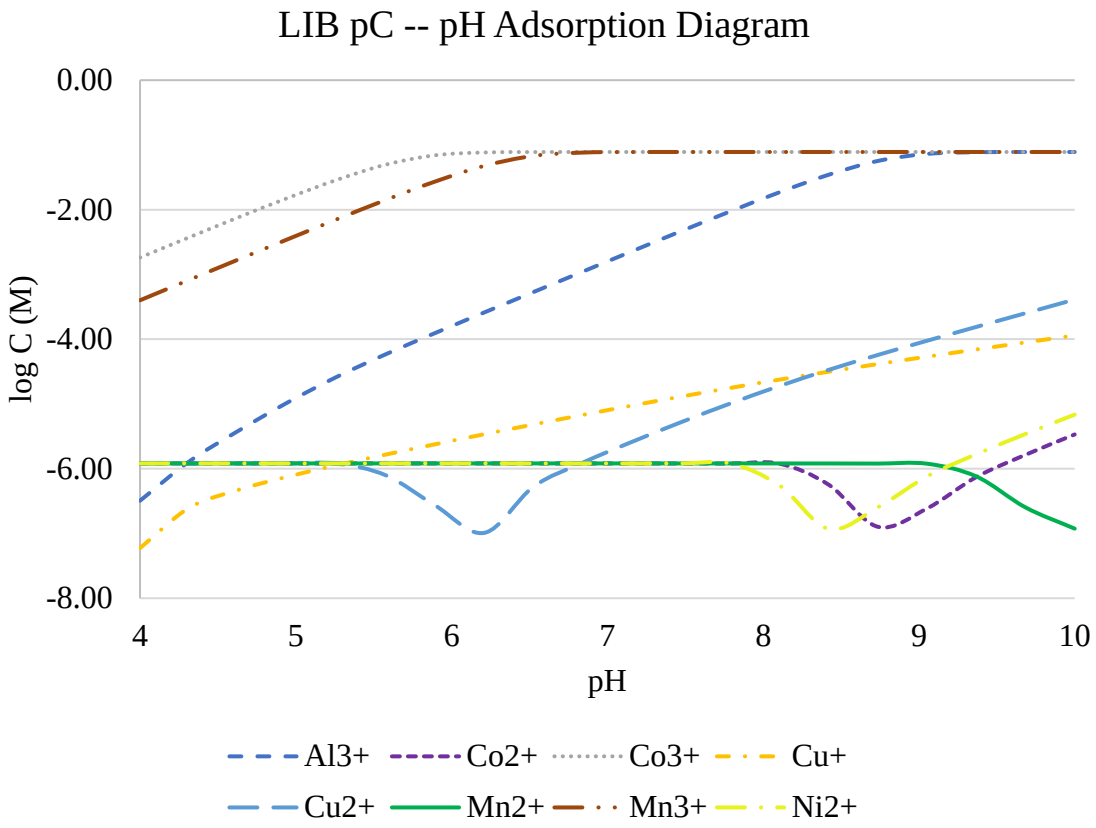

Figure 4.17: *Total LIB metal ions adsorption between pH 4 and pH 10.*

4.3.2 Water Modeling

MINEQL+ enabled the modeling the dominant species and concentrations of each LIB metal between pH 4 and pH 10. The pC – pH diagram for the LIB metals, copper, manganese, nickel, aluminum, and cobalt, is provided in Figure 4.11. Figures 4.12 through 4.16 are the pC – pH diagrams of the major species for copper, manganese, nickel, aluminum, and cobalt, respectively. The metal ion concentrations begin at LogC = 0 at pH 4 due to setting the initial concentration to 1 M and beginning the calculation at pH 4.

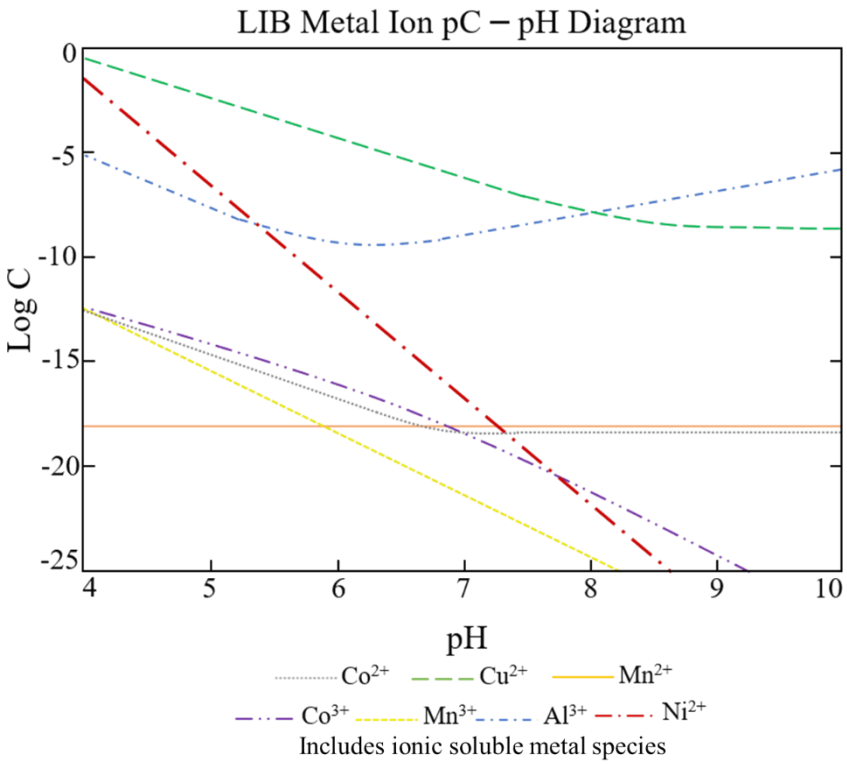

Figure 4.18: *Total LIB metal ions pC – pH diagram*

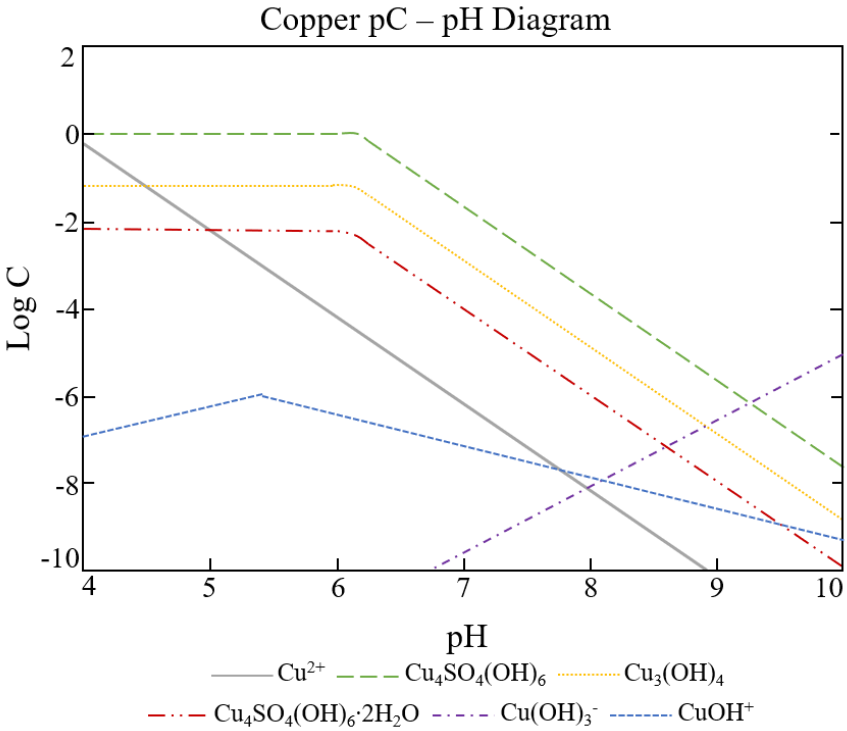

Figure 4.19: *Copper pC – pH diagram*

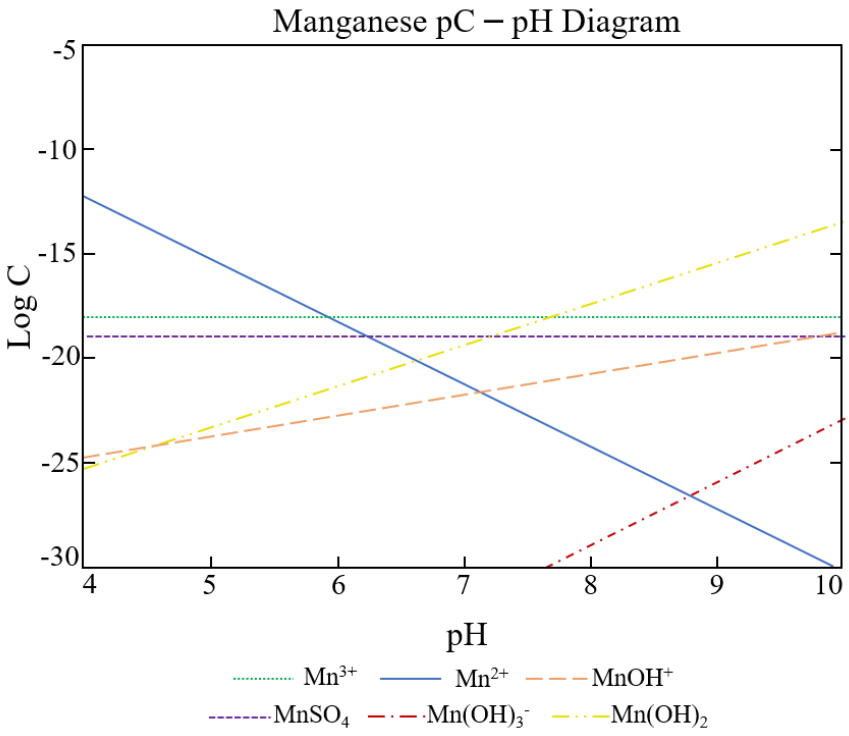

Figure 4.20: *Manganese pC – pH diagram*

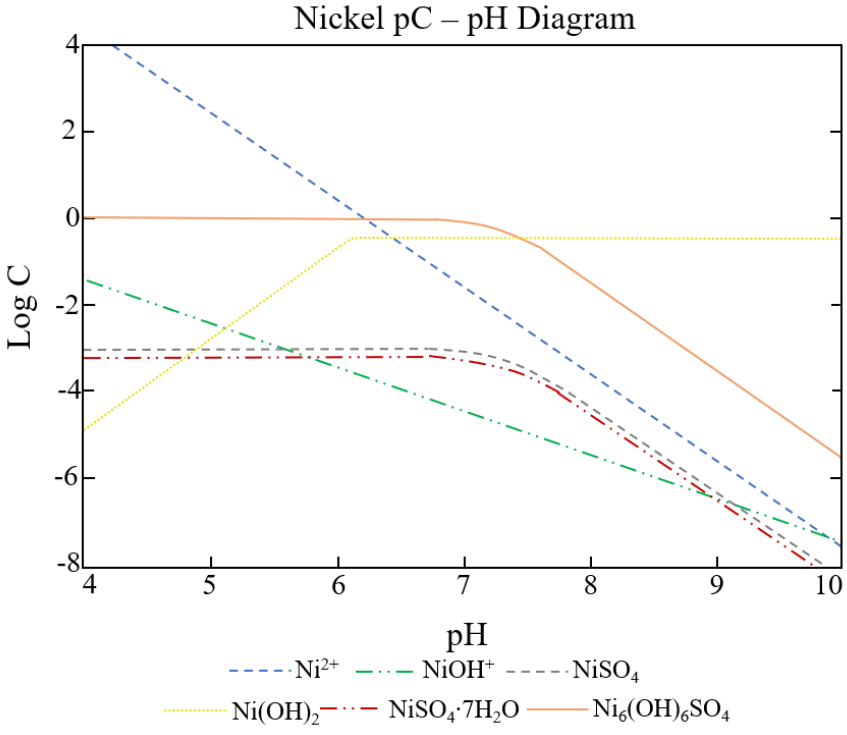

Figure 4.21*: Nickel pC – pH diagram*

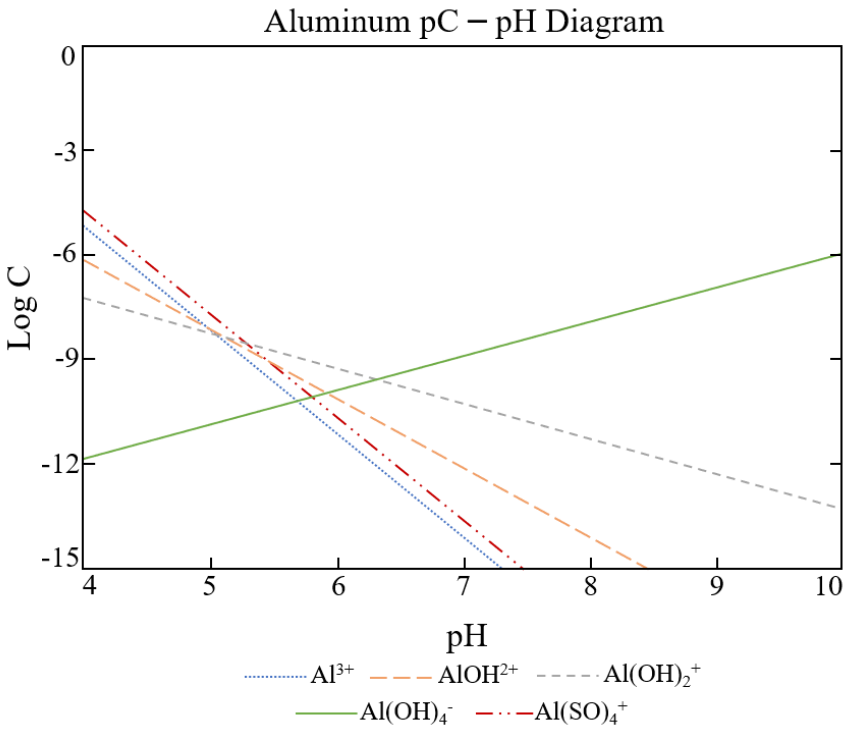

Figure 4.22: *Aluminum pC – pH diagram*

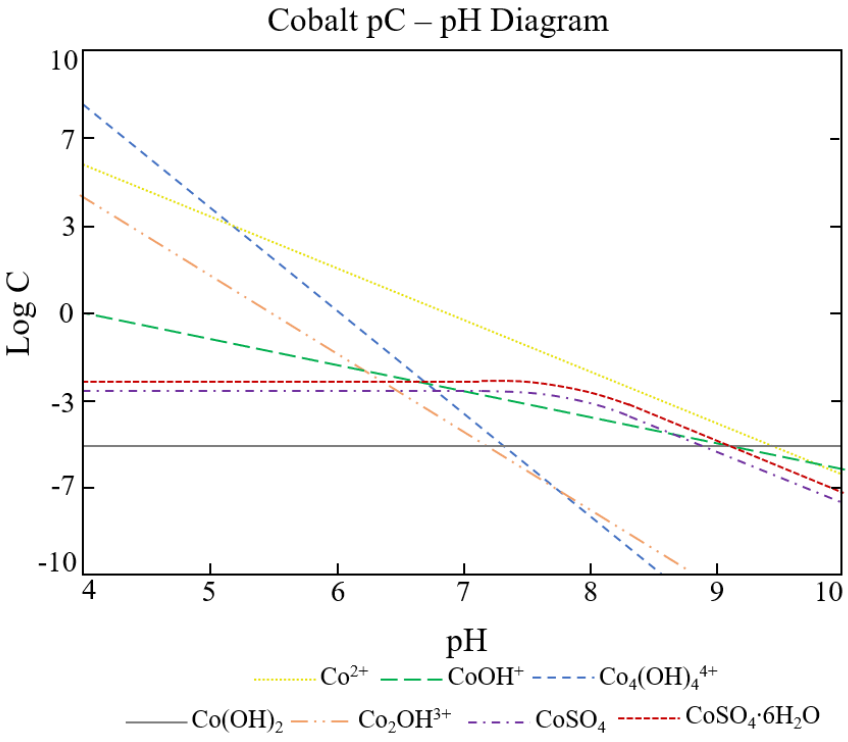

Figure 4.23: *Cobalt pC – pH diagram*

Chapter V: Discussion

5.1 Soil Analysis Discussion

The hypothesis for the soil aspect of this study states that the adsorption of LIB metals will be more significant in basic soil than acidic soil over a 24 week time period, with copper and nickel having the highest adsorption levels. The analysis of LIB metals, excluding cobalt, in pH amended soil over a 24 week time period provided statistical results between the two groups ($p < 0.05$). While it is true that some metals produce insoluble compounds that do not adsorb to the soil particles, for this study, the adsorption of these compounds includes both adsorption to the soil as well as the movement of insoluble precipitates from the LIB to the soil for the measurements and calculations. Overall, copper, manganese, and nickel adsorbed at a higher rate in the basic soil than the acidic soil, while there was no significant difference for aluminum adsorption between the two groups. When normalized to the control soil, copper and nickel adsorbed most significantly ($p < 0.05$) though aluminum had the highest overall increase in the soil. There was an attempt to normalize the adsorption to the LIB piece mass, however this increases the variation of the results. Since the majority of the non-normalized results passed the Shapiro-Wilk test, a conclusion can be made that the surface area, not the mass, of the LIB was the dominant factor for the metal interactions with the soil. Using a standardized cutting mechanism for each LIB, the range of the surface area for all LIB pieces was below ten percent, thus no normalization was required based on surface area.

Based on the XRF analysis of the LIB powder, the batteries used in this study are Ni-rich NMC batteries, $LiNi_{0.6}Co_{0.2}Mn_{0.2}O_2$ (Schipper et al., 2016). This composition of the LIB results in the oxidation states for nickel, cobalt, and manganese to be +2, +3, and +4, respectively, preceding redox degradation of the LIB (F. Lin et al., 2014). Since disposed LIB will have redox

degradation, the oxidation states of nickel, cobalt, and manganese range between +2 to +3, +3 to +2, and +4 to +2, respectively (T. Li et al., 2019; F. Lin et al., 2014; Vetter et al., 2005). The differences in oxidation states between this study and disposed LIB may cause difference in the adsorption rate of the metals to the soil because of the dynamic nature of soil. Variables including redox potential, soil pH, and oxygen and water levels all play a part in the oxidation state of metals (DeLaune et al., 2013). These naturally occurring metals in LIB are essential micronutrients for plants and animals, so the natural concentration levels in soil are not considered harmful to life. Once the concentration is above a certain limit known to cause harm to the ecosystem from sources such as landfills and recycling centers, the metal contamination requires remediation of the area to meet the concentration guidelines or standards (Alva, 1999; Lerner, 1999). The comparison between new LIB and post 24 week time period in the soil is shown in Table A.5. The decrease in both acidic soil and basic soil LIB metal is consistent with the experimental results. The lower concentration in the basic soil LIB for copper, manganese, and nickel, confirms that more adsorption occurred. The OM and OC content, 6.14% and 3.56%, respectively, which is in range for silty clay loam soil (Karlen, 2005). OM species, such as humic and fulvic acids, increases adsorption of metals at higher pH due to the negative charge on them by deprotonation. In addition to the soil particles, the positively charged LIB metal ions also adsorb to the OM, increasing the adsorption capacity of the soil that was determined in this study (Vytopilová et al., 2015). OM aids in the prevention of heavy metal uptake by plants. For this study, the adsorption capabilities and capacity of LIB metals do not distinguish between the OM and soil particle adsorption, though a future study can be performed on this soil with the removal of OM to compare the adsorption of LIB metals with and without OM.

Copper adsorption to the basic soil was shown to be more significant ($p < 0.05$) compared to the acidic soil, supporting the hypothesis. At the end of 24 weeks, the adsorption of copper in the basic soil (224.63 mg/kg) is nearly twice as high as that of the acidic soil (122.47 mg/kg). For comparison, the copper concentration in surface soil at an e-waste recycling center in the Philippines averaged at 680 mg/kg (Fujimori & Takigami, 2014). Though copper is an essential micronutrient for organisms, copper toxicity can occur in as little as 3 mg/kg. The EPA has set copper concentration limits in soil for plants, mammals, invertebrates and birds at 70, 49, 80, and 28 mg/kg, respectively (Alloway, 2019). The amount of adsorbed copper in both soil groups well surpasses the EPA limits. The best fit line used for the adsorption of copper was a first-order reaction rate. This reaction rate determined a rate constant of 0.217 and an adsorption capacity of 112.74 ± 6.64 mg/kg for acidic soil and 204.01 ± 14.77 mg/kg for basic soil. The rate constant value is in range of previous literature and the increase in adsorption capacity as pH increases coincides with previous literature, though different soils producing different rate constants and adsorption capacities (Bradl, 2004; He et al., 2020; Minamisawa et al., 2004; Xie et al., 2018). The rate constant and adsorption capacity of copper in this soil can be used to estimate and predict contamination concentrations of LIB metals surrounding landfills and recycling centers. The contamination risk of the metal is significant, notably at basic soil pH, due to the amount of copper adsorbing to the soil particles, that which can be taken up by plants with changing soil conditions.

Manganese adsorption to the basic soil was shown to be more significant compared to the acidic soil, supporting the hypothesis. At the end of 24 weeks, the adsorption of manganese in the basic soil was 479.75 mg/kg and in the acidic soil was 455.72 mg/kg. After normalizing to the control soil manganese concentration, the basic soil adsorption was 74.88 mg/kg and the acidic soil adsorption was 55.01 mg/kg. Manganese oxides are common soil minerals, with an average

soil concentration in the United States between 40 and 900 mg/kg, hence the approximate 400 mg/kg in the control soils (Control, 2012). The metal is an essential micronutrient for plants, though consensus for a toxic concentration limit has yet to be reached, as the availability of manganese to plants varies based on soil characteristics as well as the tolerance to manganese for certain plant species (Howe et al., 2005). The oxidation state of manganese in new LIB is +4, in the form of insoluble oxides, whereas in degraded LIB, the oxidation state ranges between +4 to +2, varying the bioavailability for plants. According to Alloway, 2019, in the presence of oxygen manganese (II) oxidizes rapidly to form Mn(IV) oxides at pH greater than 4, thus the Mn(II) in degraded LIB will more proportionately convert into Mn(IV) oxides rather than remaining as Mn(II). Since Mn(II) is the oxidation state that is taken up by plants, the rapid conversion to Mn(IV) is a key factor in preventing manganese toxicity to plants and animals (Millaleo et al., 2010). The increase of manganese over the 24 week time period can be accredited to the diffusion of the manganese oxides into the soil rather than the adsorption of the metal to soil particles. The best fit line used for the adsorption of manganese was a first-order reaction rate. This reaction rate determined a rate constant of 0.217 and an adsorption capacity of 46.51 ± 4.84 mg/kg for acidic soil and 72.39 ± 7.00 mg/kg for basic soil. The rate constant value is in range of previous literature and the increase in adsorption capacity as pH increases coincides with previous literature, though different soils producing different rate constants and adsorption capacities (Bradl, 2004; He et al., 2020; Minamisawa et al., 2004; Xie et al., 2018). The rate constant and adsorption capacity of manganese in this soil can be used to estimate and predict contamination concentrations of LIB metals surrounding landfills and recycling centers. With these results and the concentration range of manganese naturally in soil, the contamination risk of the metal is low due to the quick conversion to the unreactive metal oxide form.

Nickel adsorption to the basic soil was shown to be more significant compared to the acidic soil, supporting the hypothesis. At the end of 24 weeks, the adsorption of nickel in the basic soil was 101.42 mg/kg and in the acidic soil was 85.79 mg/kg. For comparison, the area surrounding an e-waste recycling center in Guiyu, China averaged 20.8 mg/kg, but the abandoned workshop was 480 mg/kg (J. Li et al., 2011). The WHO target value of nickel in soil is 35 mg/kg and remedial intervention value is 210 mg/kg (Osmani et al., 2015). The concentration of nickel for both soil groups is higher than the target value, creating a concern for the ecological effect around the contaminated soil. Nickel has a low mobility in soil, with a labile fraction between 0.1-50% of the total nickel concentration likely due to the slow reactions between nickel and iron oxides (Massoura et al., 2006). This isolates the severity of nickel contamination in soil to the immediate area. The containment of nickel is crucial to preventing contamination into the surrounding areas where it can be taken up by the agriculture or deposited into the water systems where it can bioaccumulate in aquatic and land fauna. The best fit line used for the adsorption of nickel was a first-order reaction rate. This reaction rate determined a rate constant of 0.217 and an adsorption capacity of 71.29 ± 9.42 mg/kg for acidic soil and 88.91 ± 13.51 mg/kg for basic soil. The rate constant value is in range of previous literature and the increase in adsorption capacity as pH increases coincides with previous literature, though different soils producing different rate constants and adsorption capacities (Bradl, 2004; He et al., 2020; Minamisawa et al., 2004; Xie et al., 2018). The rate constant and adsorption capacity of nickel in this soil can be used to estimate and predict contamination concentrations of LIB metals surrounding landfills and recycling centers. The sharp rise of adsorption of nickel at the beginning of the timeline may be explained by a strong affinity of nickel to the soil that adsorbs quickly then the slower diffusion of nickel oxides out of the LIB into the soil to reach an equilibrium state between the soil and LIB. The

acidic pH has more H^+ ions competing for the same adsorption sites, causing the lower nickel concentration and adsorption rate. These adsorption rates demonstrate the severity of nickel contamination from LIB, mainly at recycling centers because of the continual influx of new disposed LIB and other e-waste that is processed on-site, spreading the particulates to the surrounding area via ash in the wind and soil deposition via vehicles (Fujimori et al., 2016). With these results, the contamination risk of the metal is significant at both soil pH groups due to the amount of nickel adsorbing to the soil particles that which can be taken up by plants with changing soil conditions.

Aluminum adsorption to the basic soil was shown to have no significant difference compared to the acidic soil. At the end of 24 weeks, the aluminum concentration for the basic soil was 50,5791 mg/kg and the acidic soil was 43,761 mg/kg, although the aluminum concentration for the control soil for the basic and acidic soil differed, 43,732 mg/kg and 37,702 mg/kg, respectively. Factoring in the control aluminum concentration, the basic soil had 7,059 mg/kg and the acidic soil had 6,059 mg/kg aluminum adsorbed, both equating to a 16.1% increase in aluminum. The overall large increase of aluminum in both soil groups may be due to the aluminum being along the perimeter of the LIB cylinder, allowing more direct contact with the soil compared to the shared surface area for the four other metals, and, as an amphoteric aluminum oxide, it can react with both acids and bases to increase adsorption (Orwat et al., 2016). The best fit line used for the adsorption of aluminum was a first-order reaction rate. This reaction rate determined a rate constant of 0.217 and an adsorption capacity of 4,001.31 ± 964.12 mg/kg for acidic soil and 4,944.96 ± 973.34 mg/kg for basic soil. Based on the rate constant and fit line, the 20 and 24 week concentrations do not necessarily align with the trend that is shown with the previous time points as well as with the other LIB metals. The rate constant value is in range of previous literature and

the increase in adsorption capacity as pH increases coincides with previous literature, though different soils producing different rate constants and adsorption capacities (Bradl, 2004; He et al., 2020; Minamisawa et al., 2004; Xie et al., 2018). The rate constant and adsorption capacity of aluminum in this soil can be used to estimate and predict contamination concentrations of LIB metals surrounding landfills and recycling centers. Although there is no significant difference between the adsorption rates, there are different forms of aluminum present in each soil group, determining the degree to which it is bioavailable. In more basic pH soil, the dominant species are polymeric aluminum, including aluminum oxides and aluminum silicates, which are relatively immobile and are rarely toxic to plants. In more acidic pH soil, the dominant species is the free aluminum ion, Al^{3+}, which is the most toxic form to plants. The metal ion is absorbed by the roots, causing, followed by nutrient and water uptake, eventually leading to plant death (Bakkaus et al., 2008; Matsumoto, 2000; Panda et al., 2009). The near equal adsorption of aluminum in both soil groups is likely due to the different aluminum species formed in the soil. At a lower pH, aluminum hydroxide species are prevalent, whereas as basic pH, the main contributor is adsorbed aluminum. The stagnation in aluminum increasing between 12 to 16 weeks may be due to the primary species of aluminum reaching equilibrium in the soil and the less dominant species are then increasing in concentration. With this concentration increase through the end of the 24 week time period, it is determined that aluminum contamination risk from LIB is higher in the acidic soil due to the bioavailability of free Al^{3+} in plants. However, lowering the pH of basic soil through chemical contaminants may cause detrimental effects to the surrounding area due to the dissolution of aluminosilicates into the free aluminum ion.

Cobalt adsorption to the basic and acidic soil was below the detection limit by the XRF. As previously stated, this was not due to instrumental error as confirmed by measurements using

soil amended with LIB powder. One possible explanation for the inability to detect cobalt is the large presence of iron. Spectral interference between iron and cobalt occurs due to the K_β line of iron overlapping the K_α line of cobalt (Agency, 2007). When iron is in large quantities compared to cobalt, the XRF loses its ability to detect cobalt's K_α line. The soil used in this study has an average iron concentration of 29,101 mg/kg, which would require a large adsorption of cobalt to be detectable. Bakkaus et al. (2008) determined Co(III), deposited from anthropogenic sources, was not present in the soil the eight soils tested, but suggested any Co(III) was isotopically exchanged to Co(II). Cobalt in new and non-degraded LIB is in the +3 oxidation state, thus it must undergo a reduction to Co(II) to have significant adsorption to soil (Alloway, 2019; Sasaki et al., 2008). This is a probable explanation for the lack of cobalt detected in the soil, that Co(III) has little mobility from the LIB into the soil to undergo the reduction process to be adsorbed to the soil. Cobalt has been found to have lower bioavailability for plant uptake over time because of adsorption to the soil and the formation of lower soluble forms of cobalt (Wendling et al., 2009). This may aid in the containment of cobalt contamination depending on other environmental features that may promote the more soluble forms of cobalt. Although there are no formal concentration limits set for cobalt in soil, there are guidelines made by the EPA for avian and mammalian wildlife and plants as 120 mg/kg, 230 mg/kg, and 13 mg/kg (U.S. EPA, 2005). Further research is recommended with degraded LIB that contains the reduced form, Co(II), that has a higher reactivity with adsorption sites and is the form taken up by plants to determine the contamination risk surrounding landfills and recycling centers.

The results of the soil analysis support the hypothesis of this study, concluding that copper, nickel, and manganese had higher adsorption into the basic soil compared to the acidic soil. While there will not be such a high LIB to soil ratio in landfills and recycling centers as there was in this

study, the adsorption capabilities of soil based on soil pH can be utilized for determining the severity of LIB metal contamination. The adsorption and integration of LIB metals into soil is not a static reaction that can be summed into one equation to cover all soil types. This study focused on soil pH, however, moisture and organic content, microorganisms, and specific composition of the soil will also cause variations in the severity of LIB metal contamination in soil. The adsorption rate of the LIB metals based on soil pH can be used as part of a risk assessment for proposed landfill and LIB/e-waste recycling center locations.

5.2 Water Analysis Discussion

The hypothesis for the water aspect of this study states that the leaching of LIB metals will be more significant in acidic water than in basic water, with copper and cobalt having the highest leaching concentration. The analysis of LIB metals, excluding cobalt, in pH amended water over a 24 week time period provided statistical results between the two groups ($p < 0.05$). Similar to the soil experimental results, cobalt was below detectable limits of the XRF. Overall, there was significantly more leaching of copper, manganese, and nickel metals into the acidic water compared to the basic water, while there was a significantly larger leaching of aluminum into the basic water compared to the acidic water. The best fit line for each metal was a logistic growth rate. Though this equation cannot provide adequate information for the rate constant and solubility limits, it does provide insight into the leaching trends of each LIB metal. This insight can be utilized to develop estimations on the contamination impact via leaching LIB metals have on the environment. The comparison between new LIB and post 24 week time period in the water is shown in Table A.5. The decrease in both acidic water and basic water LIB metal is consistent with the experimental results, that leaching of LIB metals occurred. There is only a slight

difference between the acidic and basic water LIB, which demonstrates a near equal dissolution ability at both pH values. Thus, the difference of LIB metals in solution between the acidic and basic water is more based on the solubility of the metal species at each pH rather than the mobility of the metal out of the LIB into solution.

Copper leaching in the acidic water was shown to be more significant compared to the basic water. At the end of 24 weeks, the average concentration of copper in the acidic water was 0.722 mg/L and in the basic water was 0.160 mg/L. These concentrations are in a static volume, whereas in the environment, there will be a dynamic volume of water, from rain runoff and river flow, which will cause a dilution. As a comparison, the surface flow in the Lianjiang River near the e-waste recycling center in Guiyu, China, with a pH of 6.44, contained an average 1.2 mg/L, while the river sediment, with a pH of 6.26, contained 1,070 mg/kg. The amount of precipitation changed the copper surface water concentration, increasing in the rainy season compared to the dry season and regular river flow, showing the copper concentration in the surface water is not at the saturation point and can contain a higher amount of copper (Guo et al., 2009; Wong et al., 2007). These concentrations in the Lianjiang River support this study because of the copper concentration in the surface water is not at the equilibrium capacity and is capable of a higher leaching threshold. The toxicity of copper is mainly due to the copper ion, which is at higher concentrations in acidic water (Control, 2011b). As pH increases, the solubility of copper decreases and copper minerals begin to precipitate out of solution. The results of this study confirm the solubility trends between acidic and basic pH while determining the leaching rate of copper for both pH groups. The best fit line used for the leaching of copper was a logistic growth rate. This reaction rate determined a rate constant of 0.236 and a solubility limit of 0.802 mg/L for acidic water and 0.173 mg/L for basic water. The rate constant value is in range of previous

literature and the decrease in the solubility limit as pH increases coincides with previous literature, though different properties of water, such as ionic strength, produce different rate constants and solubility limits (Terrones-saeta et al., 2020). The rate constant and solubility limit of copper in water can be used to estimate and predict contamination concentrations of LIB metals in water systems surrounding landfills and recycling centers. With these results, the contamination risk of copper into water systems in highest with acidic water, which acidic water runoff is common at industrial locations such as landfills and recycling centers (Mattson, 2006).

Manganese leaching in the acidic water was shown to be more significant compared to the basic waster. At the end of 24 weeks, the average concentration of manganese in the acidic water was 0.503 mg/L and in the basic water was 0.212 mg/L. The EPA concentration limit for drinking water is 0.05 mg/L, which both of pH groups surpass, though there would a dilution factor in a real water system (Control, 2012). The majority of manganese contamination studies have focused on leachate water from landfills or on soil due to e-waste centers or landfills, but not necessarily water systems near e-waste centers. However, landfill leachate into surrounding water systems is valid for comparison. A municipal solid waste site in Tepi, Ethiopia, was studied to have a manganese leachate concentration of 0.66 mg/L, where the WHO wastewater discharge limit is 0.2 mg/L. With dilution into the nearby water system, the downstream concentration was 0.4 mg/L, double the WHO limit (Mekonnen et al., 2020). Elevated level of manganese in drinking water systems have been linked to a higher prevalence of neurological disorders after chronic exposure to the drinking water (World Health Organization, 2011). Manganese is mainly transported in rivers as suspended sediments, generally as Mn(IV), due to the pH generally being neutral to slightly alkaline. However, in low dissolved oxygen waters, manganese is able to be reduced into the more soluble Mn(II) and bioaccumulate in the plants and marine life (Howe et al.,

2005). The severity of manganese leaching in this study can be used as a guide to estimate the contamination risk over time of LIB into surrounding water systems. The best fit line used for the leaching of manganese was a logistic growth rate. This reaction rate determined a rate constant of 0.236 and a solubility limit of 0.557 mg/L for acidic water and 0.216 mg/L for basic water. The rate constant value is in range of previous literature and the decrease in the solubility limit as pH increases coincides with previous literature, though different properties of water, such as ionic strength, produce different rate constants and solubility limits (Terrones-saeta et al., 2020). These solubility limits are in range with previously reported values (Duarte et al., 2015). The rate constant and solubility limit of manganese in water can be used to estimate and predict contamination concentrations of LIB metals in water systems surrounding landfills and recycling centers. The slow initial leaching may be caused by the requirement of a reducing agent for MnO_2, the manganese species in the LIB. In disposed LIB, where the oxidation state of manganese ranges from +4 to +2, there will likely be a higher leaching rate due to the soluble reduced form of manganese.

Nickel leaching in the acidic water was shown to be more significant compared to the basic water. At the end of 24 weeks, the average concentration of nickel in the acidic water was 1.159 mg/L and in the basic water was 0.067 mg/L. The leaching of nickel into water systems near landfills and recycling centers from LIB will be diluted from rain runoff and other water sources, however, the concentration of nickel may be well above set surface water guidelines and limits. The Lianjiang River near the e-waste center in Guiyu, China had a nickel concentration of 1.4 mg/L, well above the 0.02 mg/L WHO limit (Guo et al., 2009; Wong et al., 2007). The dominant nickel species in acidic water are Ni^{2+}, which has been shown to be toxic in animal studies. The less-soluble nickel species that dominate in basic water has a lower toxicity to animals because

they are less reactive to the gastrointestinal digestive processes (Control, 2011c). The best fit line used for the leaching of nickel was a logistic growth rate. This reaction rate determined a rate constant of 0.236 and a solubility limit of 1.127 mg/L for acidic water and 0.058 mg/L for basic water. The rate constant value is in range of previous literature and the decrease in the solubility limit as pH increases coincides with previous literature, though different properties of water, such as ionic strength, produce different rate constants and solubility limits (Terrones-saeta et al., 2020). These solubility limits are in range with previously reported values (González-Siso et al., 2018). The rate constant and solubility limit of nickel in water can be used to estimate and predict contamination concentrations of LIB metals in water systems surrounding landfills and recycling centers. With these results, the acidic water poses the highest contamination risk of nickel from LIB into the water systems surrounding landfills and recycling centers.

Aluminum leaching in the basic water was shown to be more significant compared to the acidic water. At the end of 24 weeks, the average concentration of aluminum in the basic water was 3.970 mg/L and in the acidic water was 1.689 mg/L. Unlike the other LIB metals that have much higher solubility in the acidic pH range than the basic pH range, aluminum solubility varies depending on pH, with free ion Al^{3+} as the dominant species in acidic water and aluminum hydroxide, $Al(OH)_4^-$. As mentioned in Chapter 4.1, Al^{3+} is bioavailable for plants, which is then toxic to the roots by preventing essential cellular functions (Bakkaus et al., 2008; Kinraide, 1990; Matsumoto, 2000; Panda et al., 2009). $Al(OH)_4^-$, though, has no known toxicity to plants (Kinraide, 1990; Kopittke et al., 2004). The results of this study show a high leaching of aluminum at both pH groups, which poses a high contamination risk for the surrounding area and water systems. Even though over 90% of the world's lakes and streams are neutral to basic pH, high concentrations of $Al(OH)_4^-$ still pose a risk because the body of water may become acidic over

time and convert it to Al^{3+}. Bodies of water are acidified via natural or anthropogenic contaminants, including organic acids from decomposing plants and erosion products from bedrock or acid rain due to air pollution and acid mine drainage (Mattson, 2006). The best fit line used for the leaching of aluminum was a logistic growth rate. This reaction rate determined a rate constant of 0.236 and a solubility limit of 1.596 mg/L for acidic water and 3.604 mg/L for basic water. The rate constant value is in range of previous literature and the decrease in the solubility limit as pH increases coincides with previous literature, though different properties of water, such as ionic strength, produce different rate constants and solubility limits (Terrones-saeta et al., 2020). These solubility limits are in range with previously reported values (Bensadok et al., 2008). The rate constant and solubility limit of aluminum in water can be used to estimate and predict contamination concentrations of LIB metals in water systems surrounding landfills and recycling centers.

Cobalt leaching into the acidic and basic water was below the detection limit by the XRF. As previously stated, this was not due to instrumental error as confirmed by measurements using water amended with LIB powder. One possible explanation for the inability to detect cobalt is the large presence of iron. Spectral interference between iron and cobalt occurs due to the K_β line of iron overlapping the K_α line of cobalt (Agency, 2007). When iron is in large quantities compared to cobalt, the XRF loses its ability to detect cobalt's K_α line. With the analysis of the LIB pieces, iron was detected, though it should not be present in the LIB. Using the standard reference material, 2709a, the XRF analysis of the LIB piece (3.42% iron) aligned with the reference sheet (3.36% iron), so the iron levels are authentic. Thus, the iron present results in the inability to detect cobalt. Leachate water from landfills and recycling centers containing cobalt poses a risk on the ecosystem in and around the water system the leachate enters. Leachate from a municipal solid

waste dumpsite near Ibadan, Nigeria was analyzed for the heavy metal content. The average pH of the leachate was 9.25 with an average cobalt concentration of 23.09 μg/L, with a WHO discharge limit of 50 μg/L (Aromolaran et al., 2019). The leachate discharge from this dumpsite and the LIB results from this study can be used for future research to determine the contamination risk of cobalt into the water systems surrounding landfills and recycling centers.

The results of the water analysis support the hypothesis of this study, concluding the acidic water caused a higher leaching rate of copper, nickel, and manganese compared to the basic water. Aluminum had a higher leaching rate in the basic water than the acidic water, presumably due to the solubility of aluminum hydroxides. The chelation and filtration process poses a risk for error because of <100% efficiency in precipitating the dissolved metals to collect onto the filter paper. If the metal species was not suitable for chelation, it may not precipitate and be included in the XRF analysis. With this said, the standard deviation values conclude that near equal chelating and filtering efficiency over all samples was achieved so the experimental results are still valid for estimating leaching ability of the LIB metals. Although this study focused on water pH, alkalinity, dissolved oxygen, dissolved organic matter, and other variables will also cause variations in the severity of LIB metal contamination in water systems. Since natural water systems have a regular water flow, such as a stream or rain runoff, there will be a dilution of the leaching values in this study. Nonetheless, the compounding of disposed LIB into the same location over time contains the same leaching risks determined in this study.

5.3 MINEQL+ Modeling Discussion

5.3.1 Soil Modeling

The MINEQL+ modeling of LIB in acidic and basic soil was able to model and predict the adsorbed species and relative abundance of copper, manganese, nickel, aluminum, and cobalt to

one another. With the pC – pH diagrams produced by MINEQL+'s two-layer model, the dominant species throughout the pH range of 4 to 10 can be reliably used to presume which metals will have the highest adsorption rate and contamination risk. MINEQL+ uses thermodynamic parameters to determine the equilibrium states of all species of interest. However, since kinetic parameters of the chemical reactions are not modeled, the timeline to reach equilibrium is not known. Equilibration can range from seconds to months because even if the reactions are thermodynamically favorable, the kinetics determine the rate of reaction (Gee & Bruland, 2002; Y. H. Li et al., 1984). MINEQL+ modeled the thermodynamic equilibrium of the system to determine the species at the pH values while the experimental results determine the rate at which equilibrium is reached.

The parameters used for this MINEQL+ model were based on previous adsorption studies in different soil and mineral content then altered with each iteration to mirror the experimental results, resulting in $LogK^1$ equaling 1 and $LogK^2$ equaling -8.2. The surface complexation constants, LogK, were relatively consistent between quartz, feldspar, and kaolinite, allowing for a simpler iteration process. The ionic strength was chosen to represent salts and other ions in the soil, yet not overwhelm the adsorption chemistry between the soil particles and metal ions. The solids concentration at 1 g/L was verified as adequate by increasing it tenfold and seeing negligible difference.

The results of modeling the adsorption of copper into acidic and basic soil confirmed the experimental results. The model shows an increase of adsorbed copper (I) and (II) ions in the higher pH range. This supports the adsorption timeline determined by the soil sample results, having a higher adsorption of copper in the basic soil. Analyzing the major species of copper in the pC – pH diagram, concludes that desorption decreases with pH because there is less

competition from protons as well as the copper ions and binding sites' strong attractive force toward one another. The XRF results of copper may not fully be adsorbed copper, as copper oxides and hydroxides precipitate out as pH increases, which are then integrating, but not necessarily binding to the soil particles (McDowell & Johnston, 1936). Nonetheless, the results from this model verifies the experimental results of a higher adsorption of copper into basic soil.

The results of modeling the adsorption of manganese into acidic and basic soil confirmed the experimental results. MINEQL+ predicted a relatively high adsorption of Mn^{3+} over the pH range 4-10, minimizing the expected difference between the acidic and basic soil groups. The remaining major species are manganese hydroxides, which begin to decrease in solubility after approximately pH 9. It can be concluded that manganese is not a severe rick for contamination due to the adsorptive capabilities to the soil as well as the manganese oxides that are very stable compounds (Hem, 1963).

The results of modeling the adsorption of nickel into acidic and basic soil confirmed the experimental results. At the end of 24 weeks, though the basic soil group had a higher concentration of nickel compared to the acidic soil group, after five weeks, each pH group has the approximately same increasing slope. The model shows this equal adsorption with the major nickel species keeping relatively the same solubility until a slight drop after pH 8. The small difference in solubility, aiding in the adsorption, supports the experimental results.

The results of modeling the adsorption of aluminum into acidic and basic soil confirmed the experimental results. Although adsorption increases at a steady pace with increasing pH, the mobility of aluminum in both basic and acidic media provides a near equal adsorption and integration into the soil, mirroring the soil sample results. Future research could be performed to identify which aluminum species dominate the integration into the soil to determine the

contamination risk. Aluminum had a very high control soil concentration, due to the aluminosilicates and other aluminum minerals naturally occurring in soil.

The results of modeling the adsorption of cobalt into acidic and basic soil is an accurate representation of the system at equilibrium. Though cobalt was not detected by the XRF in the experimental samples, this adsorption diagram will adequately predict the degree to which cobalt integrates into the soil and the mobility it has for plant uptake. Cobalt (III) had a high adsorption throughout the pH range while cobalt (II) had a lower adsorption, with a decrease in mildly alkaline soil. With this MINEQL+ model, the adsorption capabilities of this soil based on pH can be used to predict the contamination risk of cobalt at landfills and recycling centers.

The MINEQL+ modeling of the LIB in acidic and basic soil can be reliably used to predict the adsorption profile and contamination risk. Future research with MINEQL+ is recommended to predict the adsorption and contamination risk of different LIB compositions.

5.3.2 Water Modeling

The MINEQL+ modeling of the LIB in acidic and basic water was able to model and predict the soluble species and relative abundance of copper, manganese, nickel, aluminum, and cobalt to one another. With the pC – pH diagrams produced by MINEQL+, the dominant species throughout the pH range of 4 to 10 can be reliably used to presume which metals will have the highest leaching rate and contamination risk. Similarly in the adsorption rate of metals to soils, the leaching rate of metals into water is based on kinetics (Jannasch et al., 1988; Nyffeler et al., 1984). MINEQL+ modeled the thermodynamic equilibrium of the system to determine the species at the pH values while the experimental results determine the rate at which equilibrium is reached.

The parameters for ionic strength correction and the Ca^{2+} and SO_4^{2-} concentrations were chosen based on using UltraPure water that contained a small amount of alkalinity and the addition of the calcium hydroxide and sulfuric acid to amend the pH (Goldberg & Criscenti, 2007). The starting concentration of the metal ion was zero and the metal oxide was a fixed solid to represent the remaining LIB in the water. Although the nickel, cobalt, and manganese are in a lattice or layered structure with oxygen, yielding a large interconnected unit between the metals, the standard metal oxides with the correct oxidation state were used (T. Li et al., 2019) This resulted in the beginning ion concentration at pH 4 to be 1 M, or LogC = 0 on the pC – pH diagram. The comparison between MINEQL+ predicted concentration values and experimental concentration values for acidic and basic water are in Figures A.15 and A.16, respectively. The disparities between the model and experimental values may be due to the metal oxides chosen as the fixed solids, which may have influenced the overall solubility of other metal compounds that were not necessarily considered by MINEQL+. MINEQL+ may not always have every component and species available to consider, thus the model concentrations may be higher or lower than experimental values (Tran, 2016). In this study's comparison, certain metal species may not have been considered that have a higher solubility than the species used in the model. In addition to this, though UltraPure water was used, there may have been unknown dissolved species to affect the solubility of these metals, causing a difference between the MINEQL+ model and experimental results. Although solubility relies on temperature, common ion effect, redox potential, and other parameters in addition to pH, MINEQL+ models are beneficial to predict solubility products in specific environments.

The results of modeling the leaching of copper into acidic and basic water confirmed the experimental results. The solubility of Cu(II) is highest in acidic water, mainly in the form of free

Cu^{2+}. There are dissolved copper minerals at the low pH range, however, they are thermodynamically stable and not capable to be taken up by plants (Control, 2011b; Dabinett et al., 2008). As the pH increases, $[Cu^{2+}]$ decreases and $[Cu(OH)^{-}]$ increases because of the additional hydroxide ions. However, the solubility of $Cu(OH)^{-}$ is much lower than free Cu^{2+}, so the overall soluble Cu^{2+} concentration decreases. The water based LIB leaching experimental results align with the MINEQL+ pC – pH diagram because the concentration of soluble copper was much higher in the acidic water compared to the basic water. The pC – pH diagram can be used in the prediction of major copper species at a certain pH to aid in the LIB contamination risk assessment.

The results of modeling the leaching of manganese into acidic and basic water confirmed the experimental results. MINEQL+ does not have Mn(IV), the oxidation state in new LIB, preloaded on the components list; therefore, the reduction of Mn(IV) to Mn(II) was modeled to determine the availability of Mn(II) for the formation of all potential manganese species. The reduction reaction and LogK value used were provided by Matsunaga et al., (1993), as MnO_2 converting to Mn^{2+} ion and LogK value of -0.13. The model results showing the reduction occurring at all pH values allow the use of Mn(II) and Mn(III) in solution to determine the extent of leaching into the water. The pC – pH diagram shows a higher concentration of Mn(II) in acidic water while there is an increase in Mn(II) hydroxides and the total percent of Mn(III) increases as the pH increases. This exchange between free Mn(II) ions and free Mn(III) ions reduces the availability to plants, preventing accumulation and toxic effects (Control, 2012). The experimental results show a higher concentration of manganese at the acidic pH, concluding that LIB manganese contamination risk can be accurately predicted with this pC – pH diagram.

The results of modeling the leaching of nickel into acidic and basic water confirmed the experimental results. The solubility of Ni(II) is highest in acidic water, dominantly as free Ni^{2+}. The MINEQL+ model shows dissolved nickel minerals at the low pH, however, they are thermodynamically stable and not taken up by plants (Control, 2011c). As pH increases, solubility decreases for most nickel species, precipitating into the sediment. As the pH holds in the alkaline range, nickel does not pose an immediate risk to the plants and animals that use the water system. Over a large portion of the pH range, nickel poses a contamination risk through leaching into the water systems.

The results of modeling the leaching of aluminum into acidic and basic water were considerably different. The pC – pH diagram predicted a solubility of total Al^{3+} in the acidic water higher than the basic water, though that was not the case with the experimental results. The possibility of the acidic water having a lower experimental result than the model may be due to the APDC not chelating all of the aluminum ionic compounds in the solution. Previous literature for aluminum pC – pH diagrams with sulfate included confirm the MINEQL+ model in this study is correct (Cravotta, 2006). Future research to replicate the experimental results to confirm the solubility differences with the model would be needed. Nonetheless, the pC – pH diagram can be used in the prediction of major aluminum species at a certain pH to aid in the LIB contamination risk assessment.

The results of modeling the leaching of cobalt into acidic and basic water is an accurate representation of the system at equilibrium. Though cobalt was not able to be detected by the XRF in the experimental samples, this pC – pH diagram will adequately predict the major cobalt species. The oxidation state of cobalt on this diagram is only Co(II), because Co(III) is over Log10 less in concentration, supporting the work of Bakkaus et al., 2008. As with the other LIB metals, cobalt

has a higher solubility in acidic conditions, with the mainly in the form of free Co^{2+}. As pH increases, cobalt hydroxides become prevalent, diminishing the potential toxicity to vegetation and animals (Control, 2011a; Palit et al., 1994). The pC – pH diagram can be used in the prediction of major cobalt species at a certain pH to aid in the LIB contamination risk assessment.

The combination of each LIB metal into a single model produced the total metal ion concentration over the pH range. This combination model compares the leaching risk of each metal to one another normalized to the same beginning concentration. The two highest leaching risk at pH 10 according to the model aluminum and manganese, which align with the experimental results. MINEQL+ is a powerful tool to aid in the modeling of experimental results and the prediction of end results with potential variable changes. The concentration of metals in the LIB require consideration because they vary between each other, causing the MINEQL+ model to have a qualitative conclusion on the leaching and contamination risk these metals possess.

Chapter VI: Conclusions and Future Work

6.1 Conclusions

The increased use of LIB in everyday life from cell phones, electric vehicles, and power storage creates a greater need to safely dispose and recycle them when they reach their end of life. This need can be resolved with a proactive approach by municipalities to prevent LIB entering the municipal waste systems, a curbing of illegal dumpsites, and improved transport and recycling techniques to prevent contamination of the areas surrounding the recycling centers (Agency, 1987; Alloway, 2019; Garthe & Swistock, 2005; Timpane, 2018). The metal contamination from electronic waste and other types of batteries has been well documented to cause detrimental environmental and human health effects (Aral & Vecchio-Sadus, 2008; Brewer, 2010; Klotz et al., 2017; McCauley et al., 2017). Analyses have been performed on the soil and water systems surrounding landfills and e-waste recycling centers to determine the contamination that had occurred up to that time point. However, long term analysis on the leaching and adsorption rate of LIB into water and soil based on pH has not been completed. This study successfully determines the leaching and adsorption rate for copper, manganese, nickel, and aluminum from NMC LIB.

To reiterate, the first hypothesis for this study states that the integration and adsorption of LIB metals (manganese, cobalt, nickel, aluminum, and copper) into pH amended soil over a 24 week time period will be more significant in basic soil than acidic soil. Specifically, the copper and nickel will have the highest adsorption rates onto the soil compared to the other metals, notably at the basic pH range.

The second hypothesis for this study states that the dissolution of LIB metals into pH amended water over a 24 week time period will be more significant in acidic water than basic

water. Specifically, cobalt and copper will have a higher leaching rate in the acidic water compared to the other metals.

6.1.1 Adsorption Rate of Li-ion Batteries into Soil

The adsorption of LIB metals over a 24 week period provides essential insight on the contamination risk of improperly disposed LIB. When normalized to the control soils, copper and nickel had the highest adsorption into the soil, however, aluminum had the highest adsorption outright and cobalt was below detectible limits for all time periods. Aluminum had a higher surface area compared to the other metals that share the same surface area as well as aluminum not being constrained by the oxide lattice or layering configuration in which nickel, manganese, and cobalt exist. Overall, the higher adsorption and integration rate of LIB metals into basic soil will reduce their mobility and availability for plant uptake and animal consumption.

6.1.2 Leaching Rate of Li-ion Batteries into Water

The leaching of LIB metals over a 24 week period will aid in the identification of potential contaminated water systems surrounding landfills and recycling centers. Excluding cobalt due to being below detection limit, every LIB metal had significant leaching, well above some concentration limits set by the EPA and WHO. Copper, nickel, and manganese all had a significantly higher leaching rate when comparing acidic to basic conditions. Aluminum had a higher leaching rate in the basic water compared to the acidic water.

6.1.3 Comparison of MINEQL+ Model to Sample Data

MINEQL+ successfully modeled the soil and water groups used in this study with pC – pH diagrams of individual metals as well as the LIB metals in one reaction simulation to view any reaction competition between them that will alter the solubility and adsorption abilities. The model is capable of predicting the integration of LIB metals into the soil and the leaching based on water pH. The surface complexation constants, $LogK^1$ and $LogK^2$, were confirmed to match previous literature, as 1 and -8.2, respectively. Determining the values for this soil will provide future opportunities of research and modeling equilibrium reactions.

6.1.4 Final Comments

Based on this study, future research is needed to measure and create a leaching and adsorption rate for cobalt in acidic and basic conditions. Though solubility and adsorption trends and isotherms are known for the heavy metals that compose LIB and other electronic products, the severity of the product's leaching and adsorption into the environment needs to be evaluated. With the diverse metal composition and configuration of electronics and batteries, the metal leaching into the environment will differ, potentially increasing leaching into the ecosystem or create stabilized compounds with soil minerals to prevent the toxic side effects of the metals. The results from this study conclude the severity LIB can have on the environment, the need for LIB to avoid landfills, and for LIB to be recycled and processed properly to reduce contamination of the areas surrounding the recycling centers.

References

Abe, W., Isaka, S., Koike, Y., Nakano, K., Fujita, K., & Nakamura, T. (2006). *X-ray fluorescence analysis of trace metals in environmental water using preconcentration with an iminodiacetate extraction disk. 35*, 184–189. https://doi.org/10.1002/xrs.892

Acidifying the Soil. (2012). University of California Agriculture and Natural Resources.

Afolayan, A. O. (2018). Accumulation of Heavy Metals from Battery Waste in Topsoil, Surface Water, and Garden Grown Maize at Omilende Area, Olodo, Nigeria. *Global Challenges*, *2*(3), 1700090. https://doi.org/10.1002/gch2.201700090

Agency, E. P. (1982). *Hazardous Waste Management System; Standards Applicable to Owners and Operators of Hazardous Waste Treatment, Storage and Disposal Facilities; and EPA Administered Permit Programs* (Vol. 47, Issue 143).

Agency, E. P. (1987). *Liners and leak detection for hazardous waste land disposal units* (Vol. 52, Issue 103).

Agency, E. P. (2007). Field portable X-ray fluorescence for the determination of elemental concentrations in soil and sediment. In *Environmental Protection Agency* (Issue February).

Al-Hamdan, A. Z., & Reddy, K. R. (2008). Transient behavior of heavy metals in soils during electrokinetic remediation. *Chemosphere*, *71*(5), 860–871. https://doi.org/10.1016/j.chemosphere.2007.11.028

Alloway, B. J. (2019). Heavy Metals in Soils. In *Natural Resources in U.S.-canadian Relations, Volume 2: Patterns and Trends in Resource Supplies and Policies* (3rd Editio, Vol. 2). Springer. https://doi.org/10.4324/9780429051340-10

Alva, A. (1999). Soil pollution. In *Environmental Geology. Encyclopedia of Earth Science*.

Springer.

Aral, H., & Vecchio-Sadus, A. (2008). Toxicity of lithium to humans and the environment-A literature review. *Ecotoxicology and Environmental Safety*, *70*(3), 349–356. https://doi.org/10.1016/j.ecoenv.2008.02.026

Aromolaran, O., Fagade, O. E., Aromolaran, O. K., Faleye, E. T., & Faerber, H. (2019). Assessment of groundwater pollution near Aba-Eku municipal solid waste dumpsite. *Environmental Monitoring and Assessment*, *191*(12). https://doi.org/10.1007/s10661-019-7886-1

Bakkaus, E., Collins, R. N., Morel, J. L., & Gouget, B. (2008). Potential phytoavailability of anthropogenic cobalt in soils as measured by isotope dilution techniques. *Science of the Total Environment*, *406*(1–2), 108–115. https://doi.org/10.1016/j.scitotenv.2008.07.042

Bastos, R. O., Melquiades, F. L., & Biasi, G. E. V. (2012). Correction for the effect of soil moisture on in situ XRF analysis using low-energy background. *X-Ray Spectrometry*, *41*, 304–307.

Beckingham, L. E., Mitnick, E. H., Steefel, C. I., Zhang, S., Voltolini, M., Alexander, M., Yang, L., Cole, D. R., Sheets, J. M., Ajo-franklin, J. B., Depaolo, D. J., & Mito, S. (2016). Evaluation of mineral reactive surface area estimates for prediction of reactivity of a multi-mineral sediment. *Geochimica et Cosmochimica Acta*, *188*, 310–329.

Bensadok, K., Benammar, S., Lapicque, F., & Nezzal, G. (2008). Electrocoagulation of cutting oil emulsions using aluminum plate electrodes. *Journal of Hazardous Materials*, *452*, 423–430.

Bradl, H. B. (2004). Adsorption of heavy metal ions on soils and soils constituents. *Journal of Colloid and Interface Science*, *277*(1), 1–18. https://doi.org/10.1016/j.jcis.2004.04.005

Brewer, G. J. (2010). Risks of copper and iron toxicity during aging in humans. *Chemical Research in Toxicology*, *23*(2), 319–326. https://doi.org/10.1021/tx900338d

BU-205: Types of Lithium-ion. (2019). Battery University. https://batteryuniversity.com/index.php/learn/article/types_of_lithium_ion

Carter, M. R. (1993). *Soil Sampling and Methods of Analysis* (M. R. Carter (Ed.)). Lewis Publishers.

Casalegno, C., Schifanella, O., Zennaro, E., Marroncelli, S., & Chemservice, S. (2015). Collate literature data on toxicity of Chromium (Cr) and Nickel (Ni) in experimental animals and humans 1. *European Food Safety Authority*, *12*(2). https://doi.org/10.2903/sp.efsa.2015.EN-478

Control, C. for D. (2011a). Toxicological profile for cobalt. In *Center for Disease Control*.

Control, C. for D. (2011b). Toxicological profile for copper. In *Center for Disease Control*. https://doi.org/10.1201/9781420061888_ch123

Control, C. for D. (2011c). Toxicological profile for nickel. In *Center for Disease Control*.

Control, C. for D. (2012). *Toxicological profile for manganese*.

Coronel, E. G., Bair, D. A., Brown, C. T., & Terry, R. E. (2014). Utility and limitations of portable X-ray fluorescence and field laboratory conditions on the geochemical analysis of soils and floors at areas of known human activities. *Soil Science*, *175*(5), 258–271. https://doi.org/10.1097/SS0000000000000067

Council, N. R. (2007). Assessment of the Performance of Engineered Waste Containment Barriers. In *The National Academies Press*. The National Academies Press. https://doi.org/10.17226/11930

Cravotta, C. A. (2006). Relations among pH, sulfate, and metals concentrations in Anthracite and

Bituminous coal-mine discharges, Pennsylvania. *Journal of the American Society of Mining and Reclamation, 1*, 378–404. https://doi.org/10.21000/jasmr06020378

Crook, V., Simpson, P., Rawson, B., & Wake, D. (2006). Investigation of PXRF procedures for measuring contaminated land. *Health and Safety Laboratory*, *102*, 49.

Crozier, C., & Hardy, D. (2018). *Soil acidity and liming: Basic information for farmers and gardeners*. NC State Extension Publications.

Dabinett, T., Humberstone, D., Leverett, P., & Williams, P. (2008). Synthesis and stability of wroewolfeite, Cu4SO4(OH)6.2H2O. *Pure and Applied Chemistry*, *80*(6), 1317–1323.

Davis, M. K., Jackson, T. L., Shackley, M. S., Teague, T., & Hampel, J. H. (2011). Chapter 3: Factors affecting the energy-dispersive X-ray fluorescence (EDXRF) analysis of archaeological obsidian. In *X-ray Fluorescence Spectrometry (XRF) in Geoarchaeology* (pp. 45–63). Springer Press.

DeLaune, R. D., Reddy, K. R., Richardson, C. J., & Megonigal, J. P. (2013). Soil Redoc Potential and pH Controllers. In *Methods in Biogeochemistry of Wetlands* (pp. 107–116).

Deverel, S. J., & Fujii, R. (2012). Chemistry of trace elements in soils and ground water. In *American Society of Civil Engineers, Manuals and Reports on Engineering Practice* (pp. 89–137).

Duarte, R. S., Lima, R. M. F., & Leao, V. A. (2015). Effect of inorganic and organic depressants on the cationic flotation and surface charge of rhodonite-rhodochrosite. *Mining*, *68*(4), 463–469.

Fan, Q., Li, P., & Pan, D. (2019). Radionuclides sorption on typical clay minerals: Modeling and spectroscopies. *Interface Science and Technology*, *29*, 1–38.

Fischer, J. (1999). Soil Taxonomy A Basic System of Soil Classification for Making and

Interpreting Soil Surveys. In USDA (Ed.), *Soil Survey Staff* (2nd ed.). U.S. Government Printing Office.

Foxboro. (1999). *Conductivity ordering guide* (pp. 1–2).

Fujimori, T., Eguchi, A., Agusa, T., Tue, N. M., Suzuki, G., Takahashi, S., Viet, P. H., Tanabe, S., & Takigami, H. (2016). Lead contamination in surface soil on roads from used lead–acid battery recycling in Dong Mai, Northern Vietnam. *Journal of Material Cycles and Waste Management*, *18*(4), 599–607. https://doi.org/10.1007/s10163-016-0527-7

Fujimori, T., & Takigami, H. (2014). Pollution distribution of heavy metals in surface soil at an informal electronic-waste recycling site. *Environmental Geochemistry and Health*, *36*(1), 159–168. https://doi.org/10.1007/s10653-013-9526-y

Garthe, J. W., & Swistock, B. R. (2005). Roadside dumps and water quality. *Penn State College of Agricultural Sciences*, 1–27.

Gee, A. K., & Bruland, K. W. (2002). Tracing Ni, Cu, and Zn kinetics and equilibrium partitioning between dissolved and particulate phases in South San Francisco Bay, California, using stable isotopes and high-resolution inductively coupled plasma mass spectrometry. *Geochimica et Cosmochimica Acta*, *66*(17), 3063–3083. https://doi.org/10.1016/S0016-7037(02)00907-9

Goldberg, S., & Criscenti, L. (2007). Modeling adsorption of metals and metalloids by soil components. In *Biophysico-Chemical Processes of Heavy Metals and Metalloids in Soil Environments* (pp. 216–252).

González-Siso, M. R., Gaona, X., Duro, L., Altmaier, M., & Bruno, J. (2018). Thermodynamic model of Ni(II) solubility, hydrolysis and complex formation with ISA. *Radiochimica Acta*, *106*(1), 31–45. https://doi.org/10.1515/ract-2017-2762

Gordeeva, V. P., Statkus, M. A., Tsysin, G. I., & Zoloto, Y. A. (2003). X-ray fluorescence determination of As , Bi , Co , Cu , Fe , Ni , Pb , Se , V and Zn in natural water and soil extracts after preconcentration of their pyrrolidinedithiocarbamates on cellulose filters. *Talanta*, *61*(3), 315–329. https://doi.org/10.1016/S0039-9140(03)00271-6

Gu, F., Guo, J., Yao, X., Summers, P. A., Widijatmoko, S. D., & Hall, P. (2017). An investigation of the current status of recycling spent lithium-ion batteries from consumer electronics in China. *Journal of Cleaner Production*, *161*, 765–780. https://doi.org/10.1016/j.jclepro.2017.05.181

Guilarte, T. (2010). Review Manganese and Parkinson ' s Disease : A critical review and new findings. *Environmental Health Perspectives*, *118*(8), 1071–1080. https://doi.org/10.1289/ehp.0901748

Guo, Y., Huang, C., Zhang, H., & Dong, Q. (2009). Heavy Metal Contamination from Electronic Waste Recycling at Guiyu, Southeastern China. *Journal of Environmental Quality*, *38*(4), 1617–1626. https://doi.org/10.2134/jeq2008.0398

He, G., Zhang, Z., Wu, X., Cui, M., Zhang, J., & Huang, X. (2020). Adsorption of heavy metals on soil collected from lixisol of typical karst areas in the presence of CaCO3 and soil clay and their competition behavior. *Sustainability*, *12*(18). https://doi.org/10.3390/SU12187315

Hem, J. (1963). Chemical equilibria and rates of manganese oxidation - Chemistry of Manganese in Natural Water. *US Geological Survey Water-Supply Paper 1667-A*, 71. https://pubs.usgs.gov/wsp/1667a/report.pdf

Howe, P. D., Malcom, H. M., & Dobson, D. (2005). Manganese and its compounds: Environmental aspects. In *World Health Organization*.

IAEA. (1997). *Sampling , storage and sample preparation procedures for X ray fluorescence analysis of environmental materials* (Vol. 2, Issue June).

Jacoby, M. (2019). It's time to get serious about recycling lithium-ion batteries. *Chemical & Engineering News*, volume 97, issue 28. https://cen.acs.org/materials/energy-storage/time-serious-recycling-lithium/97/i28

Jang, Y. C., & Townsend, T. G. (2003). Leaching of lead from computer printed wire boards and cathode ray tubes by municipal solid waste landfill leachates. *Environmental Science and Technology*, *37*(20), 4778–4784. https://doi.org/10.1021/es034155t

Jannasch, H. W., Honeyman, B. D., Balistrieri, L. S., & James W., M. (1988). Kinetics of trace element uptake by marine particles. *Geochimica et Cosmochimica Acta*, *52*(2), 567–577. https://doi.org/10.1016/0016-7037(88)90111-1

Jones, C., & Olson-Rutz, K. (2020). *Soil acidification: problems, causes, & testing*. Montana State University. https://landresources.montana.edu/soilfertility/documents/PDF/sscoop/SoilAcidifProbCauseTestSS.pdf

Kanchi, S., Singh, P., & Bisetty, K. (2014). Dithiocarbamates as hazardous remediation agent: A critical review on progress in environmental chemistry for inorganic species studies of 20th century. *Arabian Journal of Chemistry*, *7*(1), 11–25. https://doi.org/10.1016/j.arabjc.2013.04.026

Karlen, D. L. (2005). Productivity. In *Encyclopedia of Soils in the Environment* (pp. 330–336). Academic Press.

Kilbride, C., Poole, J., & Hutchings, T. R. (2006). A comparison of Cu, Pb, As, Cd, Zn, Fe, Ni and Mn determined by acid extraction/ICP-OES and ex situ field portable X-ray

fluorescence analyses. *Environmental Pollution*, *143*(1), 16–23. https://doi.org/10.1016/j.envpol.2005.11.013

Kinraide, T. B. (1990). Assessing the rhizotoxicity of the aluminate ion, Al(OH)4-. *Plant Physiology*, *94*, 1620–1625.

Klotz, K., Weistenhöfer, W., Neff, F., Hartwig, A., Thriel, C. Van, & Drexler, H. (2017). The Health Effects of Aluminum Exposure. *Deutsches Ärzteblatt International*, *114*(39), 653–660. https://doi.org/10.3238/arztebl.2017.0653

Kopittke, P. M., Menzies, N. W., & Blamey, F. P. C. (2004). Rhizotoxicity of aluminate and polycationic aluminium at high pH. *Plant and Soil*, *266*, 177–186. https://doi.org/10.1007/s11104-005-2229-0

Kumar, S., & Trivedi, A. V. (2016). A Review on Role of Nickel in the Biological System. *International Journal of Current Microbiology and Applied Sciences*, *5*(3), 719–727. https://doi.org/10.20546/ijcmas.2016.503.084

Lerner, D. (1999). Pollution, scientific aspects. In *Environmental Geology. Encyclopedia of Earth Science*. Springer.

Leyssens, L., Vinck, B., Straeten, C. Van Der, Wuyts, F., & Maes, L. (2017). Cobalt toxicity in humans — A review of the potential sources and systemic health e ff ects. *Toxicology*, *387*(May), 43–56. https://doi.org/10.1016/j.tox.2017.05.015

Li, J., Duan, H., & Shi, P. (2011). Heavy metal contamination of surface soil in electronic waste dismantling area: Site investigation and source-apportionment analysis. *Waste Management and Research*, *29*(7), 727–738. https://doi.org/10.1177/0734242X10397580

Li, M., Yang, B., Zhang, Z., Wang, L., & Zhang, Y. (2013). Polymer gel electrolytes containing sulfur-based ionic liquids in lithium battery applications at room temperature. *Journal of*

Applied Electrochemistry, *43*(5), 515–521. https://doi.org/10.1007/s10800-013-0535-4

Li, T., Yuan, X.-Z., Zhang, L., Song, D., Shi, K., & Bock, C. (2019). Degradation Mechanisms and Mitigation Strategies of Nickel-Rich NMC-Based Lithium-Ion Batteries. In *Electrochemical Energy Reviews* (Vol. 3, Issue 1). Springer Singapore. https://doi.org/10.1007/s41918-019-00053-3

Li, Y. H., Burkhardt, L., Buchholtz, M., O'Hara, P., & Santschi, P. H. (1984). Partition of radiotracers between suspended particles and seawater. *Geochimica et Cosmochimica Acta*, *48*(10), 2011–2019. https://doi.org/10.1016/0016-7037(84)90382-X

Lin, F., Markus, I. M., Doeff, M. M., & Xin, H. L. (2014). Chemical and structural stability of lithium-ion battery electrode materials under electron beam. *Scientific Reports*, *4*, 1–6. https://doi.org/10.1038/srep05694

Lin, J. (2009). *Performance of the Thermo Scientific Niton XRF Analyzer: The effects of particle size, length of analysis, water, organic matter, and soil chemistry*. University of California, Berkeley.

Magdaleno, A., De Cabo, L., Arreghini, S., & Salinas, C. (2014). Assessment of heavy metal contamination and water quality in an urban river from Argentina. *Brazilian Journal of Aquatic Science and Technology*, *18*(1), 113. https://doi.org/10.14210/bjast.v18n1.p113-120

Mailloux, R., Lemire, J., & Appanna, V. (2011). Hepatic response to aluminum toxicity: Dyslipidemia and liver diseases. *Experimental Cell Research*, *317*(16), 2231–2238. https://doi.org/10.1016/j.yexcr.2011.07.009

Mamindy-Pajany, Y., Sayen, S., Mosselmans, J. F. W., & Guillon, E. (2014). Copper, nickel and zinc speciation in a biosolid-amended soil: PH adsorption edge, μ-XRF and μ-XANES

investigations. *Environmental Science and Technology*, *48*(13), 7237–7244. https://doi.org/10.1021/es5005522

Mao, J., Liu, X., Chen, B., Luo, F., Wu, X., Jiang, D., & Luo, Z. (2017). Determination of heavy metals in soil by inductively coupled plasma mass spectrometry (ICP-MS) with internal standard method. *Electronics Science Technology and Application*, *4*(1), 23–31. https://doi.org/10.18686/esta.v4i1.36

Massoura, S. T., Echevarria, G., Becquer, T., Ghanbaja, J., Leclere-Cessac, E., & Morel, J. L. (2006). Control of nickel availability by nickel bearing minerals in natural and anthropogenic soils. *Geoderma2*, *136*, 28–37.

Matsumoto, H. (2000). Cell biology of aluminum toxicity tolerance in higher plants. *International Review of Cytology*, *200*, 1–46. https://doi.org/10.1016/s0074-7696(00)00001-2

Matsunaga, T., Karametaxas, G., von Gunten, H. R., & Lichtner, P. C. (1993). Redox chemistry of iron and manganese minerals in river-recharged aquifers: A model interpretation of a column experiment. *Geochimica et Cosmochimica Acta*, *57*(8), 1691–1704. https://doi.org/10.1016/0016-7037(93)90107-8

Mattson, M. D. (2006). Acid lakes and rivers. In *Environmental Geology. Encyclopedia of Earth Science* (pp. 6–9). Springer. https://doi.org/10.1007/1-4020-4494-1_4

McCauley, A., Jones, C., & Olson-Rutz, K. (2017). Soil pH and organic matter. In *Nutrient Management* (Issue 8, pp. 1–16).

McCumber, A., & Strevett, K. A. (2017). A geospatial analysis of soil lead concentrations around regional Oklahoma airports. *Chemosphere*, *167*, 62–70. https://doi.org/10.1016/j.chemosphere.2016.09.127

McDowell, L., & Johnston, H. (1936). The solubility of cupric oxide in alkali and the second dissociation constant of cupric acid. The analysis of very small amounts of copper. *Journal of the American Society of Mining and Reclamation*, *58*(10), 2009–2014.

Mehus, B., & Leroy, J. (2018). *Acute and chronic lithium toxicity*. American College of Emergency Physicians. https://www.acep.org/how-we-serve/sections/toxicology/news/august-2016/acute-and-chronic-lithium-toxicity/?_t_id=s_yGUswORhc9StQ823xZag%3D%3D&_t_q=lithium toxicity&_t_tags=andquerymatch,language:en%7Clanguage:7D2DA0A9FC754533B091FA6886A51C0D,siteid:3f8e28

Mekonnen, B., Haddis, A., & Zeine, W. (2020). Assessment of the Effect of Solid Waste Dump Site on Surrounding Soil and River Water Quality in Tepi Town, Southwest Ethiopia. *Journal of Environmental and Public Health, 2020*. https://doi.org/10.1155/2020/5157046

Millaleo, R., Reyes-Díaz, M., Ivanov, A. G., Mora, M. L., & Alberdi, M. (2010). Manganese as essential and toxic element for plants: Transport, accumulation and resistance mechanisms. *Journal of Soil Science and Plant Nutrition*, *10*(4), 476–494. https://doi.org/10.4067/s0718-95162010000200008

Minamisawa, M., Minamisawa, H., Yoshida, S., & Takai, N. (2004). Adsorption behavior of heavy metals on biomaterials. *Journal of Agricultural and Food Chemistry*, *52*(18), 5606–5611. https://doi.org/10.1021/jf0496402

Muhammad, R. H., Hassan, U. F., Mahmoud, A. A., Baba, H., Hassas, H. F., Madaki, A. A., & Madaki, A. I. (2020). Heavy metals suitability in irrigation water sources of Bauchi Suburb, Bauchi State, Nigeria. *International Journal of Research and Scientific*

Innovation, *7*(4), 216–221.

Nelson, D. W., & Sommers, L. E. (1996). Total Carbon, Organic Carbon, and Organic Matter. In *Methods of Soil Analysis: Part 3 Chemical Methods* (pp. 1001–1006). Soil Science Society of America, Inc.

Nyffeler, U. P., Li, Y. H., & Santschi, P. H. (1984). A kinetic approach to describe trace-element distribution between particles and solution in natural aquatic systems. *Geochimica et Cosmochimica Acta*, *48*(7), 1513–1522. https://doi.org/10.1016/0016-7037(84)90407-1

Olin, M., & Lehikoinen, J. (1997). *Application of surface complexation modelling :*

Orescanin, V., Mikelic, L., Roje, V., & Lulic, S. (2006). Determination of lanthanides by source excited energy dispersive X-ray fluorescence (EDXRF) method after preconcentration with ammonium pyrrolidine dithiocarbamate (APDC). *Analytica Chimica Acta*, *570*(2), 277–282. https://doi.org/10.1016/j.aca.2006.04.028

Orwat, K., Bernard, P., & Migdal-Mikuli, A. (2016). Obtaining and investigating amphoteric properties of aluminum oxide in a hands-on laboratory experiment for high school students. *Journal of Chemical Education*, *93*(5), 906–909.

Osmani, M., Bani, A., & Hoxha, B. (2015). Heavy Metals and Ni Phytoextractionin in the Metallurgical Area Soils in Elbasan. *Albanian j. Agric. Sci. 2015;14*, *14*(4), 414–419. https://www.researchgate.net/publication/304347101_Heavy_Metals_and_Ni_Phytoextractionin_in_the_Metallurgical_Area_Soils_in_Elbasan

Palit, S., Sharma, A., & Talukder, G. (1994). Effects of cobalt on plants. *The Botanical Review*, *60*(2), 149–181. https://doi.org/10.1007/BF02856575

Panda, S. K., Baluska, F., & Matsumoto, H. (2009). Aluminum stress signaling in plants. *Plant Signaling & Behavior*, *4*(7), 592–597.

Pearson, D., Chakraborty, S., Duda, B., Li, B., Weindorf, D. C., Deb, S., Brevik, E., & Ray, D. P. (2017). Water analysis via portable X-ray fluorescence spectrometry. *Journal of Hydrology*, *544*(November), 172–179. https://doi.org/10.1016/j.jhydrol.2016.11.018

Peng, Y. Z., Huang, Y. M., Yuan, D. X., Li, Y., & Gong, Z. Bin. (2012). Rapid analysis of heavy metals in coastal seawater using preconcentration with precipitation/co-precipitation on membrane and detection with X-ray fluorescence. *Fenxi Huaxue/ Chinese Journal of Analytical Chemistry*, *40*(6), 877–882. https://doi.org/10.1016/S1872-2040(11)60554-9

Perry, J. R., & Dorian, G. (1987). *Characterization of MWC ashes and leachates from MSW landfills, monofills, and co-disposal sites.*

Petrology of Banzet Lithologies. (1989). Kansas Geological Survey.

Pradzynski, A. H., Henry, R. E., & Stewart, J. S. (1976). Determination of ppb concentrations of transition metals by radioisotope-excited energy-dispersive. *Journal of Radioanalytical Chemistry*, *32*, 219–228.

Reddivari, S. (2016). *Electrode-electrolyte Interface Layers in Lithium Ion Batteries using Reactive Force Field Based Molecular Dynamics.* 1–131. https://deepblue.lib.umich.edu/handle/2027.42/133380

Reich, T. J., Das, S., Koretsky, C. M., Lund, T. J., & Landry, C. J. (2010). Surface complexation modeling of Pb(II) adsorption on mixtures of hydrous ferric oxide, quartz and kaolinite. *Chemical Geology*, *275*(3–4), 262–271. https://doi.org/10.1016/j.chemgeo.2010.05.017

Richter, C. (2015). *Sorption of environmentally relevant radionuclides (U(VI), Np(V)) and lanthanides (Nd)III)) on feldspar and mica*. Technischen Universitat Dresden.

Rivera-Mancía, S., Ríos, C., & Montes, S. (2011). Manganese accumulation in the CNS and associated pathologies. *BioMetals*, *24*(5), 811–825. https://doi.org/10.1007/s10534-011-

9454-1

Rodgher, S., Espíndola, E. L. G., Simões, F. C. F., & Tonietto, A. E. (2012). Cadmium and chromium toxicity to pseudokirchneriella subcapitata and microcystis aeruginosa. *Brazilian Archives of Biology and Technology*, *55*(1), 161–169. https://doi.org/10.1590/S1516-89132012000100020

Rodrigues dos Santos, F., de Almeida, E., da Cunha Kemerich, P. D., & Melquiades, F. L. (2017). Evaluation of metal release from battery and electronic components in soil using SR-TXRF and EDXRF. *X-Ray Spectrometry*, *46*(6), 512–521. https://doi.org/10.1002/xrs.2784

Rouillon, M., & Taylor, M. P. (2016). Can field portable X-ray fluorescence (pXRF) produce high quality data for application in environmental contamination research? *Environmental Pollution*, *214*, 255–264. https://doi.org/10.1016/j.envpol.2016.03.055

Sahraoui, H., & Hachicha, M. (2016). Determination of trace elements in mine soil samples using portable X-ray fluorescence spectrometer : A comparative study with ICP-OES Determination of trace elements in mine soil samples using portable X-ray fluorescence. *KKU Engineering Journal*, *43*(September), 162–165. https://doi.org/10.14456/kkuenj.2016.24

Sasaki, K., Matsuda, M., Urata, T., Hirajima, T., & Konno, H. (2008). Sorption of Co2+ ions on the biogenic Mn oxide produced by a Mn-oxidizing fungus, Paraconiothyium sp. *Materials Transactions*, *49*, 605–611.

Schecher, W. D., & McAvoy, D. C. (2015). MINEQL+ Chemical Equilibrium Modeling System. In *Environmental Research Software* (Vol. 5). Environmental Research Software.

Schipper, F., Dixit, M., Kovacheva, D., Talianker, M., Haik, O., Grinblat, J., Erickson, E. M.,

Ghanty, C., Major, D. T., Markovsky, B., & Aurbach, D. (2016). Stabilizing nickel-rich layered cathode materials by a high-charge cation doping strategy: zirconium-doped LiNi0.6Co0.2Mn0.2O2. *Journal of Materials Chemistry A: Materials for Energy and Sustainability*, *41*, 1–12. https://doi.org/10.1039/C6TA06740A

Schneider, A. R., Cancès, B., Breton, C., Ponthieu, M., Morvan, X., Conreux, A., & Marin, B. (2016). Comparison of field portable XRF and aqua regia/ICPAES soil analysis and evaluation of soil moisture influence on FPXRF results. *Journal of Soils and Sediments*, *16*(2), 438–448. https://doi.org/10.1007/s11368-015-1252-x

Shackley, M. S. (2018). X-Ray fluorescence spectrometry (XRF). *The Encyclopedia of Archaeological Sciences*, 1–5. https://doi.org/10.1002/9781119188230.saseas0620

Sharifi-asl, S., Lu, J., Amine, K., & Shahbazian-Yassar, R. (2019). Oxygen release degradation in Li-ion battery cathode materials: mechanisms and mitigating approaches. *Advanced Energy Materials*, *9*(22). https://doi.org/10.1002/aenm.201900551

Sharma, R., Raghav, S., Nair, M., & Kumar, D. (2018). Kinetics and adsorption studies of mercury and lead by ceria nanoparticles entrapped in tamarind powder. *ACS Omega*, *3*(11), 14606–14619. https://doi.org/10.1021/acsomega.8b01874

Shaw, C. A., & Tomljenovic, L. (2013). Aluminum in the central nervous system (CNS): Toxicity in humans and animals, vaccine adjuvants, and autoimmunity. *Immunologic Research*, *56*(2–3), 304–316. https://doi.org/10.1007/s12026-013-8403-1

Sidoryk-Wegrzynowicz, M. (2014). Impairment of glutamine/glutamate-γ-aminobutyric acid cycle in manganese toxicity in the central nervous system. *Folia Neuropathologica*, *52*(4), 377–382. https://doi.org/10.5114/fn.2014.47838

Sikora, A. L. (2018). *Soil trace metals concentrations in a mining impacted agricultural*

watershed: Comparison of analytical methods, geospatial distribution, and evaluation of risk. University of Oklahoma.

Software, E. R. (2015). *What is MINEQL+?* Mineql.Com. https://www.mineql.com/overview.html

Sparks, D. L., & Schreurs, B. G. (2003). Trace amounts of copper in water induce β-amyloid plaques and learning deficits in a rabbit model of Alzheimer's disease. *Proceedings of the National Academy of Sciences of the United States of America*, *100*(19), 11065–11069. https://doi.org/10.1073/pnas.1832769100

Stillings, L. L., & Susan, L. (1995). Feldspar dissolution at 25°C and pH 3: Reaction stoichiometry and the effect of cations. *Geochimica et Cosmochimica Acta*, *59*(8), 1483–1496.

Survey, N. C. S. (2003). *Official Soil Series Description Query Facility*.

Tang, C., Zhu, J., Li, Z., Zhu, R., & Zhou, Q. (2015). Applied Surface Science Surface chemistry and reactivity of SiO2 polymorphs: A comparative study on alpha-quartz and alpha-cristobalite. *Applied Surface Science*, *355*, 1161–1167. https://doi.org/10.1016/j.apsusc.2015.07.214

Terrones-saeta, J. M., Suárez-macías, J., Linares Del Río, F. J., & Corpas-iglesias, F. A. (2020). Study of copper leaching from mining waste in acidic media, at ambient temperature and atmospheric pressure. *Minerals*, *10*(10), 1–23. https://doi.org/10.3390/min10100873

Timpane, M. (2018). Lithium Ion Batteries in the Solid Waste System. In *Environmental Protection Agency*.

Tolonen, E. T., Hu, T., Rämö, J., & Lassi, U. (2016). The removal of sulphate from mine water by precipitation as ettringite and the utilisation of the precipitate as a sorbent for arsenate

removal. *Journal of Environmental Management*, *181*, 856–862. https://doi.org/10.1016/j.jenvman.2016.06.053

Tran, C. P. (2016). *Red Mud Minimisation and Management for the Alumina Industry by the Carbonation Method*. The University of Adelaide.

U.S. EPA. (2005). Ecological soil screening levels for cobalt. *United States Environmental Protection Agency*, *April*, 1–76. http://www.epa.gov/ecotox/ecossl/index/html

Uddin, A. H., Khalid, R. S., Alaama, M., Abdualkader, A. M., Kasmuri, A., & Abbas, S. A. (2016). Comparative study of three digestion methods for elemental analysis in traditional medicine products using atomic absorption spectrometry. *Journal of Analytical Science and Technology*, *7*(1). https://doi.org/10.1186/s40543-016-0085-6

Udristioiu, F., Bunaciu, A. A., Tanase, I. G., & Aboul-Enein, H. (2014). Paper Analysis : Nondestructive and Destructive Analytical Methods. *Applied Spectroscopy Reviews*, *47*(7), 550–570. https://doi.org/10.1080/05704928.2012.682285

Vetter, J., Novák, P., Wagner, M. R., Veit, C., Möller, K. C., Besenhard, J. O., Winter, M., Wohlfahrt-Mehrens, M., Vogler, C., & Hammouche, A. (2005). Ageing mechanisms in lithium-ion batteries. *Journal of Power Sources*, *147*(1–2), 269–281. https://doi.org/10.1016/j.jpowsour.2005.01.006

Vytopilová, M., Tejnecký, V., Borůvka, L., & Drábek, O. (2015). Sorption of heavy metals in organic horizons of acid forest soils at low added concentrations. *Soil and Water Research*, *10*(1), 1–9. https://doi.org/10.17221/144/2014-SWR

Walker, J., Cronan, S., & Patterson, H. (1988). A kinetic study of aluminum adsorption by aluminosilicate clay minerals. *Geochimica et Cosmochimica Acta*, *52*(1988), 55–62.

Wendling, L. A., Kirby, J. K., & McLaughlin, M. J. (2009). Aging effects on cobalt availability

in soils. *Environ Toxicol Chem.*, *28*(8), 1609–1617.

Williams, M., Todd, D., Roney, N., Crawford, J., Coles, C., McClure, P., Garey, J., & Citra, M. (2012). Toxicological profile for manganese. *U.S. Department of Health and Human Services*, *September*.

Wong, C., Wu, S., Duzgoren-Aydin, N., Aydin, A., & Wong, M. (2007). Trace metal contamination of sediments in an e-waste processing village in China. *Environmental Pollution*, *145*, 434–442. https://doi.org/10.1016/j.envpol.2006.05.017

World Health Organization. (2011). Manganese in Drinking-water. In *WHO Guidelines for Drinking-water Quality* (pp. 1–21).

Xie, S., Wen, Z., Zhan, H., & Jin, M. (2018). An Experimental Study on the Adsorption and Desorption of Cu(II) in Silty Clay. *Geofluids*, *2018*, 12. https://doi.org/10.1155/2018/3610921

Yeganeh, M., Afyuni, M., Khoshgoftarmanesh, A., & Khodakarami, L. (2013). Mapping of human health risks arising from soil nickel and mercury. *Journal of Hazardous Materials*, *244–245*, 225–239. https://doi.org/10.1016/j.jhazmat.2012.11.040

Zubi, G., Dufo-López, R., Carvalho, M., & Pasaoglu, G. (2018). The lithium-ion battery: State of the art and future perspectives. *Renewable and Sustainable Energy Reviews*, *89*(April 2017), 292–308. https://doi.org/10.1016/j.rser.2018.03.002

Appendix

Table A.1: *LIB NMC Powder verify cobalt is detectable by the XRF.*

LIB Powder (mg/kg)					
Sample	**Copper**	**Nickel**	**Cobalt**	**Manganese**	**Aluminum**
1	154989.80	219189.50	38460.61	40620.86	69555.35
2	155226.60	217057.30	38455.00	40272.52	67551.92
3	154784.50	219658.00	38699.00	40474.39	67430.36
Average	155000.30	218634.90	38538.20	40455.92	68179.21

Table A.2: *Control soil metal concentrations*

Control Soil Metal Concentrations (mg/kg)					
	Copper	**Nickel**	**Cobalt**	**Manganese**	**Aluminum**
Acidic	BDL	BDL	BDL	402.63	37528.50
Acidic	BDL	BDL	BDL	401.88	37660.44
Acidic	BDL	BDL	BDL	397.62	37917.54
Average	BDL	BDL	BDL	400.71	37702.16
Basic	BDL	BDL	BDL	405.68	43649.58
Basic	BDL	BDL	BDL	403.77	43427.42
Basic	BDL	BDL	BDL	405.14	44119.62
Average	BDL	BDL	BDL	404.86	43732.21

BDL = Below Detection Limit

Table A.3: *Certified standards calibration trendline and R-Squared for each LIB metal*

Certified Standards Calibration Trendline and R-Squared				
	Copper	**Nickel**	**Manganese**	**Aluminum**
Trendline	y=10,574.81x	y=11,605.04x	y=17,559.49x	y=18,978.65x
R-Squared	0.967	0.961	0.965	0.999

Table A.4: *Control water metal concentrations*

Control Water Metal Concentrations (mg/L)

	Copper	Nickel	Cobalt	Manganese	Aluminum
Acidic	0.009	BDL	BDL	BDL	BDL
Acidic	0.008	BDL	BDL	BDL	BDL
Acidic	0.009	BDL	BDL	BDL	BDL
Average	0.009	BDL	BDL	BDL	BDL
Basic	0.007	BDL	BDL	BDL	BDL
Basic	0.008	BDL	BDL	BDL	BDL
Basic	0.008	BDL	BDL	BDL	BDL
Average	0.008	BDL	BDL	BDL	BDL

BDL = Below Detection Limit

Table A.5: *LIB metal concentrations for the new LIB, post 24 weeks in soil LIB, and post 24 weeks in water LIB.*

Metal Concentrations for New, Soil, and Water LIB

	Copper	Nickel	Cobalt	Manganese	Aluminum
New	155000.30	218634.90	38538.20	40455.92	68179.21
Acidic Soil	136119.58	176944.12	28093.78	36914.31	48996.40
Basic Soil	115921.66	168273.91	26886.65	32187.04	44182.66
Acidic Water	126845.39	143989.70	24561.24	29029.90	42905.35
Basic Water	128983.67	146048.55	25582.01	32678.42	41302.88

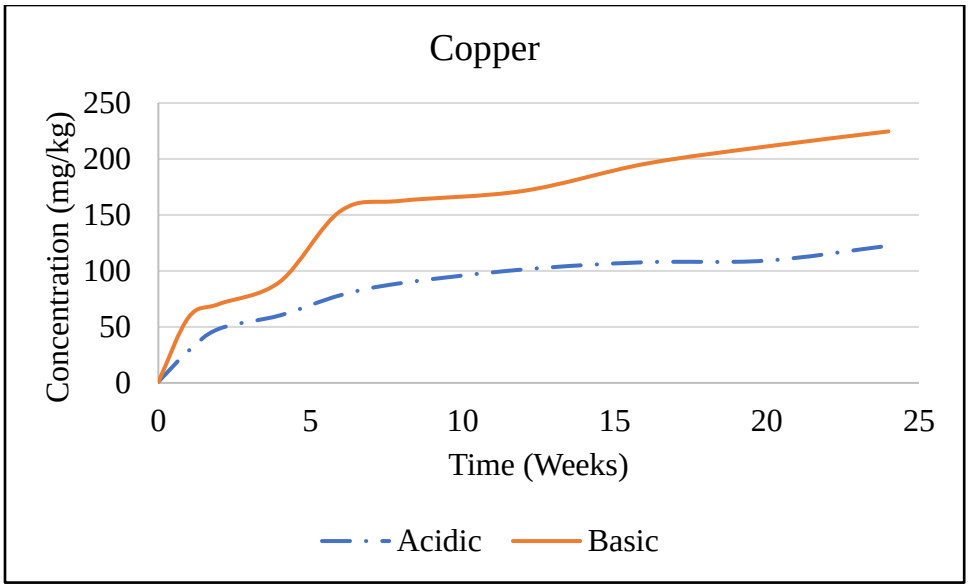

Figure A.1: *Comparison of copper concentration in acidic and basic soil, non-normalized.*

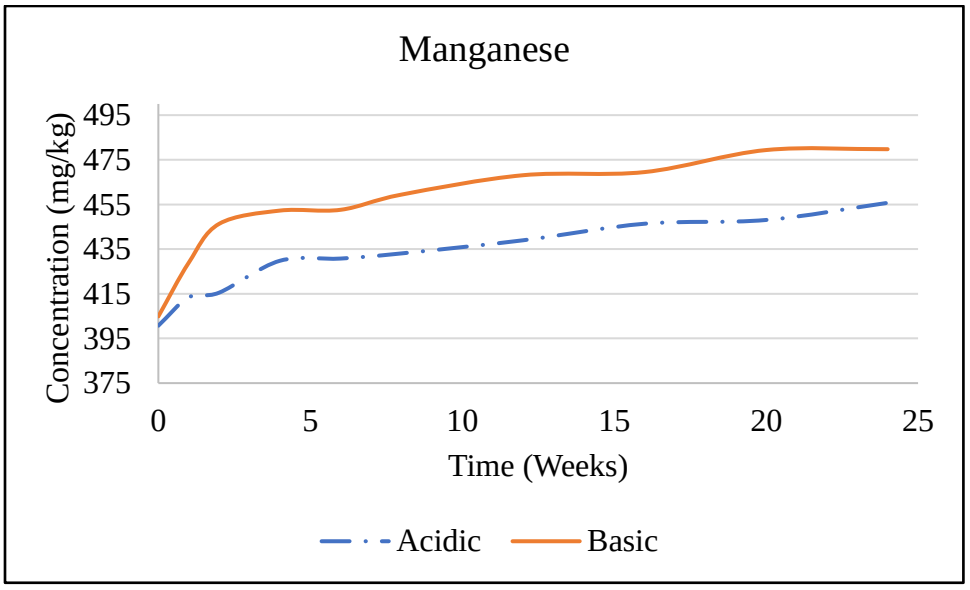

Figure A.2: *Comparison of manganese concentration in acidic and basic soil, non-normalized.*

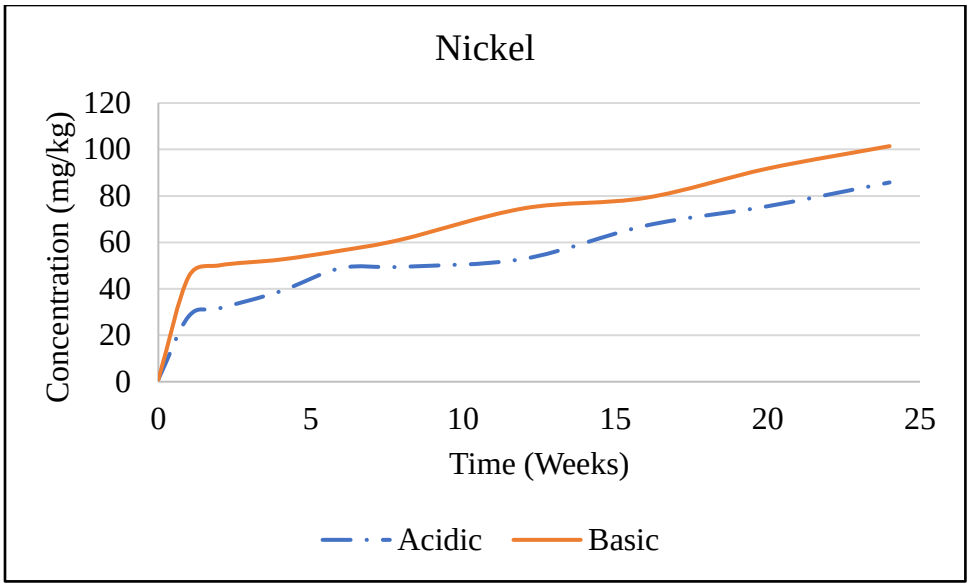

Figure A.3: *Comparison of nickel concentration in acidic and basic soil, non-normalized.*

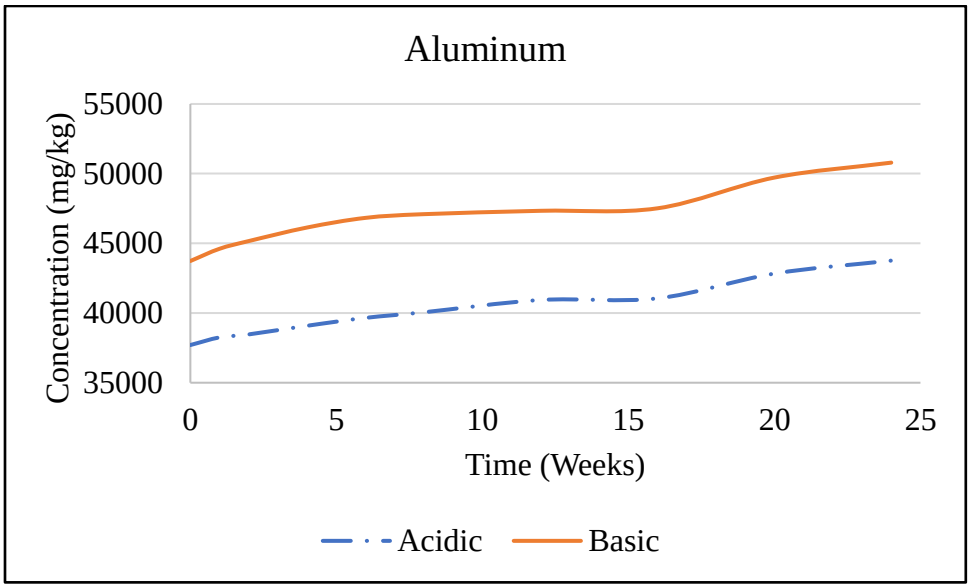

Figure A.4: *Comparison of aluminum concentration in acidic and basic soil, non-normalized.*

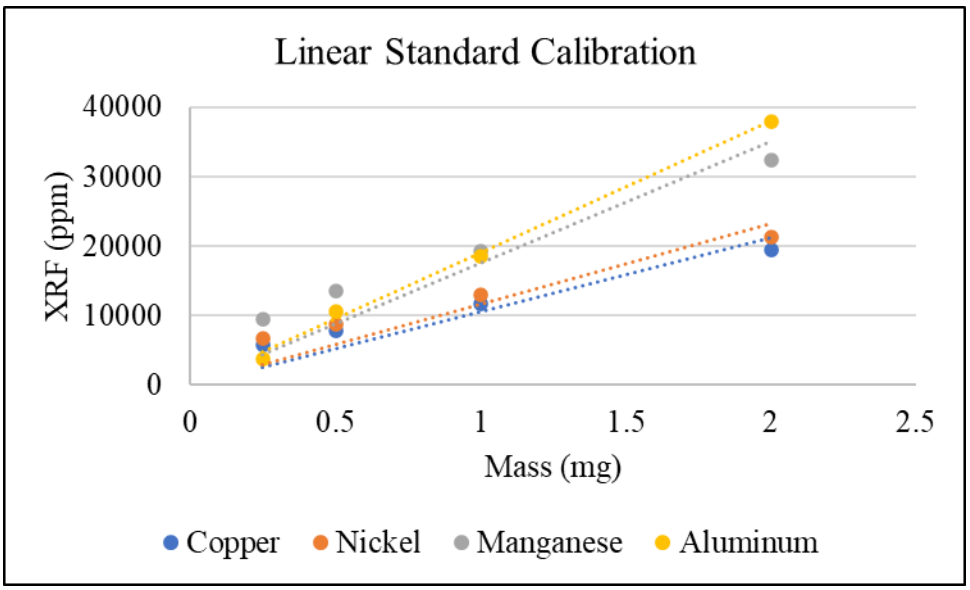

Figure A.5: *Linear standard calibration results for correcting sample XRF ppm results to actual concentrations.*

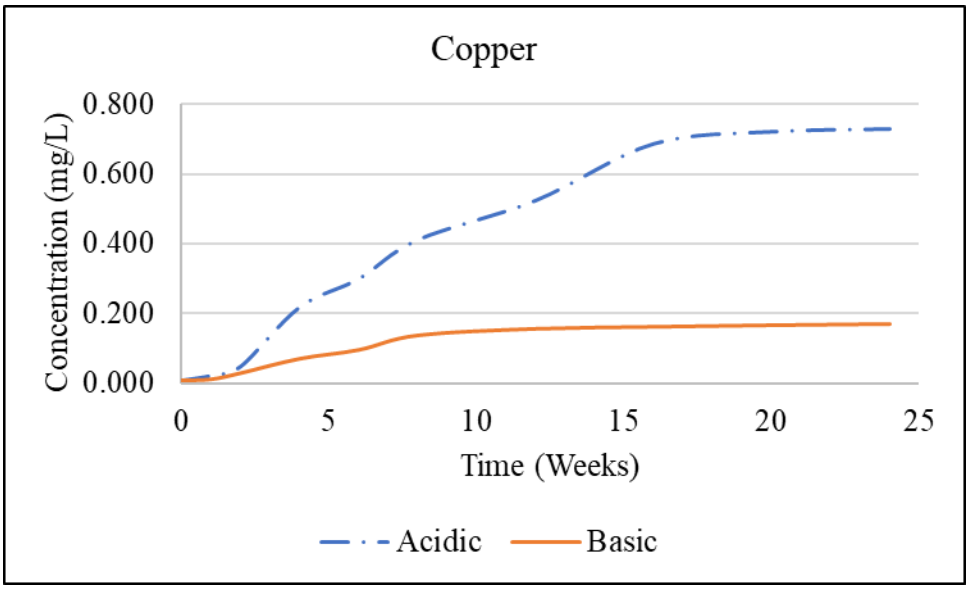

Figure A.6: *Comparison of copper concentration in acidic and basic water, non-normalized.*

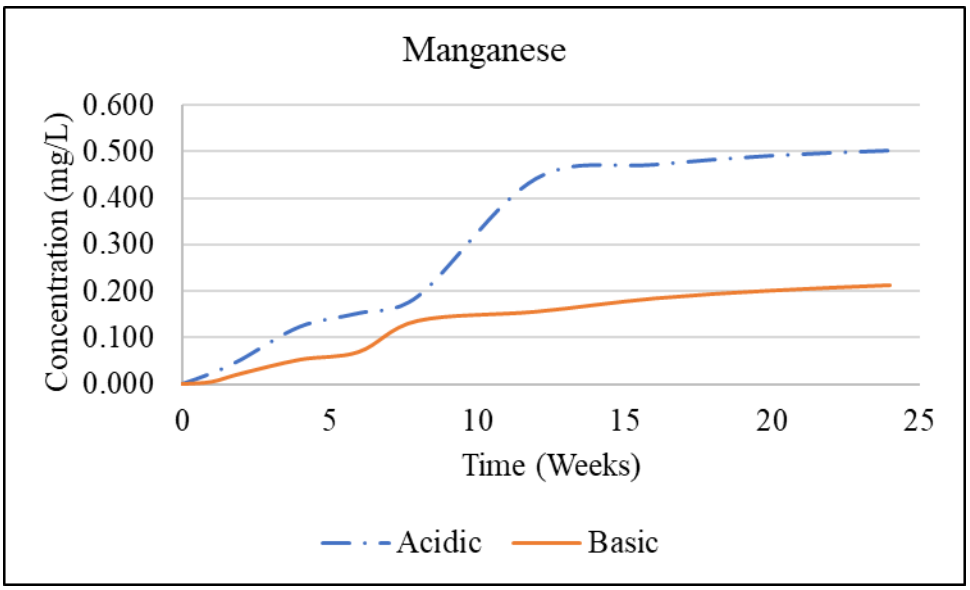

Figure A.7: *Comparison of manganese concentration in acidic and basic water, non-normalized.*

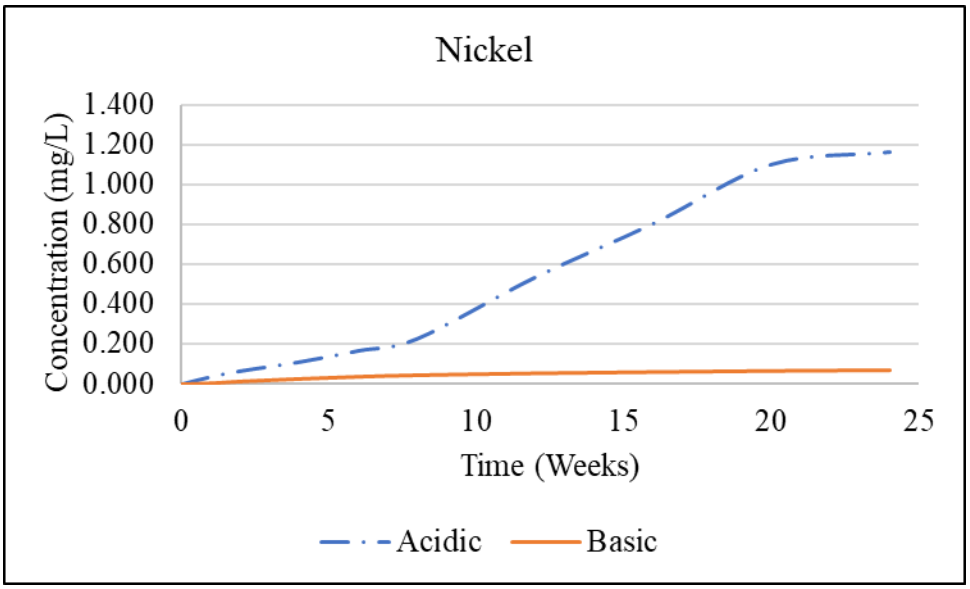

Figure A.8: *Comparison of nickel concentration in acidic and basic water, non-normalized.*

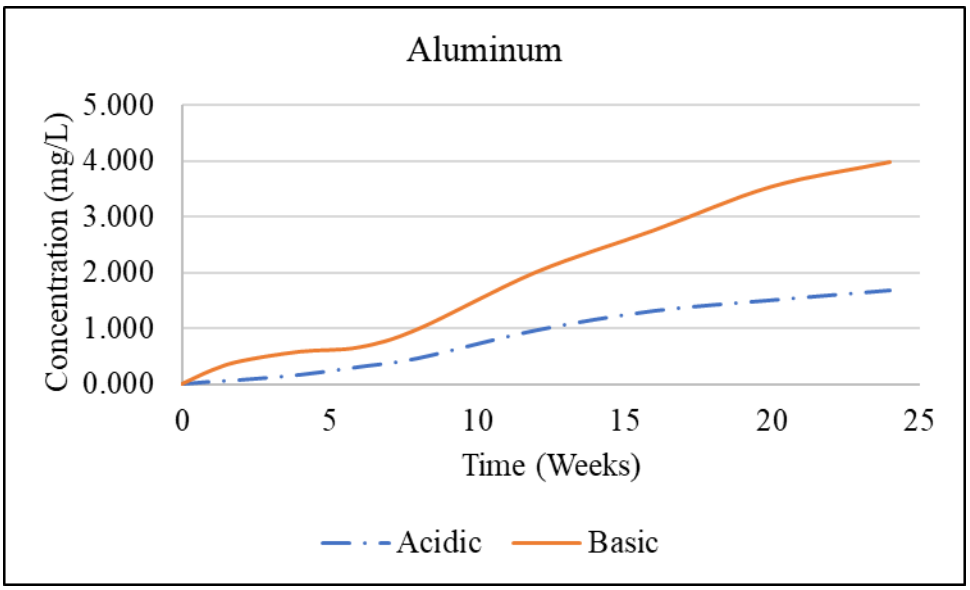

Figure A.9: *Comparison of aluminum concentration in acidic and basic water, non-normalized.*

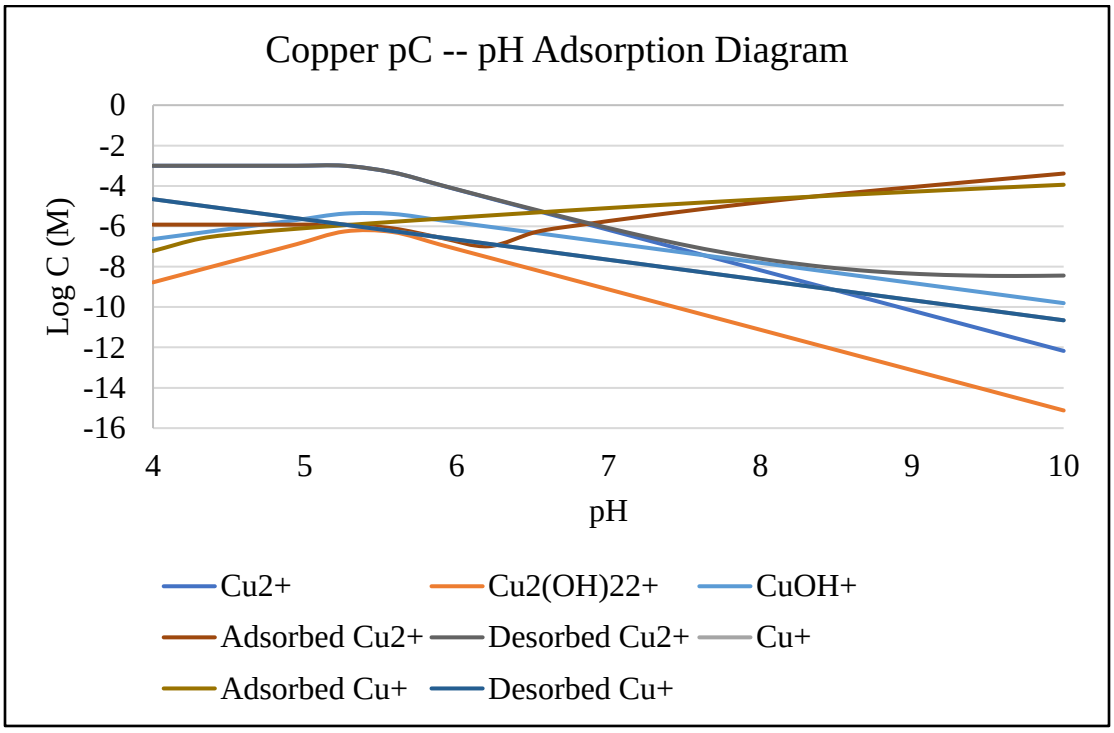

Figure A.10:*.Comparison of major copper species in the MINEQL+ adsorption model.*

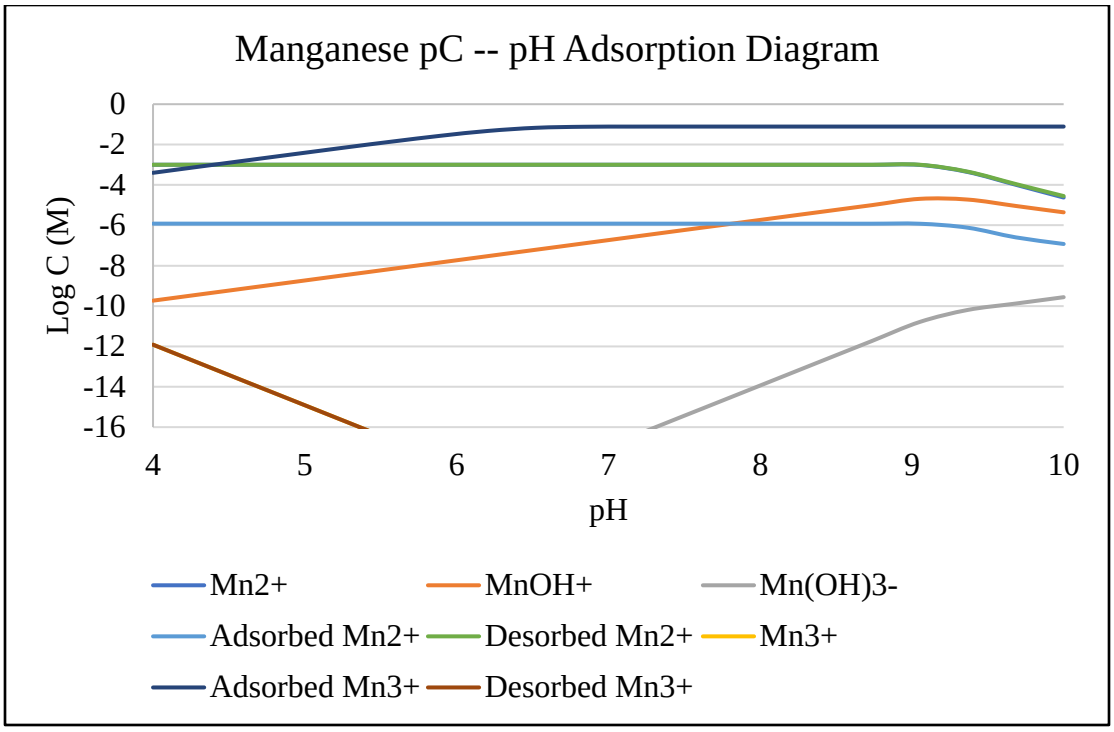

Figure A.11: *Comparison of major manganese species in the MINEQL+ adsorption model.*

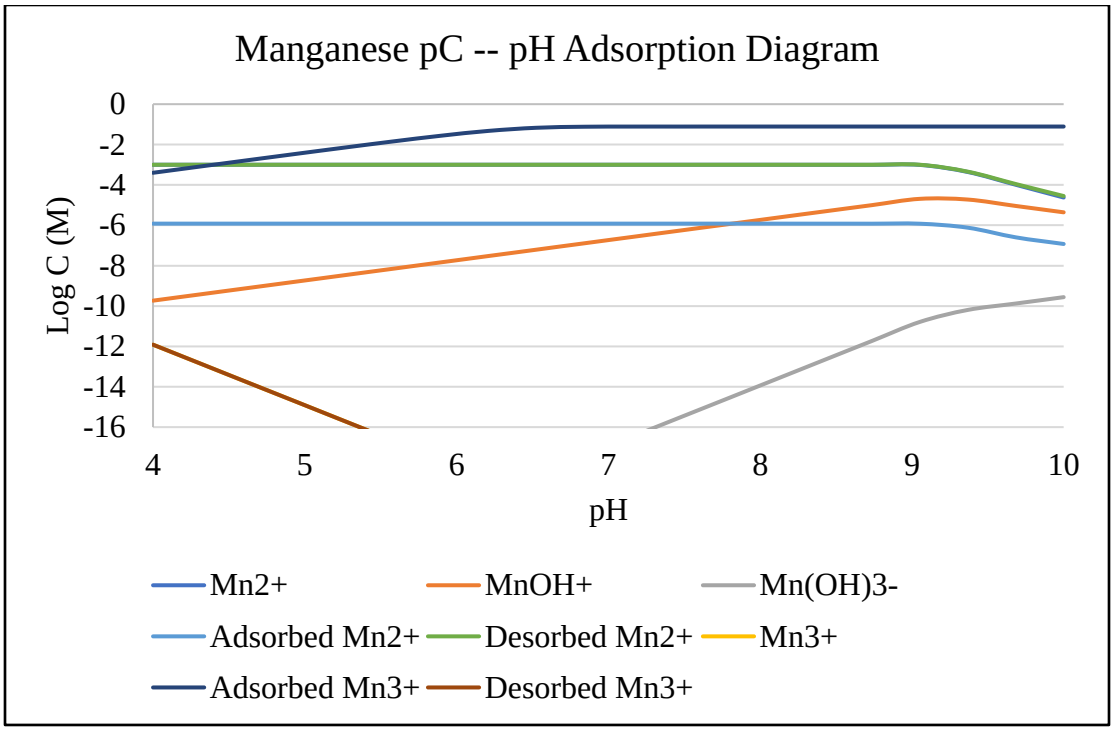

Figure A.12: *Comparison of major nickel species in the MINEQL+ adsorption model.*

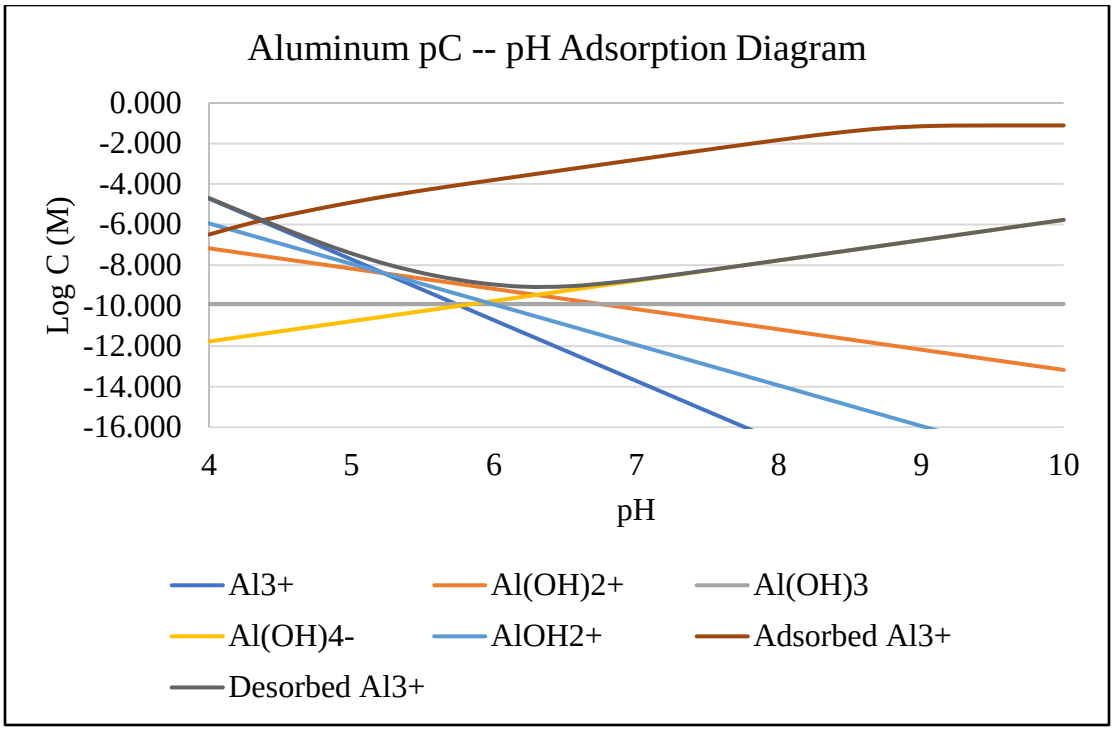

Figure A.13: *Comparison of major aluminum species in the MINEQL+ adsorption model.*

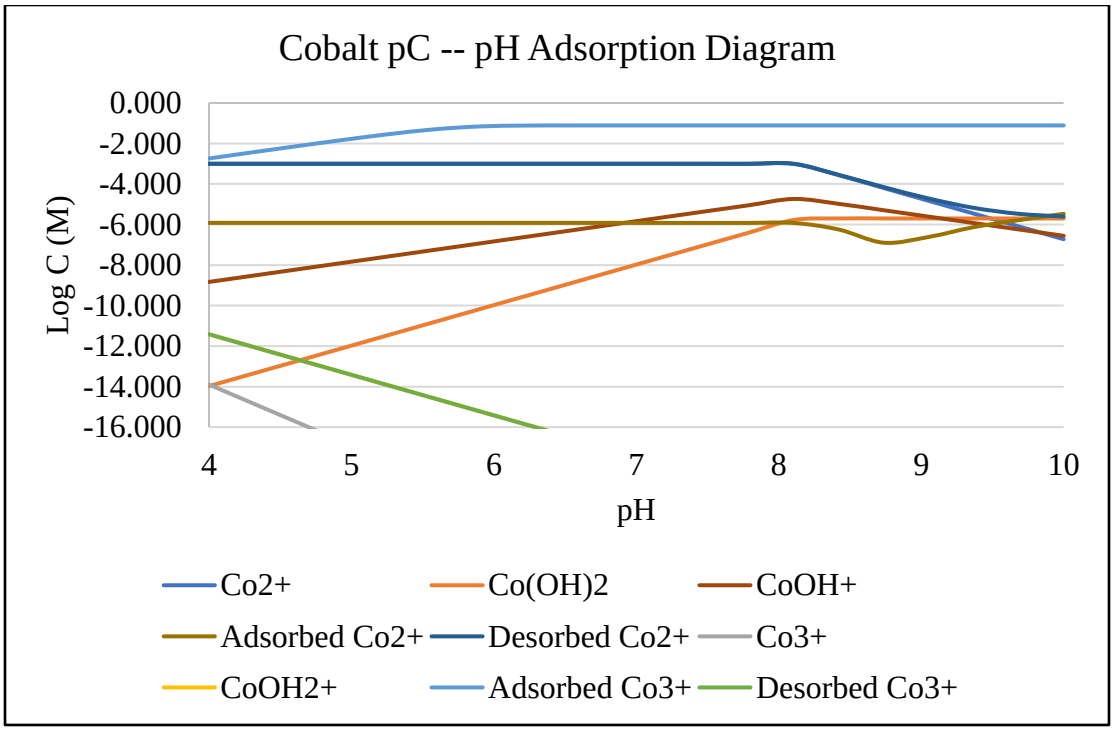

Figure A.14: *Comparison of major cobalt species in the MINEQL+ adsorption model.*

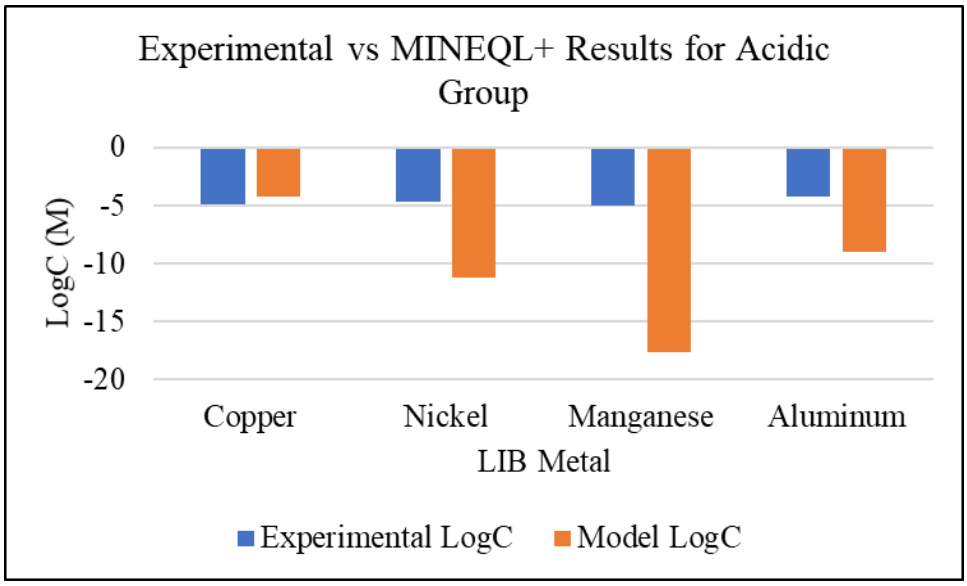

Figure A.15: *Comparison of experimental and MINEQL+ concentration results for the acidic water group.*

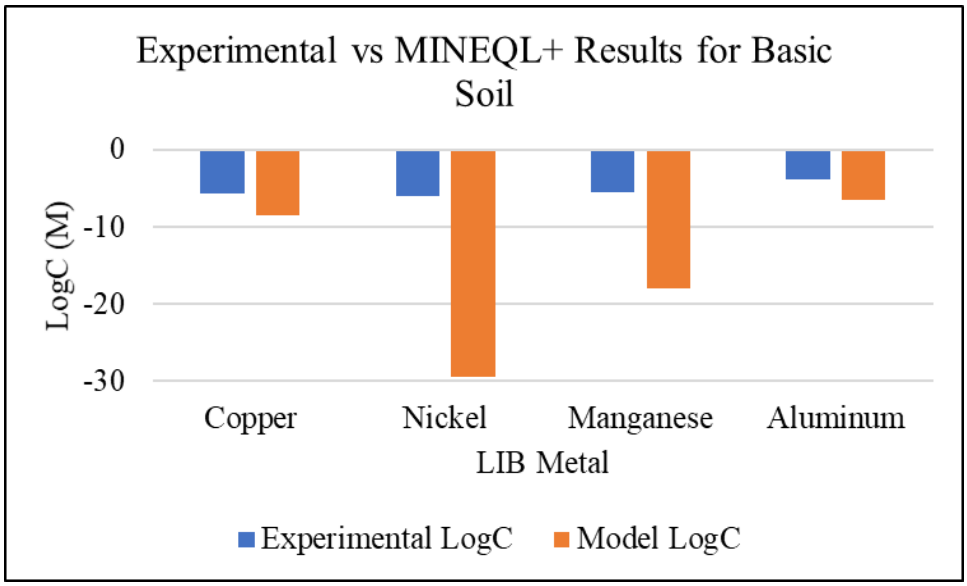

Figure A.16: *Comparison of experimental and MINEQL+ concentration results for the basic water group.*